

EFFECTS OF TOOTH QUALITY, TOOTH STRUCTURE, AND CEMENT MIXING RATIOS ON DENTAL ADHESION

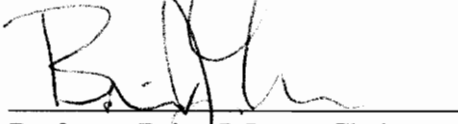
by

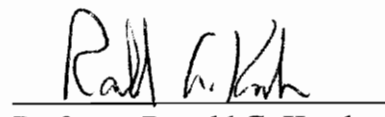
ROLA RIAD HAMANDI


Thesis submitted to the faculty of the
Virginia Polytechnic Institute and State University
in partial fulfillment of the requirements for the degree of
Master of Science
in

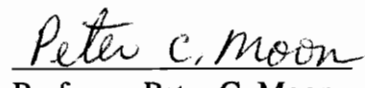
Materials Science and Engineering

APPROVED:



Professor Brian J. Love, Chairman

Professor Ronald G. Kander

Professor James P. Wightman

Professor Peter C. Moon

October, 1995
Blacksburg, Virginia

2

LD
5055
V855
1995
H353
C.2

2.7.15

Effects of Tooth Quality, Tooth Structure, and Cement Mixing Ratios on Dental Adhesion

by

Rola Riad Hamandi

Committee Chairman: B. J. Love

Materials Science and Engineering

(ABSTRACT)

Experiments were performed on a number of bovine dentin specimens with the intent of understanding the effects of dentin quality and preparation on dentinal adhesion. Dentin quality was evaluated by measuring its wetting characteristics and hardness properties. The effects of chemical treatment, thermal dehydration and rehydration on dentin quality were examined. The contribution of enamel to adhesion was evaluated by comparing the adhesion of dentin samples that had the enamel ground off prior to bonding with dentin samples that retained the enamel wall. Sulfuric acid and tannic acid etching of dentin were performed for both ground and unground teeth. Unground dentin specimens were also exposed to thermal aging at 65⁰ C. The torsional bond strength of the dental tissues under these modified processing conditions was evaluated using a commercial glass-ionomer cement. The same procedure has been repeated on unground and ground teeth by changing several different cement mixing ratio. The chemical, thermal, and mechanical properties of the cement mixing ratios were evaluated separately to provide a better understanding of adhesion. Acid etching treatment was found to improve dentin wetting characteristics and roughened the dentin surface leading to improve dental adhesion. Thermal treatment renders the dentin surface more hydrophobic and subsequently reduces adhesion. Weaker strengths were measured for untreated and ground teeth. This is related to lower mechanical interlocking and lower chemical adhesion when the smear layer covers the dentin. Mixed failure modes were detected

during dentin debonding while cohesive failure within the cement were observed during enamel debonding indicating that enamel bonded better to the cement than dentin did. Improper cement mixing decreased the bond strength of enamel and dentin.

Acknowledgments

I would like to extend my deepest thanks to my advisor, Dr Brian. J. Love, for his patience, support, and encouragement in the completion of this study. I would like to thank Dr. Ronald Kander, Dr Peter Moon, and Dr James Wightman for agreeing to be members of my committee. I would like to extend my appreciation to the department of Materials Science and Engineering which funded my project.

Special thanks to Dr Veit who provided me with bovine teeth, and to Anne Creo from 3M who sent me Vitrebond.

During my experimental work for this project, I received assistance from Mojee and Hong while performing the contact angle measurements, from Jeff May who helped me construct the torsional bond test, from Rick Clark who trained me on TGA, and Tsunou who trained me on DMA. Thank you for your assistance and help. I would like to thank Joannie Chin for being helpful in the lab.

My special thanks to Ary, Chafic, Joy, and John who were extremely helpful in checking my writing. I also thank, Marcos, Nicolas, Niomi, Vicki, and Virginie for their friendship and support, especially this summer, and to my favorite friend in the lab “Joel”.

I would like to thank my parents, Wadad and Riad, for their support and love during my bachelor’s and master’s studies and also to my host family in the U.S., Drs Solomon.

List of Figures

Figure 1: Tooth structure as described by Marsh [21]	4
Figure 2: Idealized representation of wetting of a solid by a liquid [33]	7
Figure 3: (a) Unetched enamel surface (X950); (b) etched with 85% orthophosphoric acid as described by Retief [2]	12
Figure 4: (a) Unetched enamel surface; (b) etched with 5% of aqueous tetrahydrofuran-2,3,4,5- tetracarboxylic acid for 30 sec as described by Termini [1]	13
Figure 5: (a) Dentin surface etched for two minutes with 50% phosphoric acid (X1800); (b) dentin surface etched for five minutes with 50% phosphoric acid (X1800) [35]	14
Figure 6: Structure of poly(alkenoic acid) as suggested by Ruyter [6]	21
Figure 7: Chemical reaction of Vitrebond™ as described by Mitra [48]	22
Figure 8: Different types of bond formation as described by Hull: (a) Chemical bonding between two groups; (b) mechanical interlocking; (c) electrostatic attraction; (d) molecular entanglement pursuing interdiffusion; (e) ionic bonding [59]	26
Figure 9: Mechanism of chemical adhesion of poly(alkenoic acid) to dentin collagen [6] ..	29
Figure 10: Bond strength test methods as suggested by Watanabe: (a) Illustration of cross-sectional view for tensile bond test; (b) representation of cross-sectional view of shear strength test [5]	30
Figure 11: Schematic representation of a torsional bond test method.....	30
Figure 12: Three locations of adhesive failure: (a) Adhesive failure at the interface; (b) cohesive failure in the adhesive; (c) cohesive failure in the adherend [33]	34
Figure 13: Dentin surface preparation	38
Figure 14: Schematic illustration of the Rame-Hart Goniometer	40
Figure 15: Schematic representation of Vickers indentation	40
Figure 16: Schematic illustration of tooth preparation for torsional testing	42
Figure 17: Schematic illustration of cement bonding to enamel and dentin.....	42
Figure 18: Illustration of the mechanism of debonding using a torque meter	45
Figure 19: Schematic representation of the glass-ionomer cement preparation.....	45
Figure 20: Comparison of the average polar, dispersive and total surface tension for different dentin conditions	53
Figure 21: Optical micrograph of dentin surface treated with tannic acid for 60 sec; small pores observed, indicating an opening of dental tubules (X50).....	55
Figure 22: Optical micrograph of dentin surface treated with tannic acid for 60 sec; small pores observed, indicating an opening of dental tubules (X215).....	56
Figure 23: Work of adhesion as function of aging time at 65°C in an air oven.....	57
Figure 24: Dentin surface after 3 hours of aging time at X125.....	59
Figure 25: Dentin surface after 24 hours of aging time; major cracks observed at a magnification of X25	60

Figure 26: Geometry of hardness indentation at X125.....	63
Figure 27: Effect of etching on hardness	64
Figure 28: Average hardness as function of thermal aging time at 65°C in an air oven ...	66
Figure 29: Dentin surface after 24 hours of thermal exposure and prior to hardness testing; cracks were observed at X12.5	67
Figure 30: Effects of etching on the average shear strength for the unground and ground teeth: (a) Group U _{Tannic} and Group U _{Sulfuric} ; (b) Group G _{Tannic} and Group G _{sulfuric}	70
Figure 31: Average torsional shear strength as function of thermal aging time at 65°C in an air oven.....	75
Figure 32: Variation in the average shear strength of unground and ground teeth as function of cement ratios.....	76
Figure 33: Cement trace (T) bonded to the steel rod (S) for Group U at X310.....	79
Figure 34: Cement trace (T) bonded to steel rod (S) for Group G at X300.....	80
Figure 35: The bottom part showing the cement (T) still bonded to enamel for Group U; the top part showing cement debris covering the dentin region (D) at X350	81
Figure 36: The bottom part showing the dentin (D); the top part showing the cement (T) still bonded to dentin at 295X	82
Figure 37: Dentin surface (D), dentin tubules (B) and cement debris (T) for Group G at X300	83
Figure 38: Cement trace (T) bonded to steel rod (S) for Group U _{Tannic} at X315.....	84
Figure 39: Cement trace (T) bonded to steel rod (S) for Group G _{Tannic} at X335.....	85
Figure 40: Cement trace (T) still bonded to etched enamel (S) for Group U _{Tannic} at X485	86
Figure 41: Cement trace (T) still bonded to etched dentin (R) for Group U _{tannic} at X500	87
Figure 42: Dentin surface including small pores (D), longitudinal tubules (T), and cement debris (S) shown for Group G _{Tannic} at X980.....	88
Figure 43: Micrograph of steel rod (S) for Group D ₄₈ at X300.....	89
Figure 44: Cement debris (T) covering the enamel surface (A) for Group D ₄₈ at X320	90
Figure 45: Cement debris (S) covering dentin surface (D) for Group D ₄₈ at X285	91
Figure 46: TGA plot for each cement sample ratio	96
Figure 47: Liquid Vitrebond™ spectrum.....	112
Figure 48: Powder Vitrebond™ spectrum.....	113
Figure 49: 60/40 powder to liquid cement sample ratio spectrum	114
Figure 50: 50/50 powder to liquid cement sample ratio spectrum	115
Figure 51: 40/60 powder to liquid cement sample ratio spectrum	116

List of Tables

Table 1: Surface energy contributions for the two liquids at 20 ⁰ C, used in the contact angle measurements [34].....	10
Table 2: Average Knoop hardness of dentin as function of etching time calculated by Moon [8]	18
Table 3: Stretching mode and frequencies occurring in the IR spectrum (ATR) of a setting glass-ionomer cement according to Wilson [49]	24
Table 4: Physical properties of the Vitrebond TM liquid and powder according to 3M. [47]	24
Table 5: Bond strength of a glass-ionomer cement to enamel and dentin at different surface conditions [62].....	32
Table 6: Sample conditions for each tooth.....	43
Table 7: Surface conditions of dentin specimens tested for contact angle measurements	49
Table 8: Average contact angle measurements for water and methylene iodide for each dentin specimen condition	49
Table 9: Contact angle measurements of water and methylene iodide for thermally aged dentin specimens.....	50
Table 10: Average surface tension components of untreated and treated dentin surface specimens	50
Table 11: Average work of adhesion for untreated, treated and thermally aged dentin specimens	51
Table 12: Surface conditions of etched dentin specimens tested for hardness	61
Table 13: Surface conditions of thermally aged dentin specimens tested for hardness.....	61
Table 14: Average hardness of untreated and etched dentin specimens	62
Table 15: Average hardness of untreated, thermally aged and rehydrated dentin specimens	62
Table 16: Teeth conditions used for torsional testing.....	69
Table 17: Average torque at failure and average torsional shear strength for unground, ground and etched teeth.....	69
Table 18: Average torque at failure and average torsional shear strength for the thermally aged and etched after thermally aged teeth	73
Table 19: Average torque at failure and average torsional shear strength of teeth subjected to different cement mixing ratios.....	74
Table 20: Average contact angle measurements of water and methylene iodide for each cement mixed ratio	93
Table 21: Average surface tension components for each cement mixed ratio	93
Table 22: Vibrational modes and frequencies for the liquid and powder Vitrebond TM [50]	95
Table 23: Percentage char yield for each cement ratio at 455 ⁰ C.....	95

Table 24: Average hardness of each cement sample at varying mix ratio, cured for one hour as a function of loading 98

Table of Contents

1. Background.....	1
1.1. Introduction.....	1
1.1.1. Thesis motivations.....	2
1.1.2. Thesis objectives	2
1.2. Tooth structure and composition.....	3
1.2.1 Physical and mechanical properties of enamel and dentin	3
1.3. Restorative materials used in dental applications.....	5
1.4. Factors affecting adhesion.....	5
1.4.1. Surface wetting	6
1.4.1.1. Contact angle measurements.....	6
1.4.1.2. Determination of surface tension from contact angle measurements	8
1.4.2. Effects of etching	9
1.4.3. Effects of aging of enamel and dentin	15
1.4.4. Enamel and dentin hardness measurements	15
1.4.4.1. Effects of aging on hardness	16
1.4.4.2. Effects of etching on hardness	16
1.4.5. Effects of extraction and storage	17
1.5. Light-cured glass-ionomer cements(Vitrebond TM).....	19
1.5.1. Introduction	19
1.5.2. Composition.....	19
1.5.3. Chemical reaction.....	20
1.5.4. Physical and mechanical properties	23
1.6. Theories of adhesion	25
1.6.1. Chemical adhesion.....	27
1.6.1.1. Types of chemical adhesion	27
1.6.1.2. Application of chemical adhesion to enamel and dentin	27
1.6.1.3. Adhesion based on ionic polymers	27
1.6.2. Mechanical testing.....	28
1.6.2.1. Bond strength test methods	28
1.6.2.2. Application of bond strength tests of glass-ionomer to untreated and acid treated teeth.....	28
1.6.2.3. Application of bond strength tests on thermally aged teeth.....	31
1.6.3. Adhesive failure	33
1.6.3.1. Adhesive failure in dentistry.....	33
1.6.3.2. Failure of the glass-ionomer cements.....	35
1.7. Summary	35
1.8. Thesis organization	36

2. Experimental Procedures	37
2.1. Experimental approach.....	37
2.2. Dentin sample preparation.....	37
2.3. Dentin sample surface characterization.....	37
2.3.1. Contact angle measurements	37
2.3.2. Hardness testing.....	39
2.3.3. Optical microscopy	39
2.4. Adhesion testing	41
2.4.1. Tooth preparation for torsional testing	41
2.5. Cement preparation.....	41
2.6. Torsional testing	44
2.7. Natural tissue failure analysis.....	44
2.7.1. Environmental scanning electron microscope (ESEM).....	44
2.8. Cement characterization.....	44
2.8.1. Contact angle measurements	44
2.8.2. Hardness testing.....	46
2.8.3. Fourier transform infrared spectroscopy (FTIR)	46
2.8.4. Thermogravimetric analysis (TGA).....	47
3. Results.....	48
3.1. Dentin quality results	48
3.1.1. Contact angle measurements	48
3.1.1.1. Conditions, Equations.....	48
3.1.1.2. Unetched dentin specimens.....	52
3.1.1.3. Etched dentin specimens.....	52
3.1.1.3.1. Microscopy of etched dentin specimens.....	54
3.1.1.4 Thermally aged dentin specimens.....	54
3.1.1.4.1. Microscopy of thermally aged dentin specimens	58
3.1.2. Hardness measurements	58
3.1.2.1. Conditions, Equations.....	58
3.1.2.2. Unetched dentin specimens.....	58
3.1.2.3. Etched dentin specimens.....	58
3.1.2.4. Thermally aged dentin specimens.....	65
3.1.2.4.1. Microscopy of thermally aged dentin specimens	65
3.2. Torsional testing	68
3.2.1. Conditions and equations	68
3.2.1.1. Unground and ground teeth	68
3.2.1.2. Etched unground and ground teeth	71
3.2.1.3. Thermally aged teeth	72
3.2.1.4. Analysis of glass-ionomer cement ratio on unground and ground teeth...	72
3.3. ESEM analysis.....	77
3.3.1. Unground and ground teeth.....	77
3.3.2. Etched unground and ground teeth.....	78

3.3.3. Thermally aged teeth	78
3.4. Glass-ionomer cement (Vitrebond™)	92
3.4.1. Chemical properties.....	92
3.4.1.1 Contact angle measurements.....	92
3.4.1.2. Fourier transform infrared spectroscopy (FTIR).....	92
3.4.2. Thermal properties	94
3.4.2.1. Thermogravimetric analysis (TGA).....	94
3.4.3. Mechanical properties	97
3.4.3.1. Hardness measurements.....	97
4. Discussion.....	99
4.1. Dentin quality discussion	99
4.1.1. Contact angle measurements	99
4.1.1.1. Comparison between the unetched and etched dentin specimens	99
4.1.1.2. Thermally aged dentin specimens	100
4.1.2. Hardness measurements	100
4.1.2.1. Comparison between the unetched and etched dentin specimens	100
4.1.2.2. Thermally aged dentin specimens	101
4.2. Torsional testing	102
4.2.1. Effects of etching on unground and ground teeth.....	102
4.2.2. Effects of thermal aging on enamel and dentin bond strengths.....	103
4.2.3. Effects of mixing ratios on enamel and dentin bond strengths.....	103
4.3. ESEM analysis.....	103
4.4. Glass-ionomer cement properties (Vitrebond™)	104
4.4.1. Chemical and thermal properties.....	104
4.4.2. Mechanical properties	105
4.4.3. Effects of cement mixing properties on enamel and dentin bond strength	105
5. Conclusions	106
5.1. Summary	106
5.2. Future work.....	107
Appendix A: Torsional shear strength derivation.....	109
Appendix B: Infrared Spectra	110
References	117
Vita.....	123

1. Background

1.1. Introduction:

A strong permanent bond between dental tissues and restorative dental materials is a highly desirable property for dental practice. Materials and techniques are now available which enhance measured adhesion to enamel [1]. In addition, treatment of enamel surfaces with dilute acid has improved adhesion [1,2]. Acids remove debris and increase surface wettability of enamel prior to adhesion [3]. Acid etching also creates more enamel surface area by opening up pores where the adhesive can mechanically interlock at the enamel-adhesive interface [1,3,4].

Strong dentin adhesion has been more difficult to achieve since dentin contains more water and is more heterogeneous than enamel. In addition, dentin adhesion varies with tooth type and preparation method [1,5]. Adhesion to dentin is frequently limited because bonding materials do not entirely wet dentin surface [6]. Acid treatment is thought to increase the dentin surface wettability and subsequently improve adhesion [7]. Acid etching removes the smear layer which is a weak boundary layer covering dentin. Acid etching produces more dentin surface area by opening up pores where the adhesive can mechanically interlock at the dentin-adhesive interface [1,7]. However, long exposure to acid etching demineralizes dentin surface, lowering its hardness and leading to decreasing dentin bond strength to restorative dental materials as measured by adhesion testing [8,9,10]. Most of the bond strength methods used for dental research are comprised of tensile and shear tests. Both tests have their advantages and their drawbacks [5,11,12].

Dentin aging is generally caused by trauma, diseases, dental caries, and thermal dental treatment [13]. It also occurs in geriatric dentistry. Aging is thought to change the mechanical and chemical properties of dentin due to the fact that water content is reduced and collagen is crosslinked [13,14,15].

Recently, glass-ionomer cements were introduced in the market for restorations. Glass-ionomer cements are thought to adhere to enamel and dentin without chemical treatment [6,16,17]. However, the proper proportion of powder to liquid in the glass-ionomer mixture and proper mixing ratios are expected to be routine. Unfortunately, in clinical applications, dentists do not usually weigh the components precisely prior to application. Any change from the recommended mixture will likely affect the bond strength of the cement to both enamel and dentin [18].

1.1.1. Thesis motivations:

This thesis effort is focused in the dental materials research as it relates to dentin adhesion. The effort investigated the use of a commercial dental cement (Vitrebond™) and looked at the effects of dentin quality, dentin processing and testing on dentinal adhesion as evaluated through torsional bond testing. Part of the motivation was in understanding just how robust this dental cement was to the variations most likely experienced in dental practice. The test protocol used a torsional bonding evaluation that is not extensively used in dental materials research [5,11,12]. Another interest was to evaluate how thermal aging and etching affected dentin torsional bond strength when dentin was bonded to Vitrebond.

Thesis objectives:

The objectives of the present research are to evaluate the effects of chemical treatment on dentin wettability and hardness using tannic and sulfuric acid, and to examine the effects of thermal aging on dentin hardness prior to adhesive bonding. This effort focused on evaluating the bonding characteristics to dentinal tissue under modified process conditions, determining the contributions of enamel and dentin to adhesion, analyzing the mechanism of adhesive failure, and detecting the effect of cement mixing ratios on bonding. In addition, the properties of the dental cement are assessed to provide a better understanding of adhesion.

In the following sections, the literature review focuses on the structure and properties of teeth, and the factors affecting enamel and dentin adhesion. The chemical, and mechanical properties of the dental cement are reviewed. Mechanisms of adhesion are also discussed.

1.2. Tooth structure and composition:

Teeth are mineralized tissues whose primary function is to carry load [19]. As shown in Figure 1, a tooth is comprised of two portions: the visible part known as the crown, and the root which is embedded in the gum. Each tooth is composed of four tissues: Enamel, dentin, pulp and cementum. Enamel covers the anatomical crown of the tooth, and it is the hardest substance in the tooth body. It consists mostly of inorganic components (97%), such as calcium and phosphate apatite in their hydroxy, fluoro, or carbonate forms. The remaining 3% is made up of organic constituents and water [19,20]. Dentin is the second mineralized tissue. It consists of inorganic (69%) and organic (22%) components as well as water (9%). The organic matrix of dentin consists of collagen which is found in dentinal tubules [19]. Pulp is a soft tissue that nourishes the dentin, and cementum is a calcified tissue that covers and protects the roots of the tooth [21].

1.2.1. Physical and mechanical properties of enamel and dentin:

Teeth variations in pigment and shade make restorative materials a challenge to match their natural colors. Enamel is generally blue-white and translucent as seen at the biting portion of teeth [1]. The yellowish shade of the central portion of the human teeth originates from the underlying dentin [1].

The measured strength properties of both enamel and dentin change according to testing procedure, specimen size and aging [1]. Enamel is a hard and brittle tissue with an average hardness of 350 kg/mm^2 which is lowered to 280 to 300 kg/mm^2 when ground

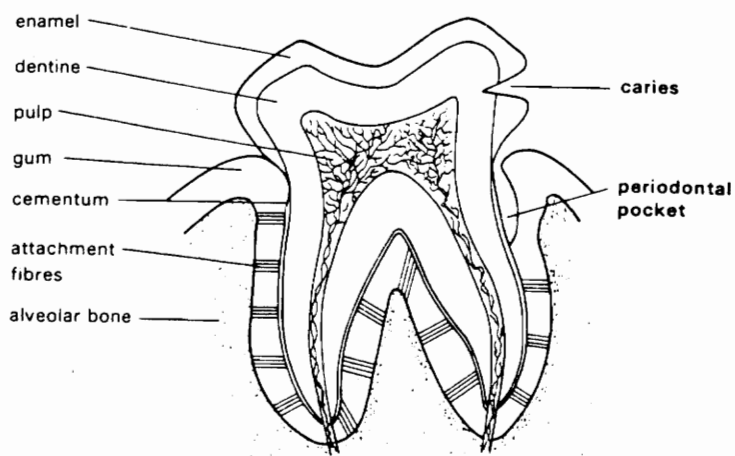


Figure 1: Tooth structure as described by Marsh [21].

[1]. Enamel has an average tensile strength of 9.8 MPa [1], a compressive strength of 241 MPa [1], and a modulus of elasticity of 48 GPa [19]. Dentin, on the other hand, is tougher and more flexible than enamel because of its increased organic and water content [1]. Vickers hardness values of dentin lie between 60 and 80 kg/mm² [1]. Dentin has a tensile strength of approximately 52 MPa [1], a compressive strength of 138 MPa [1], and a modulus of elasticity of 13.8 GPa [19].

1.3. Restorative materials used in dental applications:

Many synthetic resins can be used as restorative materials. Acrylic resin can be used for the replacement of lost tooth structure [22]. Adhesion to enamel, for example, is accomplished primarily by polymerization of methylmethacrylate and other acrylic monomers that have infiltrated pores of the treated enamel [22,23].

Acid treatments have been used to enhance adhesion between dental resins and enamel. However, acid etching alone has not improved the adhesion between dental resins and dentin [6,10,24]. Dentin bonding systems were introduced in combination with resin composites to improve adhesion [10].

Base (sealer) materials are also used in dental restoration processes [25,26]. The primary functions of a base material are to seal the dentinal tubules against bacterial attack and toxins, to prohibit the movement of tissue fluids in the tubules, and to protect the pulp from chemical irritation [25]. The two base materials that continue to be used are the calcium hydroxide and glass-ionomer materials [25]. These cements have been used under composites, amalgam, ceramic and metal restorations as well as polymeric restoration [17,25,26].

1.4. Factors affecting adhesion:

Before designing any *in vitro*, adhesion test of adhesive restorative materials it is necessary to address the factors affecting adhesion between hard dental tissues and restorative dental materials. These factors include the surface properties of enamel and

dentin such as wetting, etching, and hardening [1,7,9]. Other factors that should also be considered include teeth extraction, preparation and storage [5,7,27,28,29].

1.4.1. Surface wetting:

Good wetting is necessary to achieve a proper interfacial contact between the adhesive and its substrate [6,7]. Adhesion to dentin is frequently limited because most bonding materials do not wet entirely the solid surfaces. Poor surface wettability causes the formation of flaws at the interfaces which weakens adhesion [7]. The extent of wetting can be determined by using contact angle measurements [7,30,31,32]. From these measurements, the surface energy of the substrate can be calculated [7,32,33]. In order to complete add wetting, the surface free energy of the liquid adhesive has to be less than the surface free energy of the dentin [6].

1.4.1.1. Contact angle measurements:

The extent of wetting can be determined by measuring the contact angle [7,30,31,32]. The contact angle is defined to be the angle between the solid-liquid and liquid-vapor interfaces as illustrated in Figure 2. [32,33]. Young described the mechanism of wetting and spreading of a liquid on a solid as well as the relation of these characteristics to the equilibrium contact angle [30,34]. Young's equation can be written as

$$\gamma_{SV} - \gamma_{SL} = \gamma_{LV} \cos \theta + \pi_e \quad (1)$$

where γ_{SV} , γ_{SL} and γ_{LV} are the surface tensions at the solid-vapor, solid-liquid and liquid-vapor interface at equilibrium, respectively, and θ is the angle of contact between the solid and the liquid [30,32,34]. π_e is the spreading pressure. π_e is usually negligible when the contact angle is larger than 10° [34]. If $\theta = 0^\circ$, the solid is said to be *completely wetted*

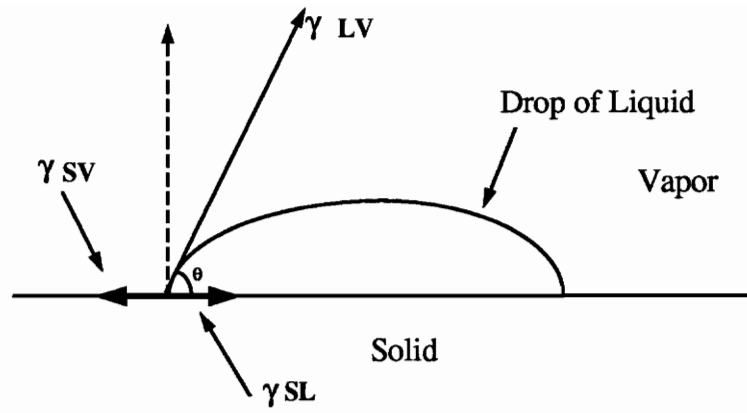


Figure 2: Idealized representation of wetting of a solid by a liquid [33].

by the liquid. If $\theta > 0^\circ$, some examiners describe the system as *partially wetted*. If $\theta > 90^\circ$, the system is described as *nonwetting* [33]. Adhesional wetting is another type of wetting to consider [32]. In adhesional wetting, a liquid which is not initially touching the solid substrate makes contact and attaches to it. Contrary to spreading wetting, the area of liquid-gas interface is reduced [32]. The work of adhesion is given by the Dupre equation:

$$W_a = \gamma_{sv} + \gamma_{lv} - \gamma_{sl} + \pi_e \quad (2)$$

where γ_{sv} , γ_{lv} and γ_{sl} are the surface tensions at the solid-vapor, liquid-vapor and solid-liquid interfaces, respectively [32]. By combining equation (2) with Young's equation (1), the Young-Dupre equation is obtained as

$$W_a = \gamma_{lv} (1 + \cos\theta) + \pi_e \quad (3)$$

If $\cos\theta = 1$, the work of adhesion is equal the work of cohesion. Therefore, the forces of attraction between liquid and solid are equal or higher than those between liquid and liquid when a zero contact angle is measured. A measurable contact angle is obtained when the liquid adheres to the solid less than it coheres to itself [32].

1.4.1.2. Determination of surface tension from contact angle measurements:

The surface tension of a solid can not be directly measured. Many indirect measuring methods have been proposed such as: the liquid homologue method (molecular weight dependent), the polymer melt method (temperature dependent), the equation of state method, the harmonic-mean method, the geometric mean method, and the critical surface tension method [34].

The geometric-mean method and the critical surface tension method are often used in dental research [1,7,30,31]. The geometric-mean method makes use of two liquids which are independently tested on the substrate [34]. Contact angles are measured for each liquid. Water being polar liquid and methylene iodide being a non-polar liquid are often suitable choices for testing [34]. The geometric-mean equation can be written as

$$\cos \theta = [2(\gamma_s^d)^{1/2} \cdot (\gamma_{lv}^d)^{1/2} / (\gamma_{lv})] - 1 \quad (4)$$

By combining equation (4) with Young's equation (1), using two liquids, the following equations are obtained:

$$(1 + \cos \theta_1) \gamma_{LV1} + \pi_e = 2[(\gamma_s^d \cdot \gamma_{LV1}^d)^{1/2} + (\gamma_s^p \cdot \gamma_{LV1}^p)^{1/2}] \quad (5)$$

$$(1 + \cos \theta_2) \gamma_{LV2} + \pi_e = 2[(\gamma_s^d \cdot \gamma_{LV2}^d)^{1/2} + (\gamma_s^p \cdot \gamma_{LV2}^p)^{1/2}] \quad (6)$$

where γ_{LV1} , γ_{LV2} , γ_{LV1}^d , γ_{LV2}^d , γ_{LV1}^p , γ_{LV2}^p are the surface tension components of liquid-vapor, liquid dispersive and liquid polar interactions of water (L_1) and methylene iodide (L_2), respectively. γ_s^d and γ_s^p are the dispersive and the polar components of the solid surface tension. Using the literature values of γ_L^p , γ_L^d , and γ_{LV} of methylene iodide and water in Table 1, the surface tension components of the solid can be determined [34]. The total surface tension of the solid, γ_r , is determined by adding its polar and dispersive components together:

$$\gamma_r = \gamma_s^d + \gamma_s^p \quad (7)$$

Busscher adapted this method using water and propanol to calculate the surface tension components of enamel. Fowkes calculated the dispersive components of human enamel, human dentin and whale dentin. He obtained values of 41.4 dyne/cm for enamel, 41.7 dyne/cm and 41 dyne/cm for human and whale dentin, respectively [1].

The critical surface tension method is widely found in dental research [1,7,31]. This concept which was developed by Zisman [34], is based on a linear relation which was found between $\cos \theta$ versus γ_{LV} for a series of various test liquids on a given solid [34]. The intercept of the line at $\cos \theta=1$ is the critical surface tension, γ_c . It is advantageous to use an adhesive with a surface tension slightly lower than the critical surface tension of the adherend [1].

1.4.2. Effects of etching:

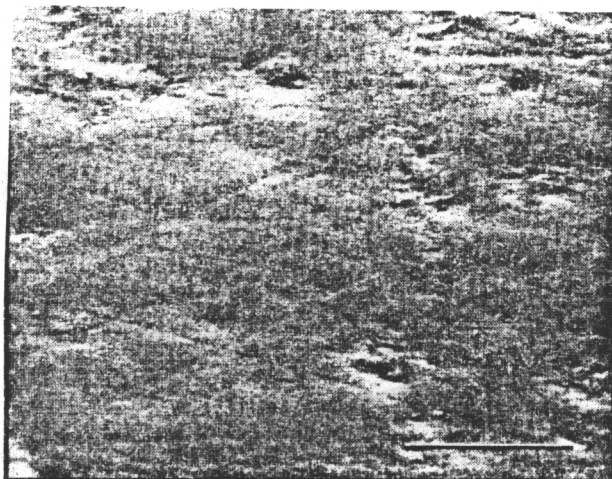
Chemical treatment of enamel and dentin surfaces has improved the bond strength between the tooth structure and dental restorative materials [1,2,3,7]. Phosphoric acid etchants have been widely used as an etchant for enamel. Phosphoric acid is non-toxic and

Table 1: Surface energy contributions for the two liquids at 20°C, used in the contact angle measurements [34].

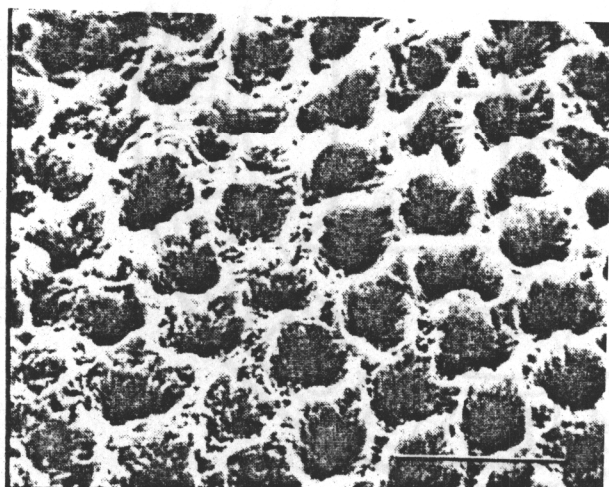
Liquids	γ_L^P (dyne/cm)	γ_L^D (dyne/cm)	γ_{LV} (dyne/cm)
Water	51	21.8	72.8
Methylene iodide	2.3	48.5	50.8

does not stain teeth like other acids do. In addition, it has gel-like properties by adding “fumed” silica. This acid is thought to increase enamel adhesion to acrylic materials by removing surface debris on enamel and making the surface more wettable [1,3]. Retief studied the effect of orthophosphoric acid etching on enamel [2]. He suggested that etching alters the surface morphology of the enamel and creates microporosity as shown in Figure 3 [2]. Termini treated enamel surfaces with different acids and chemical agents prior to adhesion testing [1]. He indicated that better wetting is obtained by treating enamel with an acid containing carboxylic acid groups as shown in Figure 4 [1]. The highest adhesion was obtained when enamel is treated with 5% tetrahydrofuran-2,3,4,5-tetracarboxylic acid. Termini recommended that a pretreatment with water soluble acid enhances adhesion [1].

The success of acid etching of enamel led to the commercial use of phosphoric acid on dentin. Most of the results show that phosphoric acid does not improve dentin adhesion [3]. Lee etched dentin surface samples for two and five minutes, respectively, using 50% phosphoric acid solution, and examined them using electron microscopy [35]. The SEM micrographs of the dentin surface are shown in Figure 5 [35]. He concluded that the two minute treatment roughened the dentin surface by dissolving the peritubular dentin. Longer etching times allowed the surface to be smoother which did not favor adhesion [35]. Okamoto studied the effects of phosphoric and hydrochloric acid followed by tannic acid treatment on dentin [36]. He proposed that phosphoric acid induces a conformational change in dentin collagen similar to that observed with 0.39M HCl which has a similar pH value. By contrast, when phosphoric acid-treated dentin was followed by tannic acid treatment for 2 hours, dentin collagen recovered its normal resistance to denaturation. Okamoto suggested that tannic acid may work as a dentin conditioner in composite resin therapy [36]. Uy and Chang used 0.1 N citric acid solution as an etchant. They indicated that the dentin surface became more wettable [1]. Baier studied the effects of citric acid and phosphoric acid on dentin by measuring its critical surface tension. He



(a)



(b)

Figure 3: (a) Unetched enamel surface (X 950); (b) etched with 85% orthophosphoric acid as described by Retief [2].

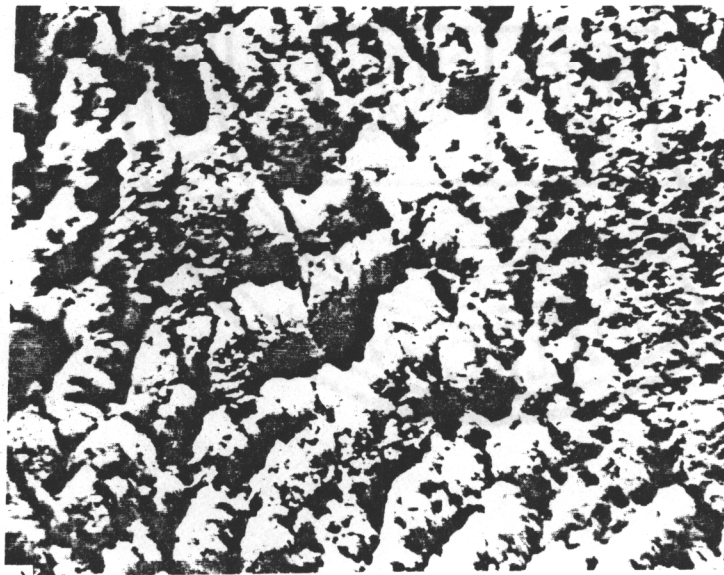
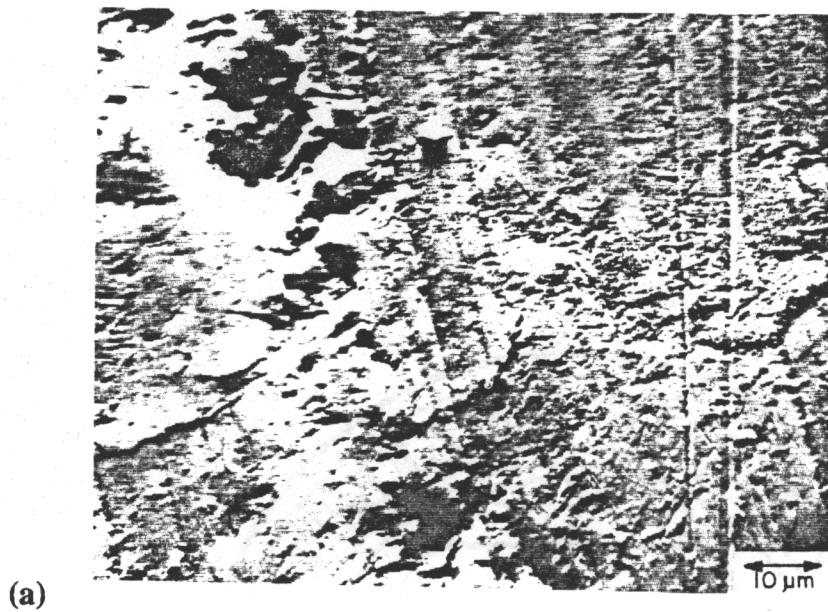
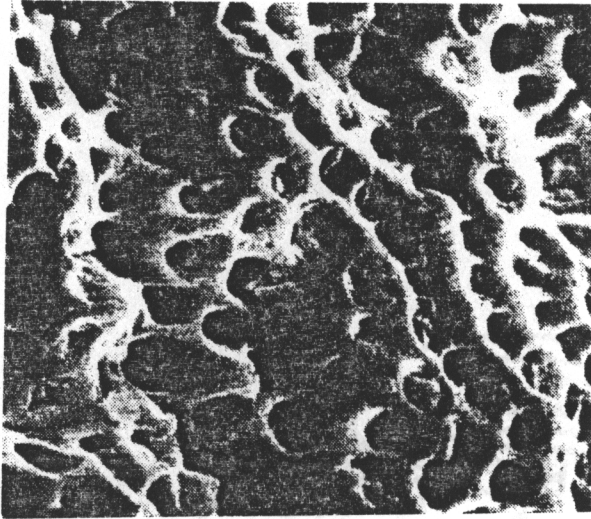
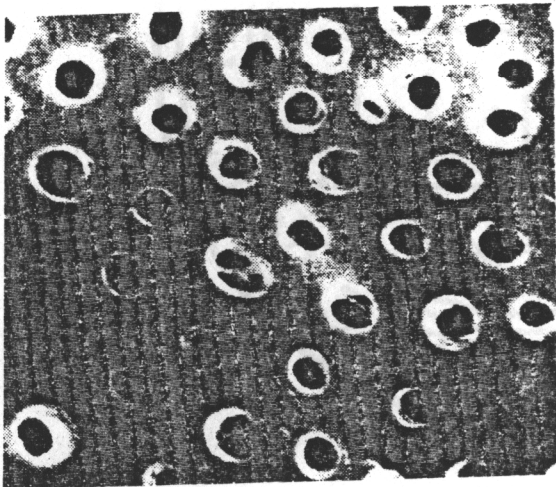


Figure 4: (a) Unetched enamel surface; (b) etched with 5% of aqueous tetrahydrofuran-2,3,4,5- tetracarboxylic acid for 30 sec as described by Termini [1].



(a)



(b)

Figure 5 : (a) Dentin surface etched for two minutes with 50% phosphoric acid (X1800);
(b) dentin surface etched for five minutes with 50 % phosphoric acid (X1800). [35].

obtained average contact angles values of 41° , 38° for unetched dentin specimens using water and methylene iodide respectively. While, average of 39° and 36° was measured for citric acid etched dentin specimens, and an average of 41° and 33° for phosphoric acid etched ones, using water and methylene iodide, respectively [7]. He commented that the two acid etchants enhance adhesion by different mechanisms. Citric acid changes the polar-polar interactions of the liquid with the solid and phosphoric acid induces better wetting of even non-polar liquids [7].

1.4.3. Effects of aging of enamel and dentin:

Aging is generally caused by trauma, diseases, fluoridation, dental caries, or thermal dental treatment such as laser treatment or drilling procedures [13,37]. Thermal aging has been thought to increase the brittleness of enamel [13]. Similarly, dentin shows remarkable thermal age-related changes due to its water and organic components [13]. Generally, heating results in dentin dehydration which lowers its flexibility [13]. Høegh conducted a study on the mass loss of human enamel and dentin using a thermogravimetric technique [38]. He exposed one gram of enamel and dentin to thermal excursion at a rate of $150^{\circ}\text{C}/\text{hour}$ under a CO_2 purge. Mass losses of 1.7 % for enamel and 9.7% for dentin around 100°C were observed due to water evaporation. At roughly 300°C , losses of 3.5% for enamel and 21.3% for dentin are thought to result from the loss of protein mass and eventually water associated with inorganic hydrates [38]. Furthermore, Van Der Graaf studied the changes in dentin dimensions upon thermal exposure [15]. He observed that dentin collagen fibers shrank upon warming at 60°C . Drying at 100°C induced some permanent shrinkage and weight loss of collagen fibers [15]. The dried collagen fibers were also thought to become more disoriented [19].

1.4.4. Enamel and dentin hardness measurements:

The hardness of a material is evaluated by pressing an indenter into its surface and measuring the size of the impression. The larger the impression, the softer the material

[39]. Hardness may also be described as the resistance of one body to another body which is attempting to occupy the same space at the same time. Hardness magnitude is related to the method used [40].

Several hardness tests have been used to evaluate hardness on enamel and dentin. These include Brinell, Rockwell, Monotron, Scleroscope, and Vickers- Knoop hardness tests [40,41]. The Vickers hardness test is used for this study. Vickers hardness is determined by the following equation [42]:

$$H_v = 1854.4 * F / [(d_1 + d_2) / 2]^2 \quad (8)$$

where F is the load in gf (gram-force), d_1 and d_2 are the diagonal length of indentation in μm . Knoop Hardness is determined using the following equation [42]:

$$H_k = (F / 7.028 \cdot d^2) \cdot 10^5 \quad (9)$$

where F is the load in gf, d is the diagonal length of indentation in μm .

1.4.4.1. Effects of aging on hardness:

Caldwell used Knoop hardness tests to determine the hardness of enamel as a function of aging. He obtained an average enamel hardness of 367 kg/mm^2 [41]. This decreased to 262 kg/mm^2 upon 10.3 hours of aging at ambient temperature. Upon grinding, the average hardness of enamel was 325 kg/mm^2 . This decreased to 155 kg/mm^2 upon 9.6 hours of aging. He indicated that the enamel surface was “softened” upon aging and grinding [41]. Totah studied the effect of drying on dentin hardness using the Beirbaum scale [43]. He suggested that dentin hardness increased upon drying at 105°C for 44 hours [43]. Investigators who measured the resistance to penetration found that this method was unsuitable for brittle teeth [40].

1.4.4.2. Effects of etching on hardness:

Panighi and G'Snell studied the change in hardness on enamel and dentin when treated with acids [9]. Vickers hardness decreased from 378 to 205 Hv for enamel and 98 to 37 Hv for dentin when they were etched with 37 wt % phosphoric acid for 60 sec and

50 wt % citric acid for 30 sec, respectively. This variation is due to a decrease in calcium concentration when hard tooth tissue surfaces are exposed to etching. They further developed an empirical relationship between hardness and calcium concentration [9]:

$$H_v = K * [Ca] \quad (10)$$

where K is equal to 9.7 for K_{enamel} and 2.65 for the K_{dentin} , [Ca] is expressed in unit percent. From this relationship, they found another correlation between the shear bond strength of enamel and dentin to methyl methacrylate resin, and their respective hardness values [9]:

$$\tau_R = (A * H_v) + B \quad (11)$$

where τ_R is the shear strength expressed in MPa, $A = 0.07$ MPa and $B = -2.8$ MPa, and H_v is the Vickers hardness number. Moon, et al. showed that a significant loss of surface hardness can occur in 15 seconds using phosphoric and citric acids as shown in Table 2 [8]. Moon et al. indicated that the decreased dentin hardness was due to surface demineralization [8]. Chiba et al. suggested that the surface hardness decreases upon etching and this reflects a decrease in the bond strength [10].

1.4.5. Effects of extraction and storage:

Bond strength may also be affected by tissue storage and preparation. Many authors reported that human dentin bond strength is influenced by the time between the extraction of the teeth and the preparation of the specimens [5,27,28,29]. Causton et al. reported that 250 minutes after extraction there is a 50% reduction in the dentin bond strength when that aged surface was bonded to polycarboxylate cement [27]. Another rise in dentin bond strength was observed after 25 days. Then, a rapid fall of dentin strength occurred between 25 and 30 days to a plateau at 45% of the original strength. This shows dentin bond quality is related to its freshness. Beech related this behavior to dentinal fluid

Table 2: Average Knoop hardness of dentin as function of etching time calculated by Moon [8].

Etching time	Average hardness (Hk) using phosphoric acid kg/mm ²	Average hardness (Hk) using citric acid kg/mm ²
0 Second	64.8	64.6
15 Seconds	37.1	45.1
30 Seconds	18.6	19.6

losses[27].

Goodis et al. studied the effects of storage in solution on human dentin shear bond strength over a period of 6-8 months [28]. Teeth were stored in distilled water, and distilled water with thymol or phosphate-buffered saline. Of all these liquids studied, saline solution lowered the measured dentin shear bond strength when these structures were exposed to a bonding agent and fitted with a composite resin [28].

1.5. Light cured glass-ionomer cements (Vitrebond™):

1.5.1. Introduction:

The clinical use of the glass-ionomer cements was primarily recommended by Wilson and Mc Lean [16]. Vitrebond™, a light cured-glass ionomer, manufactured by 3M Dental products, was the first product in the market [16]. Other products were also introduced in the market such as Kerr-XR™ Ionomer and ESPE™ Photo Applicap™ [16]. The light-cured glass-ionomer cements are used for lining/base materials under composites, amalgam, ceramic, and metal restorations [6,16,17]. Glass-ionomer cements are based on the hardening reaction between a powdered solid and polyacrylic acid solution [6,16,17,18,44]. These types of cements possess attractive properties in clinical applications such as good adhesion to tooth structure, hydrophilicity, rapid setting when they are cured with a visibly light. They also possess good aesthetics properties [16]. In addition, their ability to release fluoride appears to reduce carries attack [45]. Light cured glass-ionomer cements are thought to cause pulpal irritation, and erode dentin and enamel due to a low pH [16,46].

1.5.2. Composition:

The powder component of Vitrebond™ contains a fluoroalumino silicate glass with a photoactive initiator [6,16,17,47,48]. The liquid component is a co-polymer of acrylic/itaconic acid. The structure of this copolymer is shown in Figure 6 [6]. Water, and

hydroxyethyl methacrylate HEMA are included in the liquid [16,17,47,48]. According to the manufacturer's published specifications, the previously listed components comprise 93% of the Vitrebond liquid [47]. The remaining 7% is most probably a tetrafunctional monomer such as ethylene glycol dimethacrylate (EGDMA) which provides pendant vinyl groups for the photo initiated crosslinking. This is not specified due to the proprietary nature of the formulation. There are two main reasons to include itaconic acid in the formulation [6,16]. The primary reason is the relatively high acidity of the carboxylic acid group which provides a greater degree of reactivity in the liquid. The second reason is that itaconic acid in the polymer chain decreases the viscosity of the co-polymer [6,16].

1.5.3. Chemical reaction :

The reaction of the glass with the liquid, according to Mitra, is described by the following steps as shown in Figure 7 [16,48]. When the powder and liquid components are mixed, the ionization of polycarboxylic acid in water takes place in the presence of aluminosilicate glass. The carboxylate groups in the polymer chain form negative charges and protons. The protons attack the glass, liberating positive ions as illustrated in step 2. This is essentially an acid-base reaction. The normal setting reaction continues with the formation of a calcium aluminum polyacrylate gel matrix. By exposing the system to light, cross-linking of the pendant methacrylate groups bonded to the polycarboxylate chains occurs and gives a strong stable structure due to the covalent cross-links in addition to the ionic cross-links [16,48]. Infrared spectroscopic technique determines which functional group absorbances are present or absent from the sample [49,50]. Wilson suggested that dental cements can be observed conveniently by the technique of attenuated total reflectance (ATR) [49]. One of the major advantages of the internal-reflectance spectroscopy is that the absorption spectra are obtainable for difficult samples to deal with. These include samples with limited solubility, pastes, adhesives and powders [50].

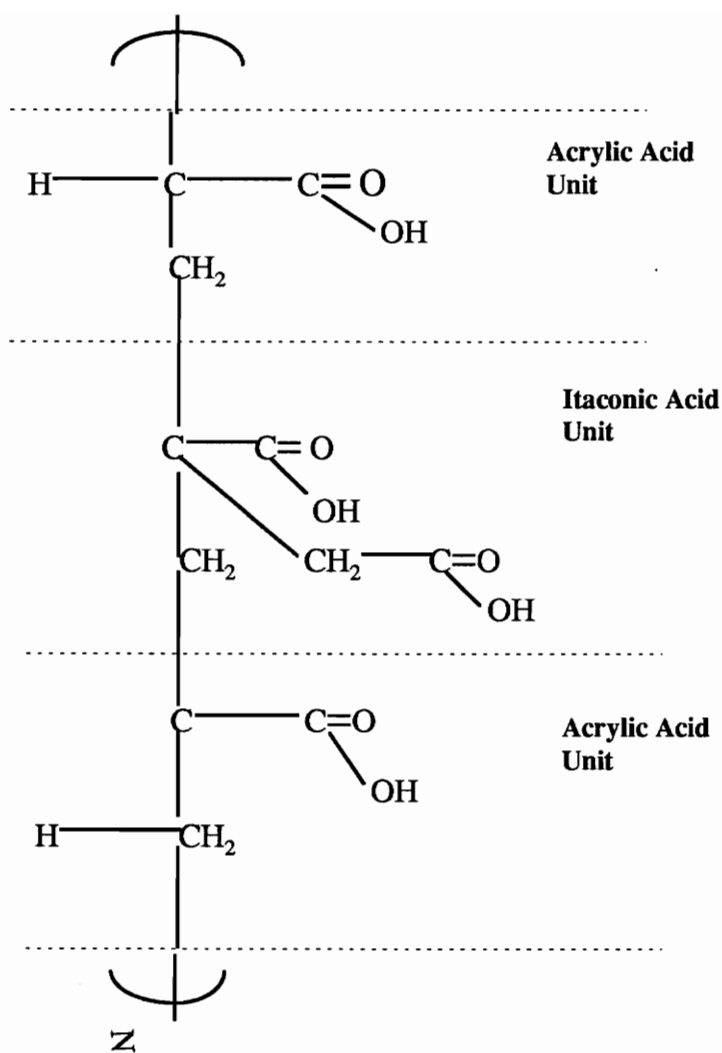
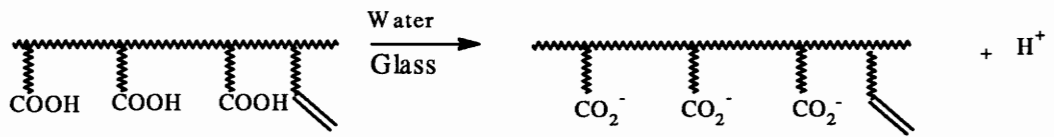
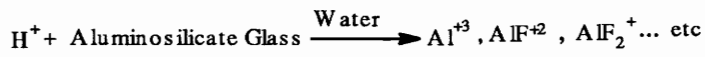


Figure 6: Structure of poly(alkenoic acid) as suggested By Ruyter [6].

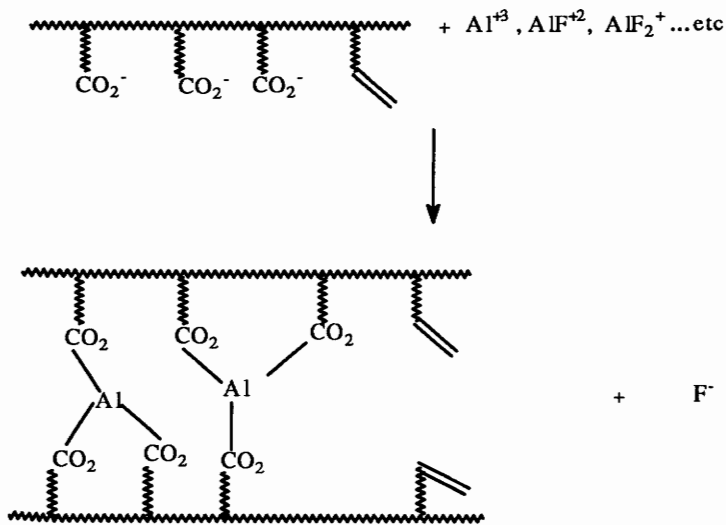
Step 1



Step 2



Step 3



Step 4

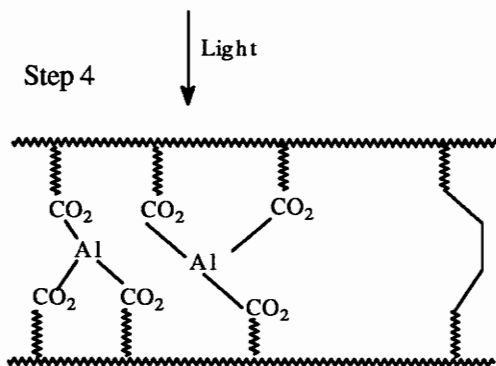


Figure 7: Chemical reaction Of Vitrebond™ as described By Mitra [48].

This technique is also useful to study the ionomer cement gel formed by the ion-binding reaction between alkali and alkaline earth metal ions and the carboxylic acid groups of the poly(alkenoic) acids [49]. In this technique, the sample is pressed against the flat surface of a crystal. The infrared beam passes through the crystal and is reflected internally from the crystalline plane face [49]. Wilson listed the ATR vibrational absorbances spectrum of a setting glass-ionomer cement as shown in Table 3 [49]. The cement paste spectrum may also be analyzed using FTIR technique.

1.5.4. Physical and mechanical properties:

The physical properties of the fluoroalumino silicate glass and the liquid acid are described in Table 4 [47]. The powder is white in color and is odorless. The liquid is slightly yellow and has a slight sweet odor [47]. The recommended powder to liquid ratio of Vitrebond is between 1.0 to 1.4 by weight [17]. The mean compressive strength of the Vitrebond paste, when made according to Hegarty et.al., is 52.03 (\pm 30.08) MPa and 56.25 (\pm 17.49) MPa after 1 and 24 hours of setting, respectively [51]. However, by allowing Vitrebond to chemically set in a photographic dark room, the mean compressive strength decreases to 5.1 (\pm 0.38) MPa and 8.69 (\pm 2.39) MPa after 1 and 24 hours of setting, respectively [51]. Besides Vitrebond, other glass-ionomer cements are used in clinical practice such as ASPA, and Chem Fill II where the poly(alkenoic) acid is mixed with the glass and vacuum dried. Water is added to the powder [52]. According to Crisp et al., an excess in the powder fraction in the ASPA cement, leads to a lower working time and higher stiffness, compressive strength and hardness in the paste which provide greater resistance to moisture [53]. By increasing the powder fraction in the paste, the rate of the reaction is accelerated because there is a greater specific area of the powder per unit volume of paste [53]. However by increasing the acid concentration in the paste, the reaction is retarded [54]. As with all cements, the exact powder to liquid ratio and proper

Table 3: Stretching mode and frequencies occurring in the IR spectrum (ATR) of a setting glass-ionomer cement according to Wilson [49].

Species	Vibrational Mode	Frequency (cm ⁻¹)
COO ⁻ (Al)	Asym. stretch	1600-1530
	Sym. stretch	1390
COO ⁻ (Ca)	Asym. stretch	1533
	Sym. stretch	1404
COO ⁻ (Na)	Asym. stretch	1540
	Sym. stretch	1406
Silica Gel	Si-O Stretch	1050

Table 4: Physical properties of the Vitrebond™ liquid and powder according to 3M [47].

Physical Properties	Vitrebond Liquid	Vitrebond Solid
Boiling Point	N/D	N/A
Solubility in Water	Complete	nil
SP.Gravity	1.2 gm/ml	3.2 mg /ml
Percent Volatile	35% by wt	N/A
Volatile Organics	N/D	N/A
pH	2.5-3.0	N/A
Viscosity	300. CPS	N/A
Melting Point	N/D	N/D

mixing are important to obtain strong adhesion [18,52,55]. Major problems encountered improper mixing of powder/liquid ratio. This includes the lack of understanding in handling the paste during mixing, especially the failure to incorporate the exact powder ratio in the mix [55,56]. Hand mixed glass-ionomer cement is another problem affecting the mechanical properties of the cement. According many authors, an inexperienced operator obtained lower cement paste strength values than did a skilled operator [57,58].

1.6. Theories of adhesion:

There are six possible adhesion mechanisms. These include adsorption and wetting, interdiffusion, electrostatic attraction, chemical bonding and mechanical adhesion. These mechanisms are illustrated in Figure 8 [59]. The first mechanism was reviewed in section 1.4.1. The interdiffusion mechanism occurs when the molecules entangle and interact across the interface. These kind of interactions include Van der Waals, dipolar or electrostatic forces, but not necessarily chemical or mechanical interactions [33]. The electrostatic adhesion mechanism occurs between surfaces when one surface possesses an excess positive charge and the other possesses negative charge. The bond strength of the interface will be related to the charge density. Electrostatic attraction may also be involved in chemical bonding. Chemical adhesion involves the formation of bonds across the interface such as covalent, electrostatic or metallic bonds [4,6]. Mechanical adhesion involves the mechanical interlocking and interpretation of the surface features of one adherend [33,59].

Bonding to tooth structure is achieved by an initial wetting of a polymeric restorative material to the tooth followed by chemical and mechanical bonding [4,7,6]. Chemical bonding is attained between the organic and inorganic components of the tooth and the restorative material. Mechanical interlocking depends on the available area, and the surface roughness, and will likely be affected by the level of etching at the surface [33,59].

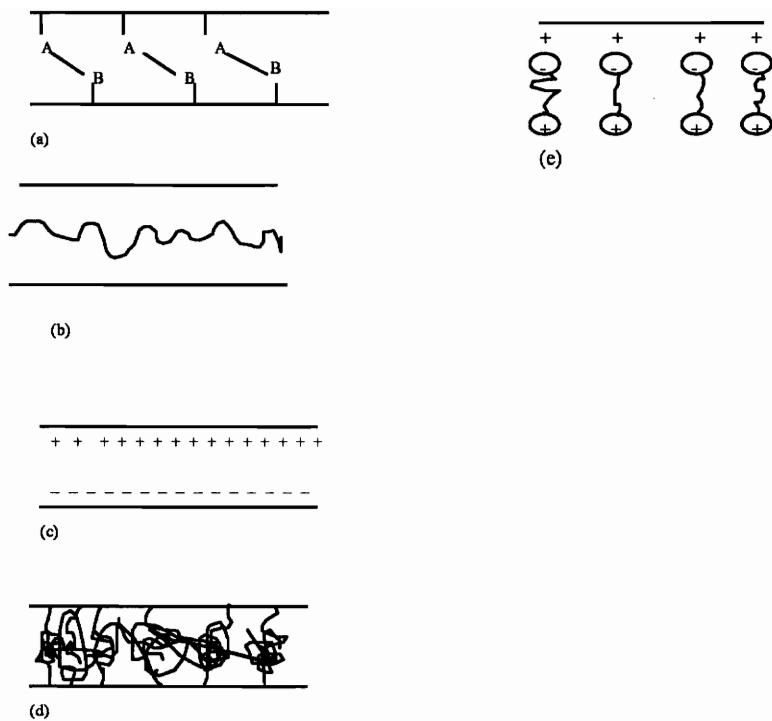


Figure 8 : Different types of bond formation as described by Hull : (a) Chemical bonding between two groups; (b) mechanical interlocking; (c) electrostatic attraction; (d) molecular entanglement pursuing interdiffusion; (e) ionic bonding [59].

1.6.1. Chemical adhesion:

1.6.1.1. Types of chemical adhesion:

Primary valence forces and secondary valence forces are the two principal types of chemical adhesion. The primary valence bonds are the covalent and coordinate. Both of them are electron pair bonds. These types of bonds are the strongest and the most stable. Ionic bonds may also be included in this category because they also form strong bonds. The secondary valence bonds, known also as intermolecular bonds, are the Van Der Waals bonds and the hydrogen bonds [6].

1.6.1.2. Application of chemical adhesion to enamel and dentin:

Chemical adhesion is associated with chemical reaction across the interface. Chemical adhesion can be enhanced by coupling agents and grafting techniques to change surface reactivity. Adhesion based on ionic polymers is also a chemical reaction which may occur across the natural tissue interface [6,60].

1.6.1.3. Adhesion based on ionic polymers:

There are two types of dental materials that are grouped as polyelectrolytes. These are zinc carboxylate cements and glass-ionomers or glass-poly(alkenoates). The glass-poly(alkenoates) are based on poly(acrylic acid) and copolymers of acrylic and maleic acid or acrylic acid-itaconic acid [6]. VitrebondTM adhesive, for example, is a combination of acrylic acid and acrylic acid-itaconic acid [47]. The mechanism of adhesion of poly-(alkenoic acid) base materials to apatite such as enamel is attained by ionic bonding with calcium ions acting as bridges[6]. In addition to apatite, dentin has an organic phase. The organic phase is mainly collagen with free carboxylic acid and amino

groups. The hydrogen from the amino group of the collagen can form a hydrogen bond to the carboxyl groups of the poly(alkenoic acid) [6]. Ions diffusing from the glass-ionomer or dentin apatite allow cation bridges to be formed between the carboxyl group of the poly(alkenoic acid) and the collagen as shown in Figure 9 [6]. However, during etching, calcium ions are separated from the dentin apatite and the possibility of bonding between the carboxylic acid groups of poly(alkenoic acid) and the acid groups of both apatite and collagen is decreased [6].

1.6.2. Mechanical testing:

1.6.2.1. Bond strength test methods:

The bond strength test methods employed on dentin are comprised of tensile and shear tests as illustrated in Figure 10 [5]. These tests have their advantages and their drawbacks [5,11,12]. The measured bond strength from both tensile and shear tests, for example, will depend upon flaws or defects in the zone of increased stress at the bond edge [11,61]. However, *in vivo* tests are complex in nature, so neither tensile nor shear bond strength tests effectively simulate the interoral forces [5].

Bending tests for measuring cement-dentin bond have been used by researchers in order to more effectively control the stress state [11,12]. Torsional testing is another technique that can be used to measure the bond strength of the adhesive to enamel and dentin. The geometry of the test is illustrated in Figure 11. The torsional shear strength equation is derived in appendix (A).

1.6.2.2. Application of bond strength tests of glass-ionomer to untreated and acid treated teeth:

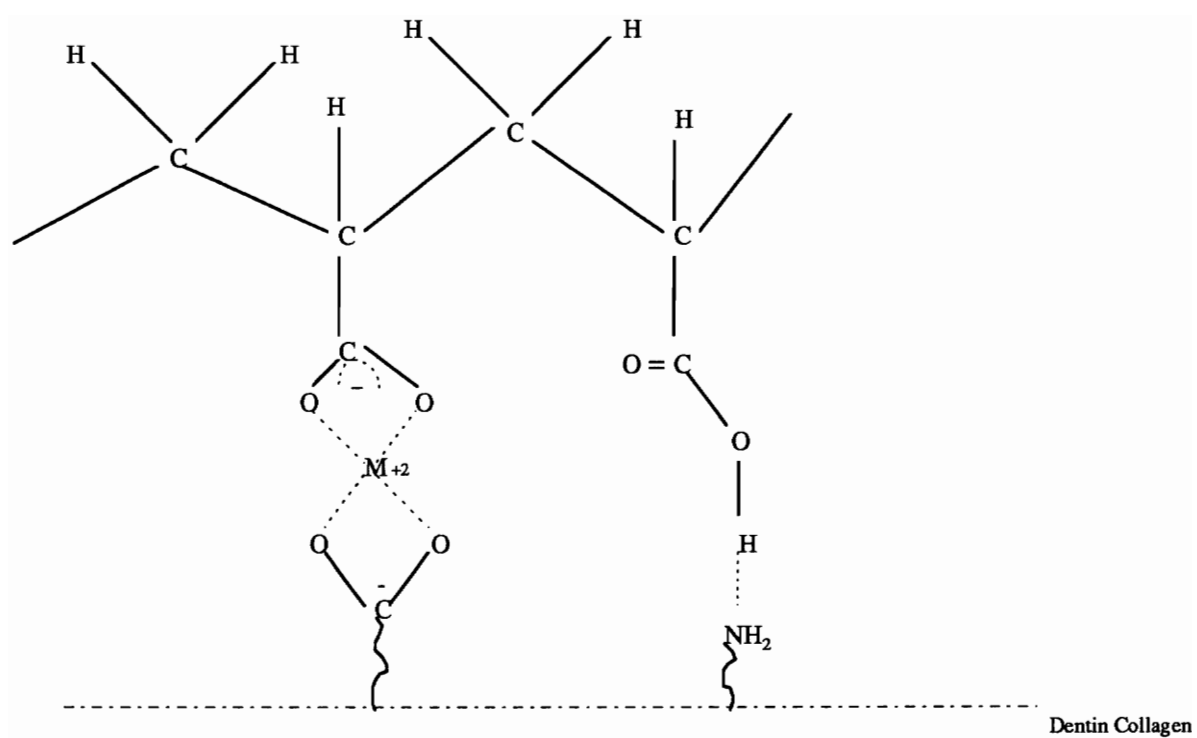


Figure 9: Mechanism of chemical adhesion of poly(alkenoic acid) to dentin collagen [6].

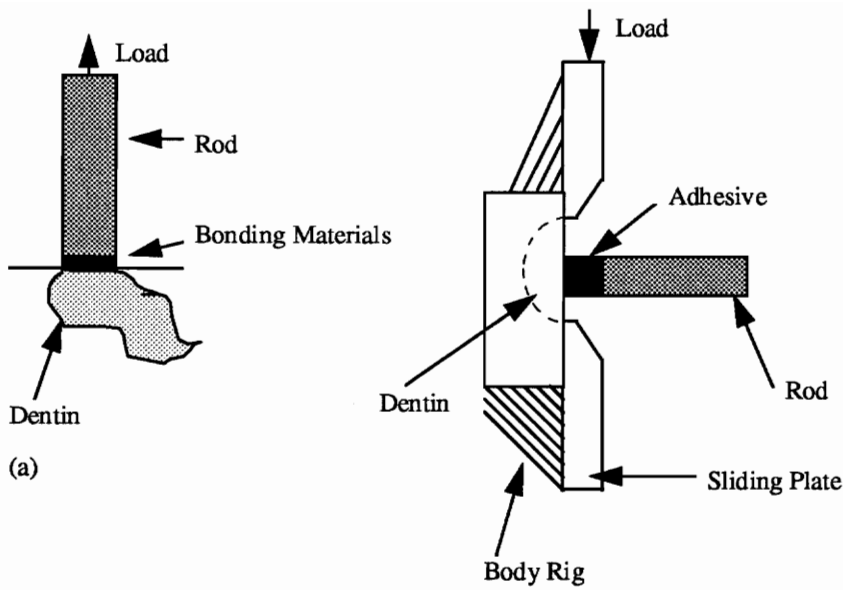


Figure 10: Bond strength test methods as suggested by Watanabe: (a) Illustration of cross-sectional view for tensile bond test; (b) representation of cross-sectional view for shear strength test [5].

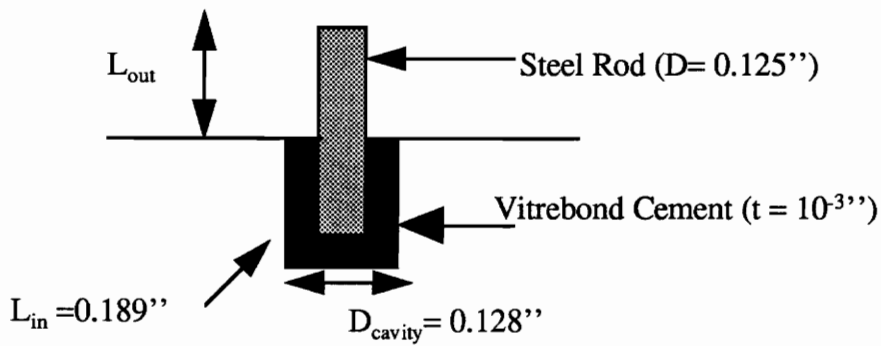


Figure 11: Schematic representation of the torsional bond test method.

Many authors have studied the bond strength of a glass-ionomer cement on both enamel and dentin using shear and tensile techniques [1,16,48,61,62,63,64]. Wilson et al. performed tensile tests to study the mechanisms of adhesion of the glass-ionomer cement (ASPA) on both enamel and dentin [62]. The data obtained for the tensile bond strength for untreated and treated samples with different etchants are shown in Table 5 [62]. They concluded that high molecular weight conditioners such as tannic acid, interacted with the substrates without forming soluble complexes. They showed that tannic acid treatment enhanced adhesion [62]. Smith and others suggested that tensile tests of bond strength of glass- ionomer cements to dentin show that the average tensile strength was much above 5 to 6 MPa [16]. When the dentin was etched with phosphoric acid, the bond strength values were remained as conflicting data [16].

Evje et al. performed a bending test on cylindrical cement/ dentin/composite sandwich glued to stainless steel [11]. The observed bond strength values of untreated dentin were 2 to 4 times greater than the values determined in traditional tensile bond tests. However, by treating the dentin with tannic acid prior to their test, they found that microleakage effects at the interface created by the acid prevented the increase adhesion of glass-ionomer cement to dentin [11].

1.6.2.3. Application of bond strength tests on thermally aged teeth:

Maldonado evaluated the tensile bond strength of glass-ionomer cements (ASPA) on enamel and dentin treated with tannic acid and thermally cycled in a water bath at 45 °C for 30 sec. An average value of 2.48 MPa was obtained for glass-ionomer bonded to enamel. The average value of 1.62 MPa and 0.9 MPa were obtained for uncycled and thermally cycled interfaces, respectively [63]. He proposed that the bond strength of glass ionomer cement on enamel was stronger than dentin. Thermal cycling did not have a major effect on the glass ionomer-enamel bond, but significantly reduced the bond strength of the cement to dentin [63]. Another high molecular weight conditioner,

Table 5: Bond strength of a glass-ionomer cement to enamel and dentin at different surface conditions [62].

Teeth Surface Conditions	Tensile bond strength of cement to enamel (MPa)	Tensile bond strength of cement to dentin (MPa)
Untreated	3.18	3.13
Etched with tannic acid (25%), for 60 Sec	7.02	6.32
Etched with citric acid (50%) for 30 Sec	5.57	3.75

poly(acrylic acid), was used by Barakat et al. to evaluate its effects on the *in vitro* tensile bond strength of glass ionomer base cements (GBC) to human dentin stored in water for 24 hours at 37 °C prior to adhesion testing [64]. The bond strength data obtained for the untreated dentin specimens were 1.2 MPa while the etched ones with 10 % and 25 % of poly(acrylic acid) were respectively 2.57 MPa and 2.22 MPa [64]. Jameson and his colleagues investigated the effects of hydration, dehydration and rehydration on dentin specimens prior to adhesion testing using tensile and three point bending tests [14]. They demonstrated that dehydrated dentin specimens exhibited greater elastic energy, a complete absence of plastic energy and required less energy to induce fracture than hydrated and rehydrated dentin. They observed that dehydration in the bulk of dentin induced a brittle behavior [14].

1.6.3. Adhesive failure:

An adhesive joint can fail in three modes. The first failure mode occurs at the adhesive-adherend interface and is known as adhesive failure. The second failure mode occurs within the adhesive layer and is known as cohesive failure. The third failure mode occurs within the adherend and is known as cohesive failure. These types of failures are illustrated in Figure 12 [33]. The first case is the result of poor adhesion. The other two cases are related to the weakness in the adhesive or the adherent. In a joint, a combination of the three failure modes may also occur. It has been proposed that a bond failure in a “proper” adhesive joint never occurs at the interface. Failure will occur in a weak boundary layer close to the interface, or within the weaker of the two bonded phases [33].

1.6.3.1. Adhesive failure in dentistry:

Most of the adhesive joints prepared for dental purposes fail adhesively [61]. Adhesion to enamel and dentin is thought to be dependent on their surface morphology. It

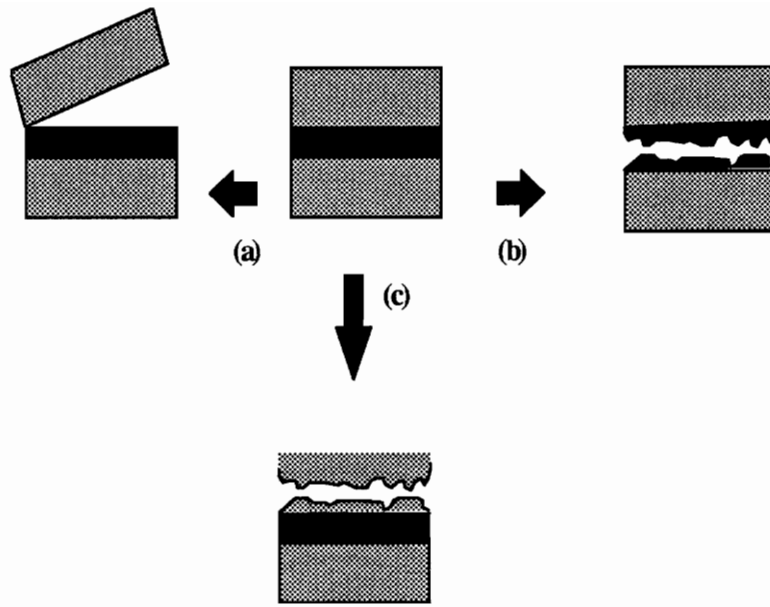


Figure 12: Three locations of adhesive failure: (a) Adhesive failure at the interface; (b) cohesive failure in the adhesive; (c) cohesive failure in the adherend [33].

may also depend upon the chemical variations which occur on the surface and the bulk of the dental hard tissues [61].

1.6.3.2. Failure of the glass-ionomer cements:

From SEM observations, Smith showed that failure at the etched dentin interface with the glass-ionomer indicated an adhesive failure including evidence of penetration of the cement into the tubules and cohesive failure in the cement. According to Smith, this behavior is related to bonding micromechanical interlocking to the etched surface where the cement penetrates into the tubules, and chemical interactions [16]. Charlton also investigated the locus of failure using a light cured glass ionomer cement of Fuji II TM and Vari GlassTM on both untreated and treated dentin with 10% of polyacrylic acid loaded in shear [65]. He suggested that the majority of the failures were mixed, indicating a combination of adhesive failure which occurred between the dentin and cement, or cohesive failure occurring within the cement. None of the cohesive failures occurred completely within the dentin [65].

1.7. Summary:

It is necessary to address the factors affecting bonding to dentin prior to an adhesion test. Being a natural and heterogeneous tissue, dentin quality varies after extraction, and storage [1,5,27,28,29]. According to many researchers, the extent of dentin wetting influences adhesion [1,6,7]. It has been suggested that acid treatment may improve dentin bonding which depends on the acid concentration, and its exposure time [1,35]. Acid etching is also thought to decrease the surface hardness upon etching and reflects a decrease in adhesion [8,9,10]. Dentin shows remarkable thermal age related changes because of its water content and organic components [13,15,19,38]. Thermal aging induces dehydration of dentin and can lead to crosslinking of collagen [13,15]. Bonding to tooth structure is achieved first by initial wetting of a polymeric restorative material to it, followed by chemical bonding and mechanical interlocking [4,7,6]. Most of

the bond strength test methods employed on dentin are comprised of tensile and shear tests [1,16,48,61,62,63,64]. Both tests have their advantages and drawbacks [5,11,12]. Inappropriate mixing strongly affects the mechanical and chemical properties of the cement paste. From the SEM observations, most of the adhesive joints for dental purposes are believed to fail adhesively [61].

1.8. Thesis organization:

The present background reviewed important concepts and components to conduct the experimental procedures which will be used in this study.

- The extent of wetting for untreated, etched and thermal aging dentin specimens will be determined from the contact angle measurements using the two liquid method.
- The hardness measurements of untreated, etched and thermally aged and rehydrated dentin specimens will be determined using a Vickers probe.
- The bond strength of unground and ground teeth specimens exposed to etching thermal aging and different mixing ratios will be determined using a torsional testing.
- The mechanism of adhesion failure will be characterized using the environmental scanning electron microscope (ESEM).
- The properties of the glass-ionomer cement will be determined using the two liquid method, and the infrared spectroscopy. The thermal properties of the cement paste will be studied using the thermogravimetric analysis (TGA). While the mechanical properties of the cements will be estimated using a Vickers hardness testing.

2. Experimental Procedures

2.1. Experimental approach:

The experimental work was conducted using three approaches: the first approach was to prepare dentin specimens where the surface can be tested. The second approach was to prepare specimens where adhesion can be tested. The final one was to mix the glass-ionomer cement and to study its properties.

2.2. Dentin sample preparation:

Extracted anterior bovine teeth were collected from the Virginia Maryland Regional College of Veterinary Medicine and kept frozen until needed. Each dentin specimen was prepared by diamond wheel saw sectioning using two parallel cuts as shown in Figure 13. The first cut removed the roots and the second cut removed the occlusal enamel. Sixteen specimens were prepared in this way. Specimens were then transferred to a mounting press. A thermoset casting resin, PSI Testing System 203, was added to each dentin specimen and pressed at 72.5 MPa for ten minutes at high temperature. All specimens were mechanically polished using a set of 60-600 grit sand papers.

Two samples were left untreated, two were etched with 20% w/w tannic acid for 60 seconds, and two were treated with 8.5 % w/w sulfuric acid for 60 seconds to mimic clinical processing. Ten specimens were exposed to a temperature of 65⁰C for varying lengths of time (1,2,3,24,48 hours) to mimic aging of the dentin.

2.3. Dentin sample surface characterization:

2.3.1. Contact angle measurements:

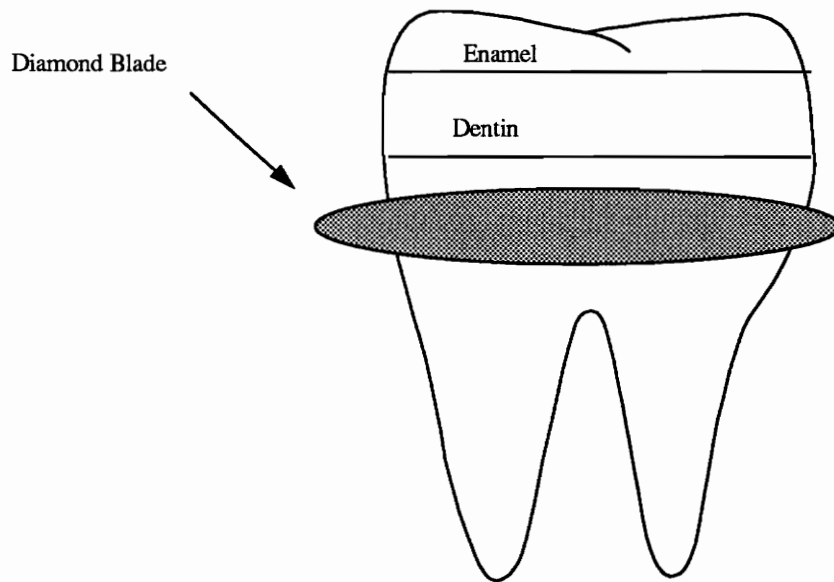


Figure 13: Dentin surface preparation.

The polar γ_s^P and dispersive γ_s^D components of the surface tension of initial, etched, and aged dentin mounted specimens were determined using the two liquid method. This method has been used to estimate the surface tension of solids [34]. The surface tension requires the measurement of contact angles using water and methylene iodide drops with respect to the dental surface. As shown in Figure 14, the contact angle of a 5 μ l drop for each liquid was measured using a 25 μ l syringe and observed under Rame-Hart Goniometer attached to a screen where the contact angle of each liquid on a solid was measured after 30 seconds. Eight measurements were traced for each sample. The mean and standard deviations were recorded. Using the literature values of γ_L^P , γ_L^D , and γ_{LV} of methylene iodide and water, the surface tension was calculated for each condition.

2.3.2. Hardness testing:

Hardness tests were conducted using a Leco DM 400 Digital Measuring Microscope, using a Vickers probe. Each initial, etched, and aged dentin specimen was placed and focused under the microscope. The two measuring lines of the ocular lens were adjusted to zero. The load was preset to 200 g. A diamond shape was observed as shown in Figure 15. The hardness was calculated from X diagonal length d_1 (μ m), Y diagonal length d_2 (μ m), and load F (gm). The group of aged samples following thermal exposure were rehydrated at 86% RH for two days at 45⁰C in an oven and their hardness values were measured. This was done in order to investigate the level of elastic recovery following rehydration. Five measurements were taken for each specimen.

2.3.3. Optical microscopy:

The specimen surfaces for each condition were evaluated using an Olympus PM-10 AD optical microscope.

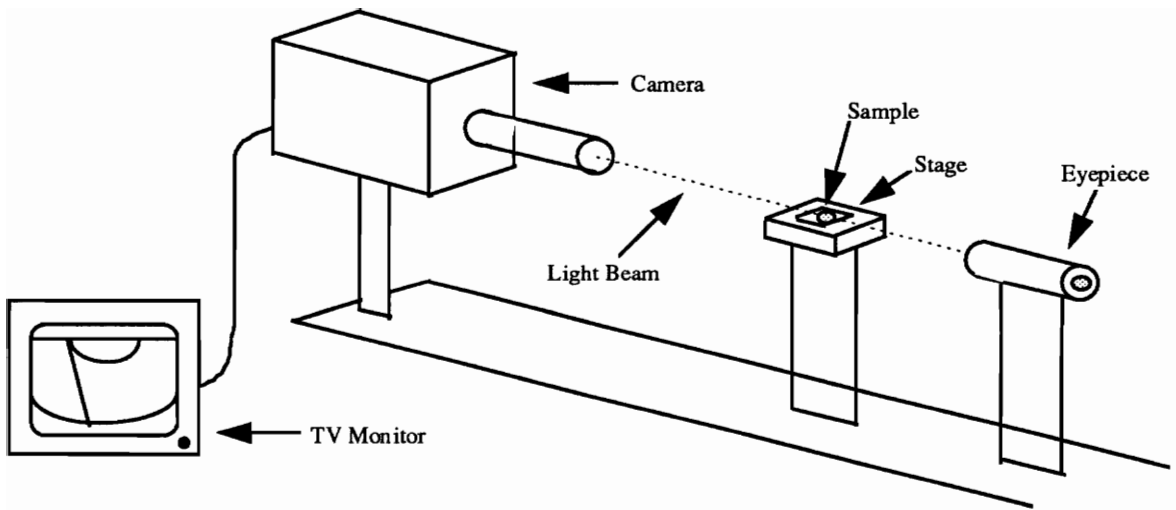
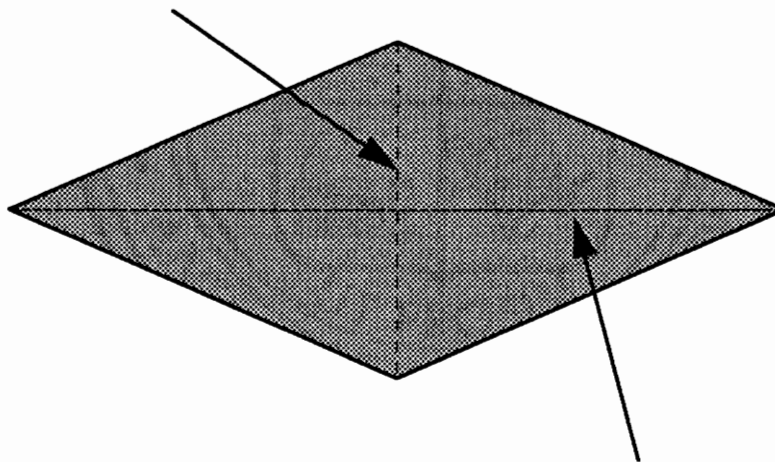


Figure 14: Schematic illustration of the Rame- Hart Goniometer.

d_1 Diagonal Length of Indentation (μm)



d_2 Diagonal Length of Indentation (μm)

Figure 15: Schematic representation of Vickers indentation.

2.4. Adhesion testing:

2.4.1. Tooth preparation for torsional testing:

Torsional adhesive testing was performed on forty eight bovine specimens. These specimens were prepared to evaluate whether mechanical bonding to the enamel dominates the adhesion of the cement. A cavity was prepared by drilling through the enamel of each tooth using a 0.125 inch bit to a standard depth of 0.189 inch and reaming each sample with a 0.128 inch reamer to yield a well prepared 0.128 inch diameter hole as shown in Figure 16. Each cavity was cleaned with water and blown dry. This was performed on eight initial specimens. A second group of eight specimens was prepared by drilling through the enamel of each tooth then grinding it. Each ground tooth was drilled again, then reamed to obtain a cavity depth of 0.189 inch. A third group of twenty was drilled then exposed to 65°C for periods of times ranging from 1 to 48 hours. Ten of them were etched after drilling with 20 % tannic acid for 60 seconds following thermal exposure.

In a separate comparison study, two unground and two ground specimens were etched with 8.5% sulfuric acid , and two unground and two ground were etched with 20% tannic acid for 60 seconds after drilling and prior to adhesive bonding. Table 6 describes the dentin specimen conditions.

2.5. Cement preparation:

A light cured glass-ionomer cement (Vitrebond, 3M) was first mixed according to the manufacturer's instructions [17]. As shown in Figure 17, the cement was mixed then placed in the cavity, and a 0.125" diameter steel rod was inserted into the

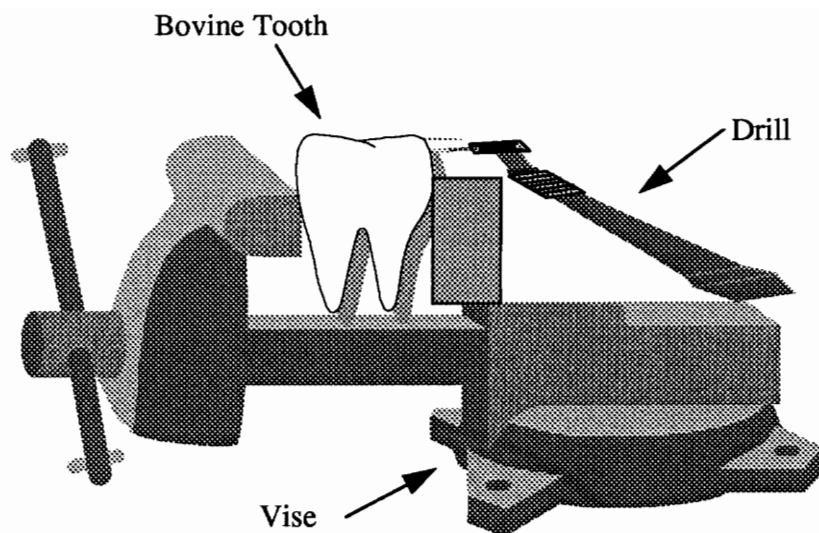


Figure 16: Schematic illustration of tooth preparation for torsional testing.

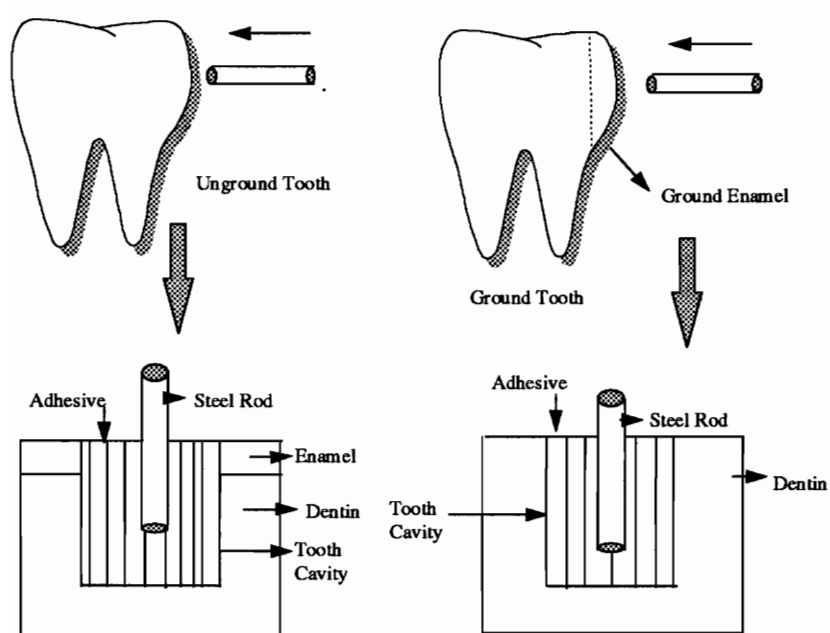


Figure 17: Schematic illustration of cement bonding to enamel and dentin.

Table 6: Sample conditions for each tooth.

Tooth Type	Etched	Thermally aged	Mixed at different ratios	Thermally aged and Etched
Unground	X	X	X	X
Ground	X	–	X	–

cavity of each specimen while the cement self-cured. The same procedure was repeated on ten unground and ten ground teeth by changing the powder/ liquid ratio of the cement using a weight % of : (50/50,55/45, 60/40, 45/55, 40/60).

2.6. Torsional testing:

The steel tooth joints were subjected to hand held torsional testing. For each sample, a rod was attached to a chuck which was joined to a torsion meter for adhesion testing as shown in Figure 18. The samples were allowed to react for a day before testing. Torque and shear stress failure were recorded for each sample type. The potential to prevent bending moment during torque application was controlled.

2.7. Natural tissue failure analysis:

2.7.1. Environmental scanning electron microscope (ESEM):

After torsional loading to failure, each rod was removed and observed under ESEM. Each tooth was ground parallel to the cavity and mechanically polished using 320 grit sand paper. Teeth cavities were studied by ESEM to characterize the failure surfaces.

2.8. Cement characterization:

The different cement ratios were characterized separately using contact angle measurements, Vickers microprobe, TGA, and IR, in order to determine their hardness, thermal and chemical properties.

2.8.1. Contact angle measurements:

Five cement samples with various ratios were mixed and pressed to a 0.3 mm thickness using a shim between two rectangular glass slides as shown in Figure 19.

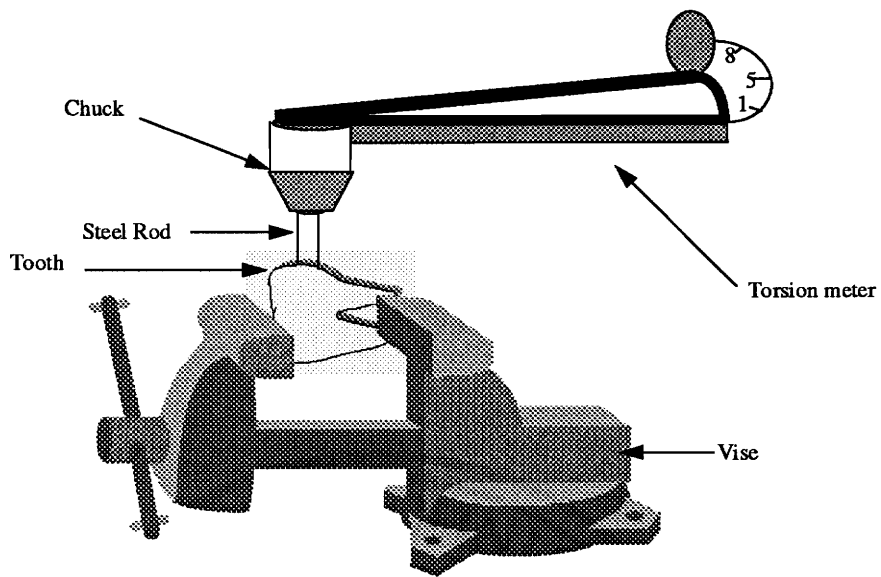


Figure 18: Illustration of the mechanism of debonding using a torque meter.

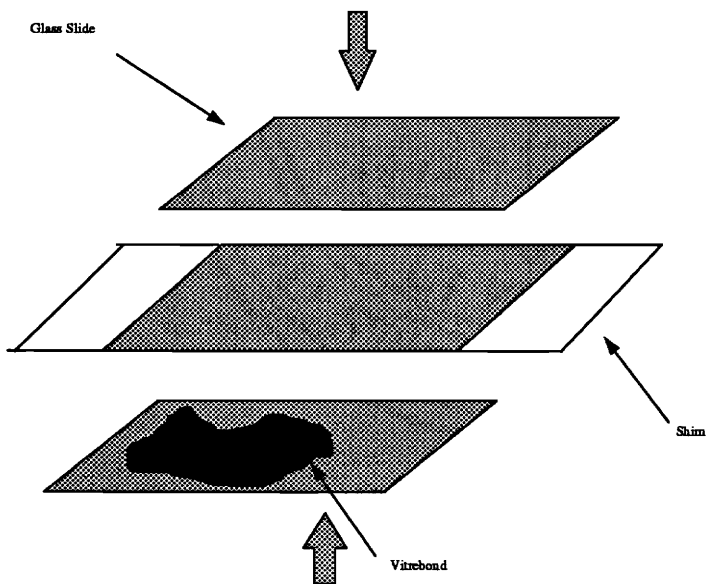


Figure 19: Schematic representation of the glass-ionomer cement preparation.

The samples were removed after pressing and exposed to blue light for curing, TCL 390, Patterson. The samples were left for at least one hour before testing. The edges of each cement sample were ground using a 320 grit sand paper. Water and methylene iodide were the two liquids chosen for this experiment. The contact angle of a 0.5 μl drop for each liquid was observed using a Rame- Hart Goniometer attached to a screen. The contact angles of water and methylene iodide on each cement sample were measured after 30 seconds. At least eight measurements were taken for each sample. The polar γ_s^P and dispersive γ_s^D components of the surface tension of the cement samples were also determined.

2.8.2. Hardness testing:

Five cement samples with various ratios were mixed and pressed to a 0.3 mm thickness using a shim between two rectangular glass slides as shown in Figure 19. The cement samples were carefully removed after blue light curing. The edges of each cement sample were ground using a 320 grit sand paper and then mounted with a thermoset casting resin (PSI Testing System 203). The Vickers microprobe was set at three different loads: 100g, 200g, and 300g to determine the variation in the microhardness of the mixed samples. These loads are lower than the loads of a typical hardness test. At least ten measurements were taken for each sample. The mean and the standard deviations were calculated.

2.8.3. Fourier transform infrared spectroscopy (FTIR):

Transmission Infrared analysis was performed with a Nicolet 750 FTIR spectrometer and TGS detector. Four KBr disks were cleaned with methylene chloride. One disk was used to record the background. Fifty-two scans were collected for the background file. Vitrebond powder and liquid were coated on two different disks. Then, each cement sample with a percentage weight powder to liquid ratio of 60/40, 50/50 and

40/60 was mixed with a dental cement spatula on each disk. Fifty-two absorbance scans were also collected for each sample.

2.8.4. Thermogravimetric analysis (TGA):

Thermogravimetric analysis was performed with a DuPont 1090 Thermal Analyzer and 951 Thermogravimetric Analyzer. This technique records the mass loss of a sample in a controlled atmosphere as its temperature increases.

10 mg of different sample ratios were transferred to panels. The sample thermocouple was placed inside the sample boat close to the sample. Temperature profiles were analyzed between room temperature and 455^o C at 10^o C/min. Data were transferred to Origin software. Plots of % weight loss vs temperature were obtained for each specimen.

3. Results

3.1. Dentin quality results:

3.1.1. Contact angle measurements:

3.1.1.1. Conditions, Equations:

Dentin specimens were characterized in their virgin state, after acid etching and thermal aging for various times as shown in Table 7.

The average and standard deviation of the contact angle of water and methylene iodide for each group measured are listed in Tables 8 and 9. Using these results, the surface tension was determined using relations 5 and 6 [34] which can be solved simultaneously in the form of:

$$\cos\theta_{1,2} + 1 = 2(\gamma_s^D * \gamma_{LV}^D)^{1/2} / \gamma_{LV} + 2(\gamma_s^P * \gamma_{LV}^P)^{1/2} / \gamma_{LV} + \pi e \quad (12)$$

where $\cos\theta_{1,2}$ is the contact angle of water and methylene iodide placed on dentin surface. $\gamma_{LV}^D, \gamma_{LV}^P$ and γ_s^D, γ_s^P are the liquid surface tensions for dispersive and polar components of the liquid and the solid respectively. πe , the spreading pressure, is negligible because the contact angle is larger than 10° [34]. By knowing the values of θ_1 and θ_2 from experimental, and $\gamma_{LV}^D, \gamma_{LV}^P$ from literature [34], the mean and standard deviation of the polar and the dispersive components of the surface tension were determined.

The total surface tension of each group was determined by employing equation (7). γ_s is the sum of dispersive and polar components of the surface tension [34]. The surface tension of each group as well as the standard deviations were determined and are shown in Table 10. The work of adhesion for each group was also determined using equation (3) [32].

Table 7: Surface conditions of dentin specimens tested for contact angle measurements.

Group	Conditions
Group V	Unetched dentin specimens
Group E _{Tannic}	Etched dentin specimens with 20% w/w tannic Acid for 60 sec
Group E _{Sulfuric}	Etched dentin specimens with 8.5% w/w sulfuric acid for 60 sec
Group D ₁	Thermally aged dentin for 1 hour
Group D ₂	Thermally aged dentin for 2 hours
Group D ₃	Thermally aged dentin for 3 hours
Group D ₂₄	Thermally aged dentin for 24 hours

Table 8: Average contact angle measurements for water and methylene iodide for each dentin specimen condition.

Conditions	Average θ_1 (Water)	Average θ_2 (Methylene Iodide)
Group V	57° (± 6)	38° (±7)
Group E _{Tannic}	22° (±5)	34° (±4)
Group E _{Sulfuric}	17° (±3)	13° (±4)

Table 9: Contact angle measurements of water and methylene iodide for thermally aged dentin specimens.

Conditions	Average θ_1 (Water)	Average θ_2 (Methylene Iodide)
Group D ₁	67° (±4)	7° (±6)
Group D ₂	66° (±6)	11° (±11)
Group D ₃	72° (±4)	0°
Group D ₂₄	73° (±5)	6° (±8)

Table 10: Average surface tension components of unetched and etched surface dentin specimens.

Conditions	Average polar components (dyne/cm) γ_s^p	Average dispersive components (dyne/cm) γ_s^d	Total surface Tension (dyne/cm) γ_s
Group V	23 (±3)	33 (±6)	55 (±6)
Group E _{Tannic}	42 (±1)	29 (±1)	71 (±2)
Group E _{Sulfuric}	38 (±1)	33 (±1)	70 (±2)

Table 11: Average work of adhesion for unetched, etched and thermally aged dentin specimens.

Conditions	Average work of adhesion (mJ/m ²)	Standard deviation (σ) (mJ/m ²)
Group V	121	±5
Group E _{Tannic}	143	±2
Group E _{Sulfuric}	141	±1
Group D ₁	108	±5
Group D ₂	111	±6
Group D ₃	108	±6
Group D ₂₄	106	±7

The average work of adhesion as well as the standard deviation of work for each group were determined and are shown in Table 11.

3.1.1.2. Unetched dentin specimens:

For Group V, average contact angles of $57^{\circ} (\pm 6)$ and $38 (\pm 7)$ were noted for water and methylene iodide droplets respectively. Knowing these values, equation (12) was used to determine the average dispersive and polar components of the surface tension for Group V as shown in Table 10. From equation (7), the total surface tension is determined to be $55 (\pm 6)$ dyne/cm. In addition, from equation (3) [32], the average work of adhesion for the Group V is $121 (\pm 5)$ mJ/m².

3.1.1.3. Etched dentin specimens:

Etching dentin with tannic acid lowered the average contact angles to $22 (\pm 5)$ and $34^{\circ} (\pm 4)$ for water and methylene iodide droplets. Using sulfuric acid, the contact angles decreased to $17^{\circ} (\pm 3)$ and $13^{\circ} (\pm 4)$ for water and methylene iodide. Knowing these values, equation (12) was used to determine the average dispersive and polar components of the surface tension for the etched dentin specimens. These are shown in Table 10. The total surface tension has an average value of $71(\pm 2)$ dyne/cm for Group E_{Tannic} and $70 (\pm 2)$ dyne/cm for Group E_{Sulfuric}. The work of adhesion has increased to values of $143 (\pm 2)$ mJ/m² and $141 (\pm 1)$ mJ/m² for Group E_{Tannic} and Group E_{Sulfuric}, respectively.

Etching results in better wetting as evidenced by the decrease in the contact angle made with the polar component and the corresponding rise in the polar surface tension. Group E_{Tannic} led to the highest polar surface tension. The average dispersive component of Group E_{Sulfuric acid} and Group V is the highest as shown in Figure 20.

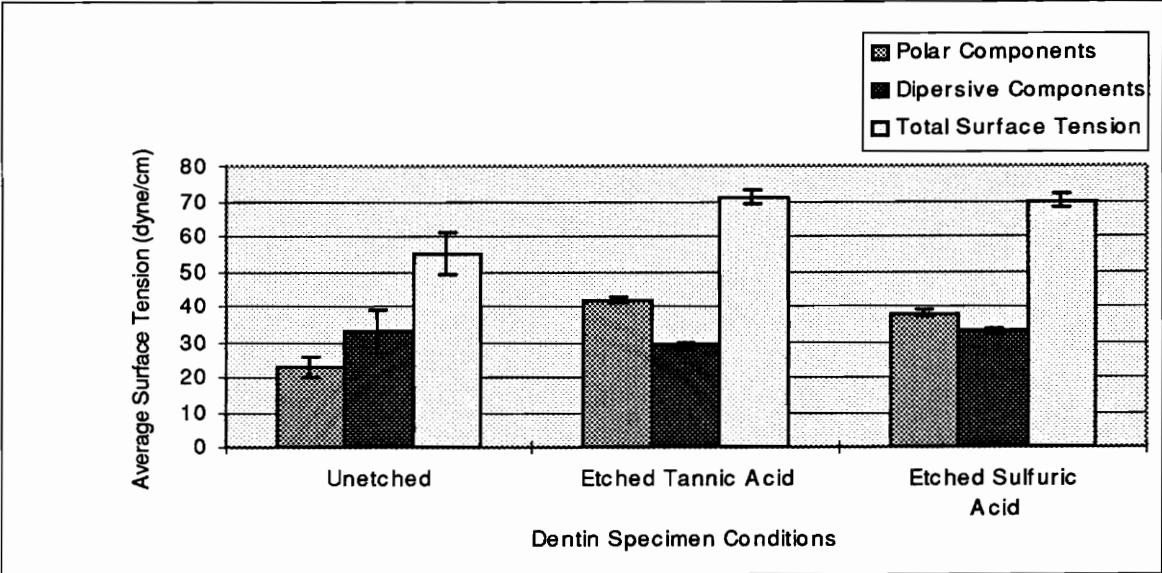


Figure 20: Comparison of the average polar, dispersive and total surface for different dentin conditions.

3.1.1.3.1. Microscopy of etched dentin specimens:

Group E_{Tannic} specimens were observed under the optical microscope at different magnifications. Figures 21 and 22 show the effect of etching on the surface of a tannic acid treated dentin specimen for the first 60 sec. Small pores are seen on the surface of dentin indicating that an opening of dentin tubules occurs with etching. These pores may explain why the contact angles of water and methylene iodide are lower if they penetrate the pores.

3.1.1.4. Thermally aged dentin specimens:

The average and standard deviation of the contact angle of water and methylene iodide for Group D are listed in Table 9. As methylene iodide was placed on the aged surface, it was readily absorbed into the bulk of the dentin. However, the contact angle, θ_p , of water for all aged specimens was less than 90° indicating a partial wetting for all specimens. The two liquid method for determining the surface tension was not applicable since methylene iodide was absorbed into dentin. Equation (3) [32] was used to determine the average work of adhesion for Group D, the results of which are summarized in Table 11. Figure 23 is a plot of the average work of adhesion versus the aging time which shows no change in the work as function of increases thermal aging, indicating that this change in work was essentially complete by the first hour of thermal exposure.

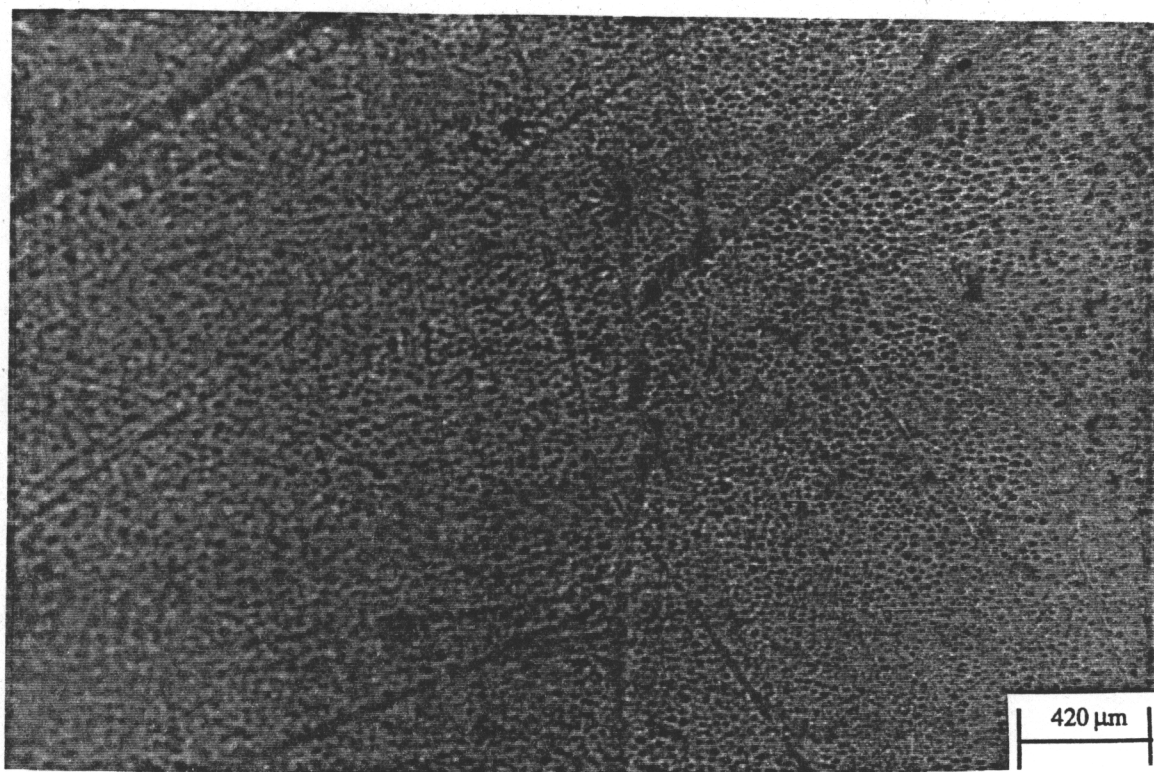


Figure 21: Optical micrograph of dentin surface treated with tannic acid for 60 sec; small pores observed, indicating an opening of dental tubules (X50).

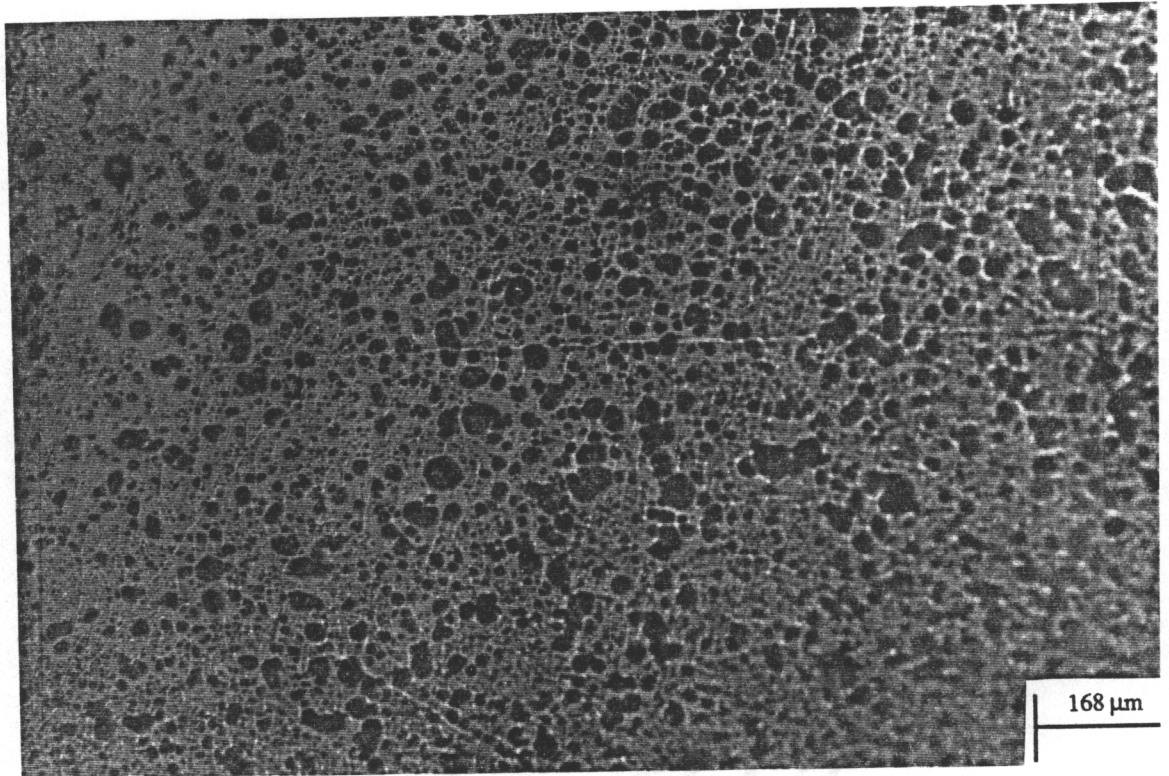


Figure 22: Optical micrograph of dentin surface treated with tannic acid for 60 sec; small pores observed, indicating an opening of dental tubules (X125).

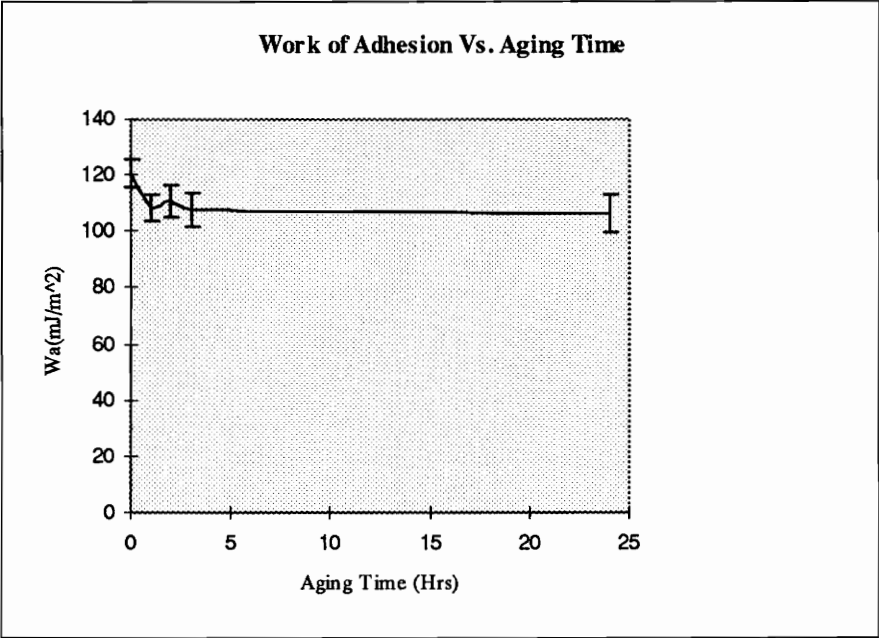


Figure 23: Work of adhesion as function of aging time at 65°C in an air oven.

3.1.1.4.1. Microscopy of thermally aged dentin specimens:

Figure 24 shows the dentin surface after 3 hours of thermal aging time. However, upon 24 hours of thermal aging at 65⁰C, cracks were observed on the dentin as seen in Figure 25.

3.1.2. Hardness measurements:

3.1.2.1 Conditions, Equations:

The dentin surface conditions for each group are listed in Table 12 and 13.

The average Vickers hardness, and its the standard deviation, were determined for Group V, Group E, and Group D using equation (8) [42]. The results are listed in Tables 14, and 15. Figure 26 illustrates the geometry of the hardness indentation.

3.1.2.2. Unetched dentin specimens:

The average and standard deviation of the Vickers hardness for Group V was determined using equation (8). A value of 76 (± 3) Hk was determined.

3.1.2.3. Etched dentin specimens:

The average Vickers hardness of Group E are summarized in Table 14. The calculated hardness decreased with etching as shown in Table 14. Further etching caused a loss of surface hardness. These results were compared with Group V as illustrated in Figure 27 and are lower to other results published in the literature [9].

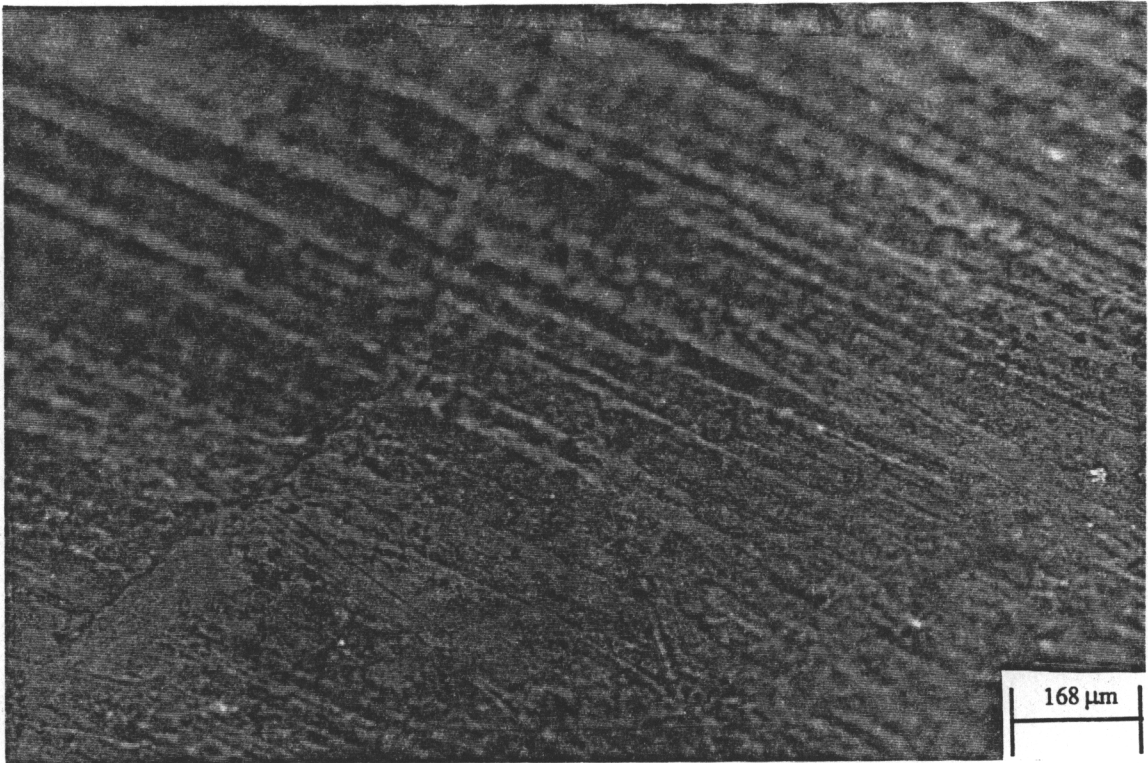


Figure 24: Dentin surface after 3 hours of aging time at X125.

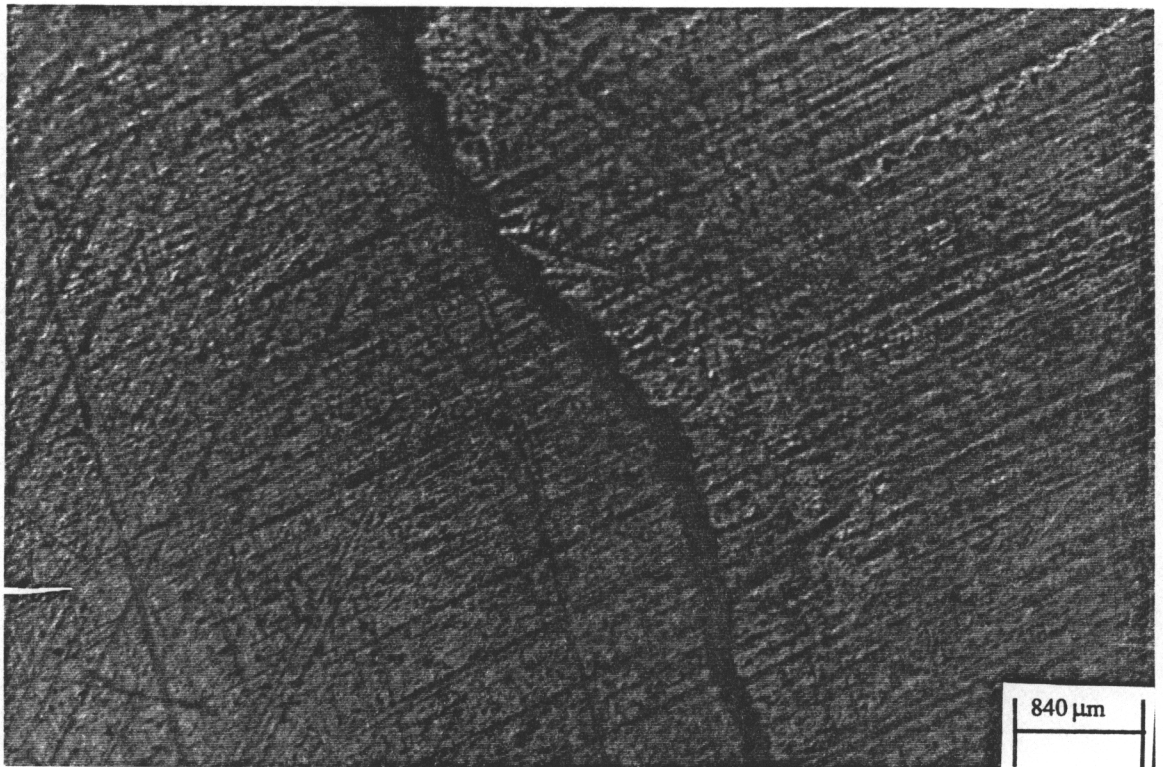


Figure 25: Dentin surface after 24 hours of aging time; major cracks observed at a magnification of X25.

Table 12: Surface conditions of etched dentin specimens tested for hardness.

Dentin specimens	Conditions
Group V	Unetched dentin specimens
Group E _{Tannic}	Etched dentin specimens with 20% w/w tannic acid for 60 sec
Group E _{Tannic} 1	Etched Group E _{Tannic} with additional 20 sec with 20% w/w tannic acid
Group E _{Sulfuric}	Etched dentin specimens with 8.5 % w/w sulfuric acid for 60 sec
Group E _{Sulfuric} 1	Etched Group E _{Sulfuric} with additional 20 sec 8.5% w/w sulfuric acid

Table 13: Surface conditions of thermally aged dentin specimens tested for hardness.

Dentin specimen conditions	Denaturing time (Hours)	Rehydration time (Days)
Group V	0	for 2 days, 86% RH, at 45 ⁰ C
Group D ₁	1	for 2 days, 86% RH, at 45 ⁰ C
Group D ₂	2	for 2 days, 86% RH, at 45 ⁰ C
Group D ₃	3	for 2 days, 86% RH, at 45 ⁰ C
Group D ₂₄	24	for 2 days, 86% RH, at 45 ⁰ C
Group D ₄₈	48	for 2 days, 86% RH, at 45 ⁰ C

Table 14: Average hardness of unetched and etched dentin specimens.

Sample conditions	Average hardness (kg/mm ²)	Standard deviation (σ) (kg/mm ²)	Load (g)
Group V	76	± 3	200
Group E _{Tannic}	68	± 1	200
Group E _{Tannic1}	44	± 3	200
Group E _{Sulfuric}	61	± 4	200
Group E _{Sulfuric1}	50	± 3	200

Table 15: Average hardness of unetched, thermally aged and rehydrated dentin specimens.

Sample conditions	Average hardness (kg/mm ²) after aging	Standard deviation (σ) (kg/mm ²)	Average hardness (kg/mm ²) after rehydration	Standard deviation (σ) (kg/mm ²)	Load (g)
Group V	75	± 2	82	± 2	200
Group D ₁	62	± 1	72	± 5	200
Group D ₂	56	± 3	63	± 1	200
Group D ₃	52	± 3	60	± 2	200
Group D ₂₄	46	± 2	54	± 1	200
Group D ₄₈	38	± 3	47	± 2	200

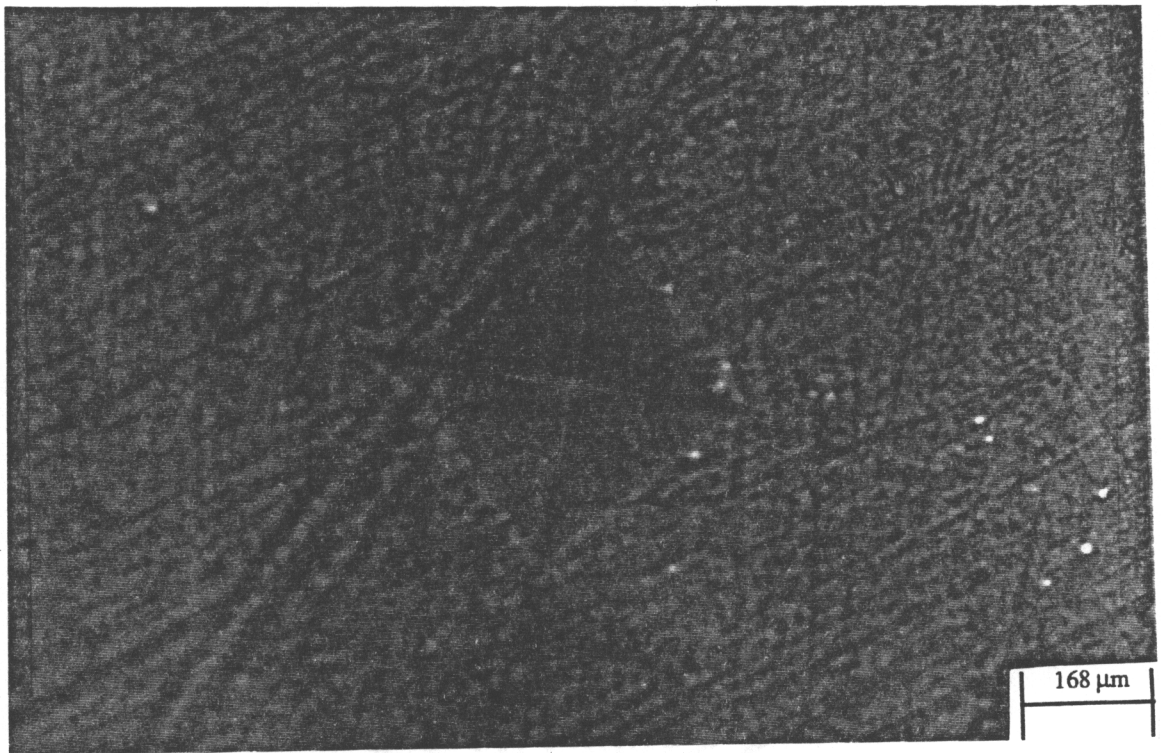


Figure 26: Geometry of hardness indentation at 125X.

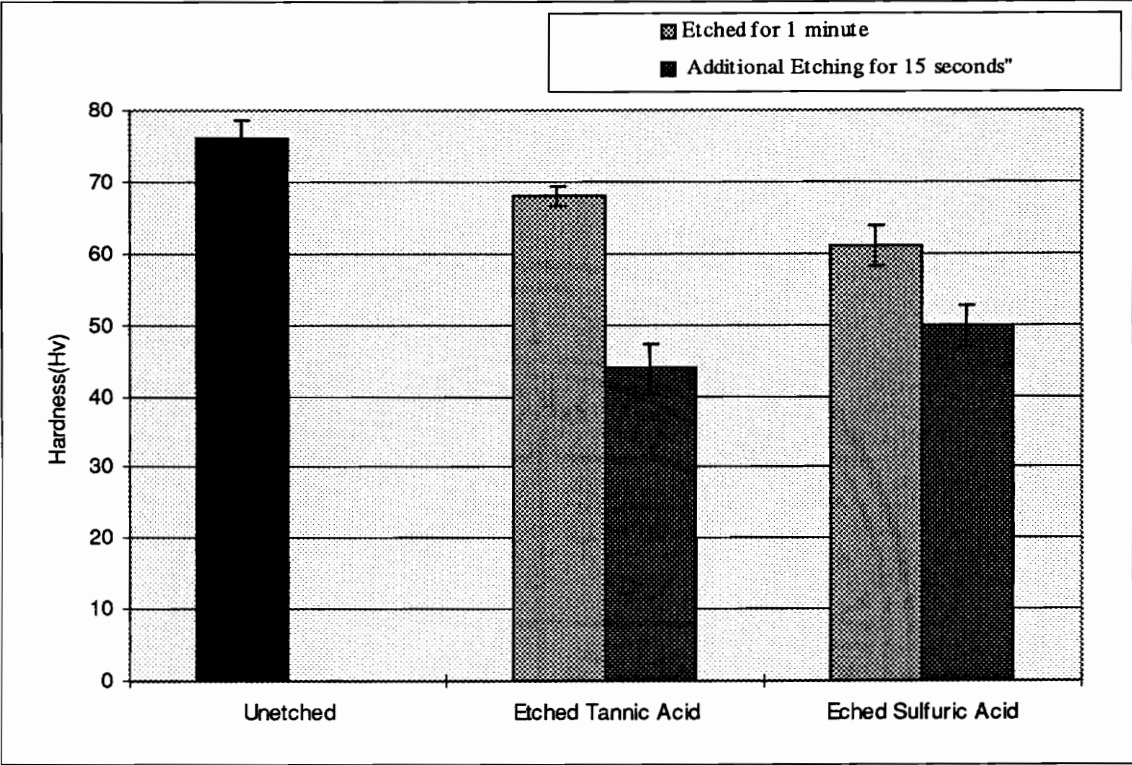


Figure 27: Effect of etching on hardness.

3.1.2.4. Thermally aged dentin specimens:

The average hardness and its standard deviation were determined for Group D as shown in Table 15. By exposing Group D to a temperature of 65⁰C, the dentin hardness progressively decreases with time. Following exposure to the humid environment (86% RH) for two days at 45⁰C, the hardness was only partially recoverable. The hardness results of aged dentin specimens were compared with the rehydrated ones as shown in Figure 28 where the variation of hardness was affected by thermal aging time and rehydration. It was observed that dentin hardness was slightly recoverable when it was exposed to the humid environment. This may be associated with water content restoring dentin toughness.

3.1.2.4.1. Microscopy of thermally aged dentin specimens:

Figure 29 illustrates a major crack in the dentin region after 24 hours of aging time prior to hardness testing.

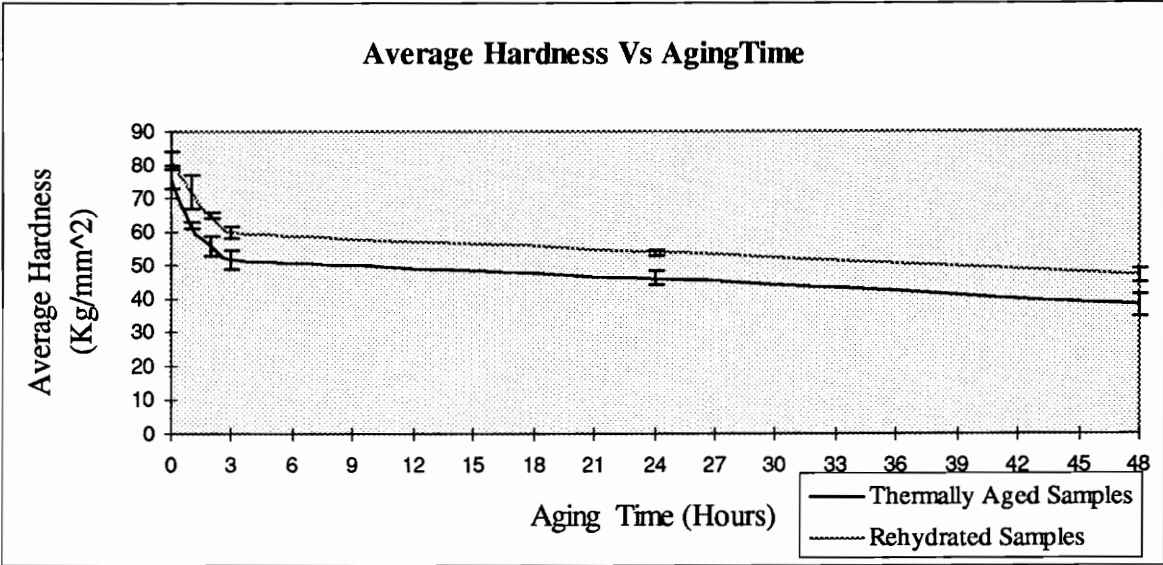


Figure 28: Average hardness as function of thermal aging time at 65 °C in an air oven.

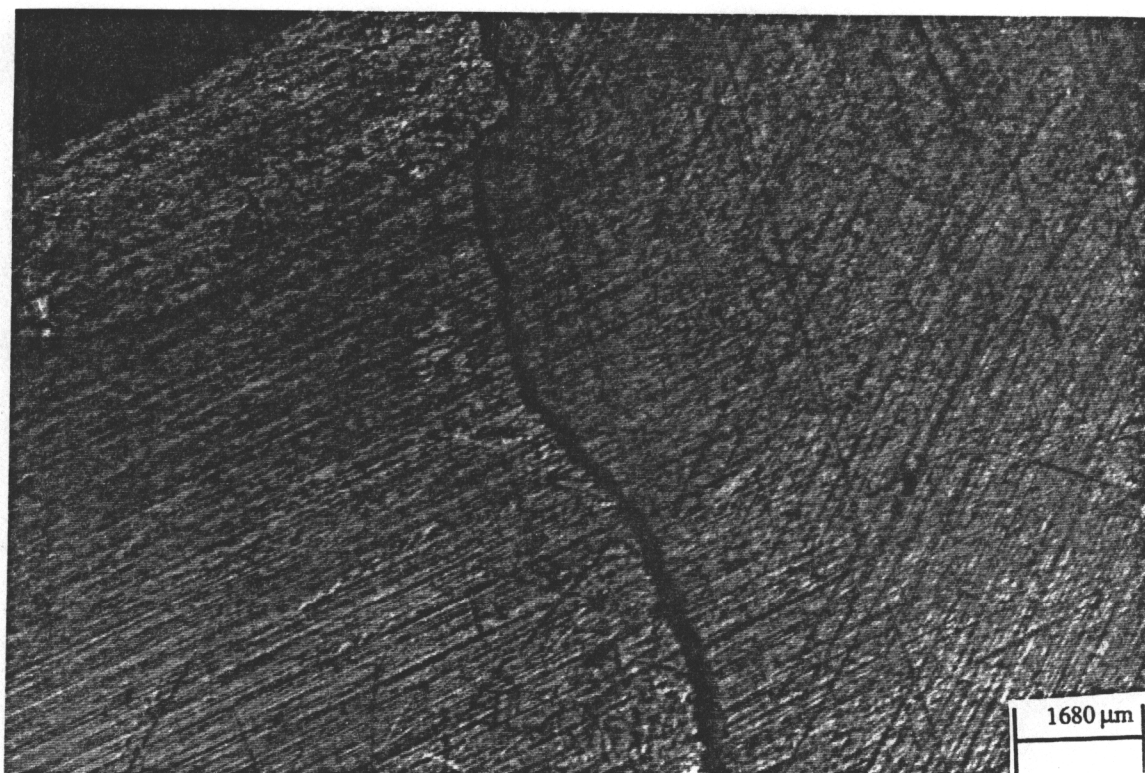


Figure 29: Dentin surface after 24 hours of thermal exposure and prior to hardness testing; cracks were observed at 12.5X.

3.2 Torsional testing :

3.2.1. Conditions, Equations:

Torsional adhesion tests were performed on dentin exposed to different conditions as listed in Table 16. From these tests, the average shear strength (τ) for each group was determined using the derived relationship from appendix (A):

$$\tau = 2 * T / \pi * (D)^2 * L \quad (VI)$$

where T is the torque at failure in N.m, D is the rod diameter in m, and L is the cavity length in m. From the average torque at failure, the average shear strength and its standard deviation in MPa were determined for each dentin specimen condition.

3.2.1.1. Unground and ground teeth:

Using equation (VI) from Appendix A, average torsional shear strengths of 10.3 (\pm 0.6) MPa and 8.3 (\pm 0.3) MPa were measured for the adhesive bonded to Group U and Group G, respectively. The average torsional shear strength was reduced when the enamel was ground as shown in Figure 30. The increase in the torsional bond shear strength for Group U is attributed to more mechanical interlocking of the cement with the enamel. Compared to dentin, enamel is stiffer (E= 48 GPa) [19], harder (Hv= 280 to 300) [1] and higher in compressive and tensile strength than dentin. The addition of enamel results in higher torsional shear bond strengths. Contrary to dentin, enamel contains more hydroxyapatite, carbonate, and magnesium and contains significantly less water. Cement may infiltrate better to the inorganic components of enamel, increasing the average shear bond strength.

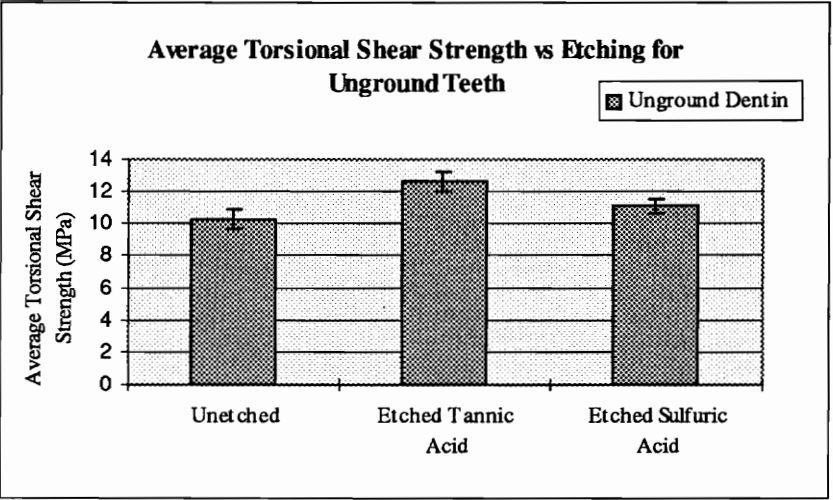
Weaker strengths were measured for Group G. This may be associated with a lower dentin stiffness (E= 13.8 GPa) [19], and hardness (Hv= 60 to 80 kg/mm²) [1]. In

Table 16: Teeth conditions used for torsional testing.

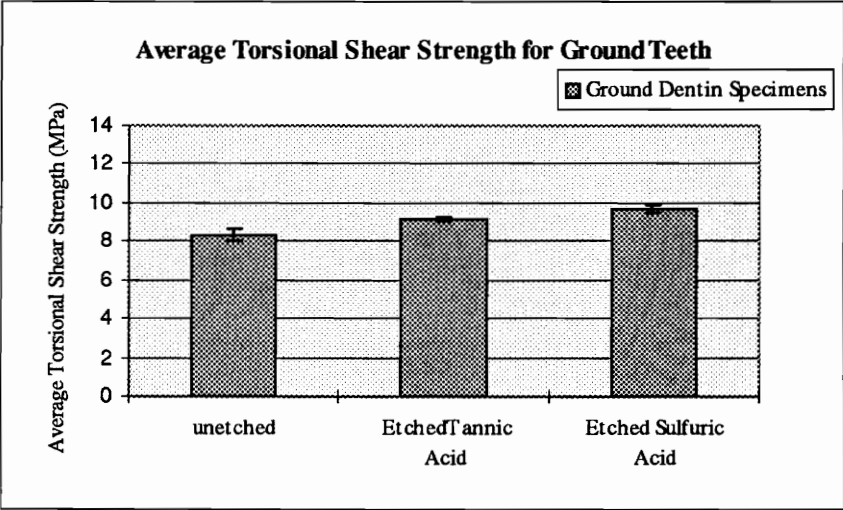
Conditions	Unground teeth	Ground teeth	Etched with tannic acid	Etched with sulfuric acid	Thermal aging	Mixed at varied ratios
Group U	X					
Group U _{Tannic}	X		X			
Group U _{Sulfuric}	X			X		
Group G		X				
Group G _{Tannic}		X	X			
Group G _{Sulfuric}		X		X		
Group D	X				X	
Group D _{Tannic}	X		X		X	
Group R _U	X					X
Group R _G		X				X

Table 17: Average torque at failure and average torsional shear strength for unground, ground and etched teeth.

Conditions	Average torque at failure T (N.m)	Average torsional shear strength τ (MPa))
Group U	0.76 (± 0.05)	10.3 (± 0.6)
Group U _{Tannic}	0.93 (± 0.04)	12.6 (± 0.6)
Group U _{Sulfuric}	0.82 (± 0.03)	11.1 (± 0.4)
Group G	0.63 (± 0.03)	8.3 (± 0.3)
Group G _{Tannic}	0.7 (± 0.1)	9.2 (± 0.1)
Group G _{Sulfuric}	0.72 (± 0.21)	9.7 (± 0.2)



(a)



(b)

Figure 30: Effects of etching on the average shear strength for the unground and ground teeth; (a) Group U_{Tannic} and Group U_{Sulfuric} ;(b) Group G_{Tannic} and Group G_{Sulfuric} .

addition, the cement may infiltrate poorly to the smear layer. All these factors may lower the torsional shear strength for Group G

3.2.1.2. Etched unground and ground teeth:

The average shear strength and standard deviation were determined for unground and ground teeth that when etched with tannic and sulfuric acids as shown in Table 17. Average torsional shear strengths of 12.6 (± 0.6) MPa, and 11.1(± 0.4) MPa were achieved for Group U_{Tannic} and Group U_{Sulfuric}, respectively. In addition, average torsional shear strengths of 9.2 (± 0.1) MPa and 9.7 (± 0.2) MPa were obtained for Group G_{Tannic} and Group G_{sulfuric} , respectively.

Adhesion tests reveal that Group U_{Tannic} and Group U_{Sulfuric} exhibit higher shear strength than Group G_{Tannic} and Group G_{sulfuric}. Acid etching of enamel increases the surface area available for bonding and increases the wettability of the etched enamel surface. The cement will be more likely to infiltrate the etched enamel and dentin surfaces and bond mechanically to them resulting in increased torsional shear strength. In addition, acid treatment exposes the dentin collagen tubules, leaving pores as discussed earlier. Thus, the cement can enter dentin tubules creating a mechanical keying action increasing the observed torsional shear strength. By treating both enamel and dentin with tannic acid, the average shear strength was higher than the sulfuric acid treatment as shown in Figure 30 (a). This may be associated with the increasing the polar surface tension of dentin when etched with tannic acid as discussed earlier. Knowing that the cement is hydrophilic [19,48], this may reflect an increase in the bond strength of dentin when it is etched with tannic acid. In general, etching with sulfuric and tannic acid increase the total dentin surface tension of dentin which may also reflect in an increase in the bond strength.

Group G_{Tannic} and Group G_{Sulfuric} exhibit a higher average torsional shear bond strength than Group G as shown in Figure 30 (b). It is more likely that etching removes the smear layer and opens the dental tubules. This may also increase the surface area available for bonding and increase the wettability of the etched dentin surface as discussed

in the contact angle results. The cement may flow more easily into the pores in the dentin surface and the cement can bond mechanically to the etched dentin surface, increasing the average torsional shear strength.

3.2.1.3. Thermally aged teeth:

The average torque at failure and the average torsional shear strength and its standard deviation were calculated for Group D as shown in Table 18. An average of 9.1 (± 1.1) MPa was obtained for Group D₁ which decreased dramatically to 0.8 (± 0.1) MPa after 48 hours. The average shear strength of Group D_{Tannic} slightly increased as shown in Figure 31, indicating that tannic acid may act as a hydrating conditioner prior to adhesive bonding.

3.2.1.4. Analysis of glass-ionomer cement ratio on unground and ground teeth:

The average torque at failure and the average shear strength and its standard deviation were determined for Group R_U and Group R_G as shown in Table 19. By examining the effects of changing the liquid to powder ratio, the highest shear strength values were obtained for the unground dentin were 11.1 (± 0.3) MPa and 10.8 (± 0.2) MPa at 50/50 and 55/45 ratios, respectively as shown in Figure 32. The average shear strength decreased with an excess in the powder ratio at 60/40 to 8.4 (± 0.1) MPa. There is insufficient liquid available to bind the glass particles together into the cement. Consequently, the shear strength decreased. In addition, an excess of liquid ratio at 45/55 and 40/60 decreased the values of the average shear strength to 9.4 (± 0.4) MPa and 8.9 (± 0.2) MPa, respectively.

Table 18: Average torque at failure and average shear strength for the thermally aged teeth.

Thermal aging conditions	Average torque at failure (N.m)	Average torsional shear strength (τ) (MPa)
Group D ₁ 1 Hour	0.7 (± 0.1)	9.1 (± 1.1)
Group D _{Tannic} 1 Hour	0.8 (± 0.1)	10.4 (± 1.4)
Group D ₂ 2 Hours	0.6 (± 0.2)	8.7 (± 1.6)
Group D _{Tannic} 2 Hours	0.71 (± 0.04)	9.5 (± 0.5)
Group D ₃ 3 Hours	0.49 (± 0.02)	6.6 (± 0.3)
Group D _{Tannic} 3 Hours	0.55 (± 0.02)	7.4 (± 0.2)
Group D ₄ 24 Hours	0.15 (± 0.03)	2.1 (± 0.3)
Group D _{Tannic} 24 Hours	0.36 (± 0.04)	4.8 (± 0.4)
Group D ₅ 48 Hours	0.06 (± 0.01)	0.8 (± 0.1)
Group D _{Tannic} 48 Hours	0.12 (± 0.02)	1.7 (± 0.2)

Table 19: Average torque at failure and average torsional shear strength of teeth subjected to different mixing ratios.

Mixing conditions	Average torque at failure (N. m)	Average torsional shear strength τ (MPa)
Group R _u 60/40	0.62(\pm 0.01)	8.4 (\pm 0.1)
Group R _u 55/45	0.81(\pm 0.02)	10.8 (\pm 0.2)
Group R _u 50/50	0.83(\pm 0.02)	11.1 (\pm 0.3)
Group R _u 45/55	0.71(\pm 0.03)	9.4 (\pm 0.4)
Group R _u 40/60	0.66(\pm 0.02)	8.9 (\pm 0.2)
Group R _G 60/40	0.48(\pm 0.04)	6.4 (\pm 0.5)
Group R _G 55/45	0.59(\pm 0.04)	8.0 (\pm 0.6)
Group R _G 50/50	0.69(\pm 0.06)	9.3 (\pm 0.8)
Group R _G 45/55	0.59(\pm 0.04)	7.6 (\pm 1.1)
Group R _G 40/60	0.42(\pm 0.03)	5.8 (\pm 0.4)

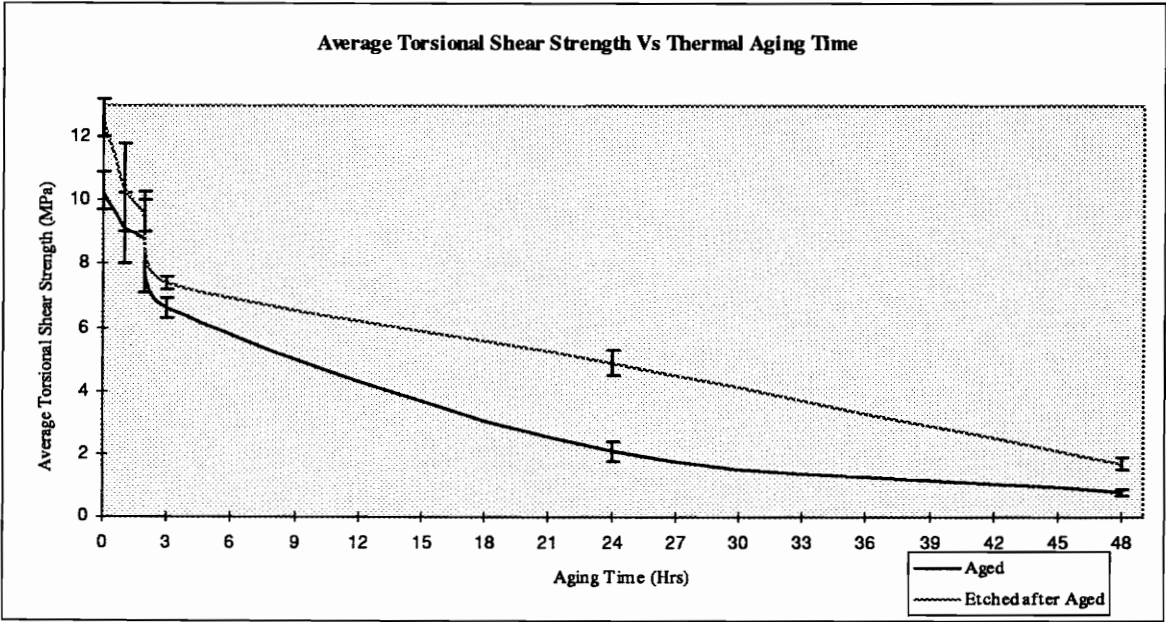


Figure 31: Average torsional shear strength as function of thermal aging time at 65°C in an air oven.

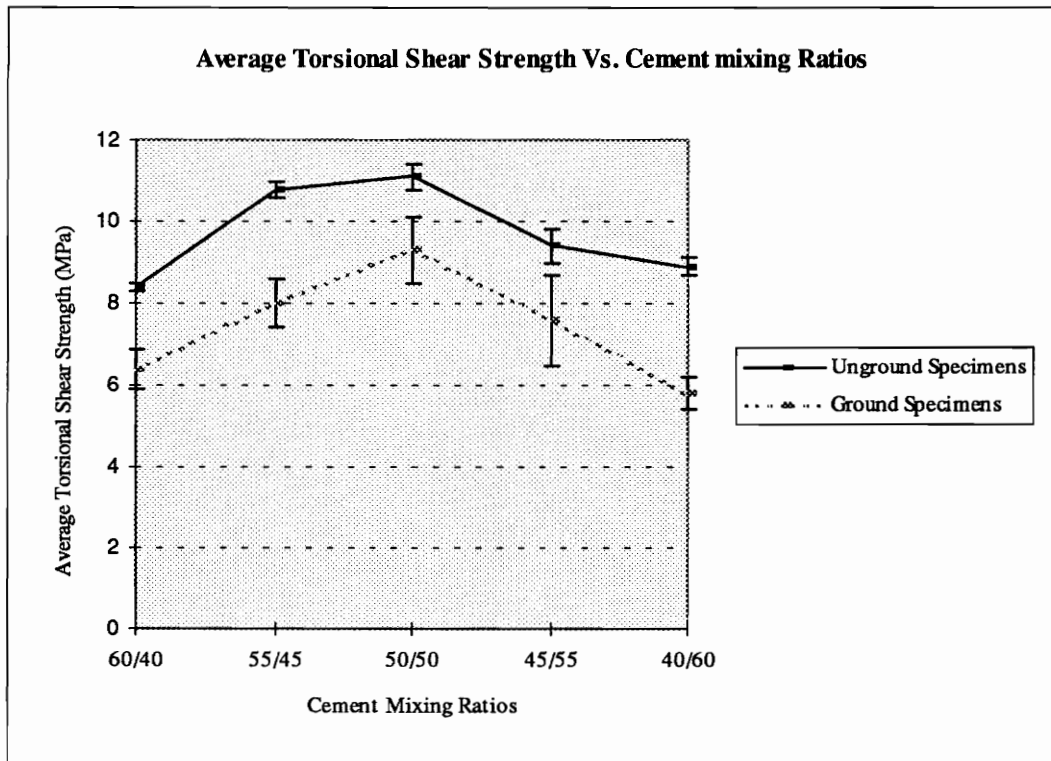


Figure 32: Variation in the average shear strength of unground and ground teeth as function of cement ratios.

The excess of liquid in the paste may overhydrate the cement due to the water and HEMA content. The excess acid may additionally etch the dentin and enamel surface due to its high reactivity. The paste may become softer due to its excess of liquid and takes longer to set.

By examining the effects of changing the liquid to powder ratio for Group R_G, the 50/50 and 55/45 ratios have the highest torsional shear strength. As discussed for Group R_U, the same ratio factors may also affect the average shear strength of the ground ones. In addition, by grinding the enamel, the average shear strength was reduced as shown in Figure 32 suggesting mechanical interlocking into the enamel may be the main factor in stronger adhesion.

3.3. ESEM analysis:

To understand the mechanism of failure, the debonded teeth specimens and the steel rods were observed under ESEM. The results for the different teeth structure surfaces are shown in the next sections.

3.3.1. Unground and ground teeth:

Representative micrographs of the steel rod for Group U and Group G after torsional debonding are shown in Figures 33 and 34. These pictures show debris of cement left on the steel rod for both groups. By examining the debonded Group U, some cement still covers the enamel region as shown in Figure 35. Few cracks are observed within the cement-enamel region. This may indicate a cohesive failure occurs within the cement-enamel region. By examining the dentin side of the fracture surface, some cement is missing as shown in Figure 36. The other part is still bonded to dentin. Dentin exhibits an adhesive and cohesive failure.

The cement is bonded to the steel rod for Group G. However by looking on the dentin surface of the fracture surface as shown in Figure 37, cement debris is observed. The tubules of the dentin are also seen, indicating the smear layer was removed even

though it was not treated in this case. There are two explanations for this observation. The first is that the smear layer was removed while drilling the cavity prior to adhesion bonding. The second approach is that the smear layer was removed during torquing. For the first case, adhesive failure may be occurred within the dentin. For the second case, failure seems to occur cohesively within the smear layer.

3.3.2. Etched unground and ground teeth:

By examining the steel rod for Group U_{Tannic} and Group G_{Tannic} shown in Figures 38 and 39, the cement particles are left on the steel rod. Figure 40 shows cement is still bonded to enamel fractured surface. The treated enamel specimens may exhibit a cohesive failure within the cement. The fractured surface of the dentin is shown in Figure 41. Cement residue is still attached to the dentin surface for Group U_{Tannic}. However more cement was removed and the dentin tubules were more visible. This suggests a cohesive and adhesive failure mechanism at the dentin interface.

Figure 42 shows the ground etched dentin after failure. Part of debonded the dentin surface shows dentin tubules indicating that cement was removed after failure. However some cement is still bonded to dentin. The treated ground teeth seem to exhibit adhesive and cohesive failure.

3.3.3. Thermally aged teeth.

By examining the steel rod of Group D₄₈ specimens in Figure 43, no trace of cement was detected on the rod. By examining the fractured enamel surface shown in Figure 44, a thin layer of cement covers the enamel surface. In addition, cracks within the enamel are observed. Figure 45 shows few trace of cement still overlays the dentin. Major dentin cracks were observed in this region. These cracks show a brittle behavior.

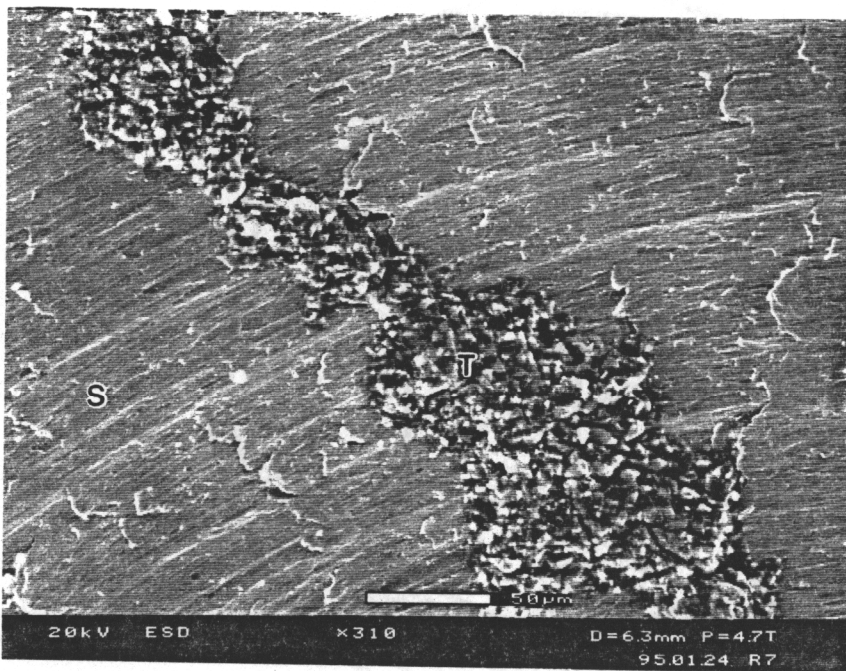


Figure 33: Cement trace (T) bonded to steel rod (S) for Group U at X310.

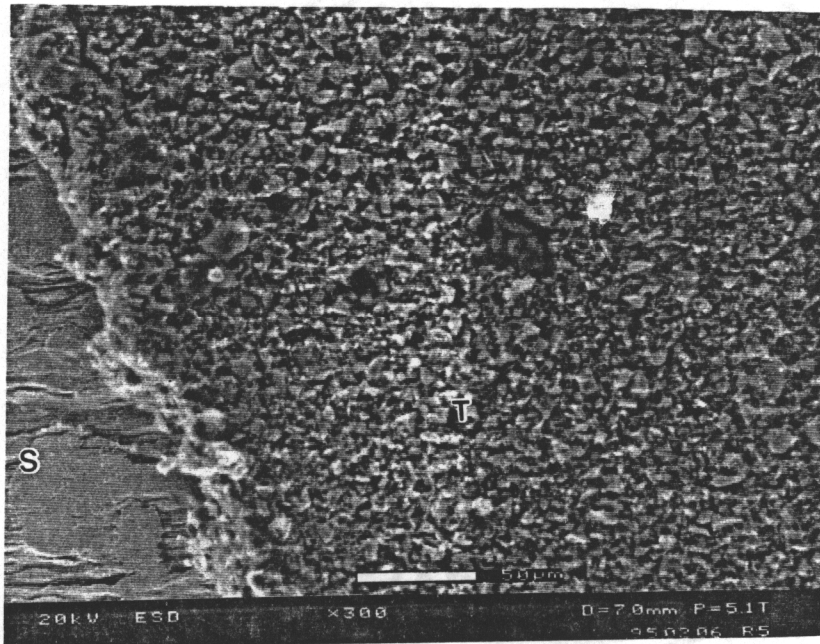


Figure 34: Cement trace (T) bonded to steel rod (S) for Group G at X300.

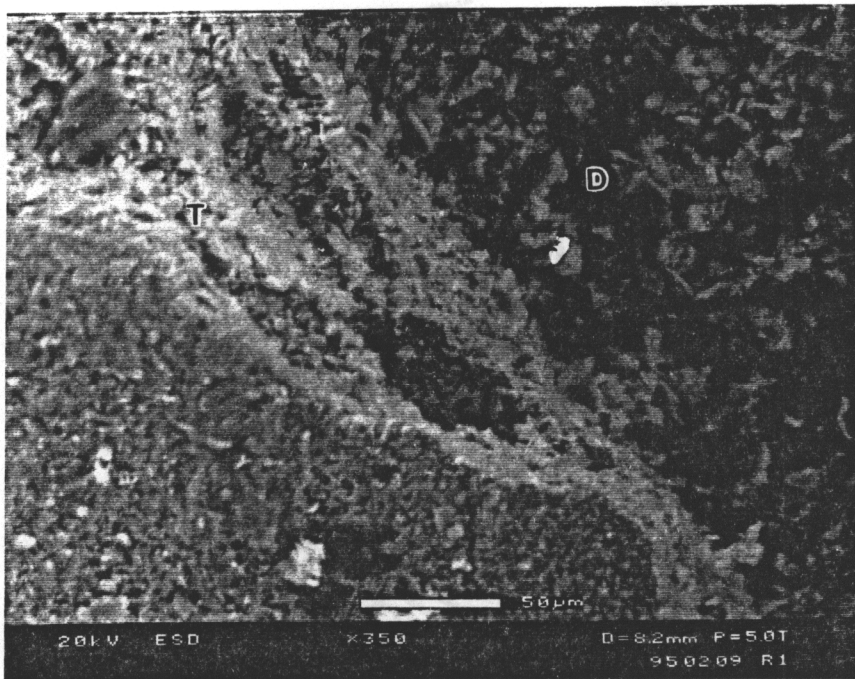


Figure 35: The bottom part showing the cement (T) still bonded to enamel for Group U;
The top part showing cement debris covering the dentin region (D) at X350.

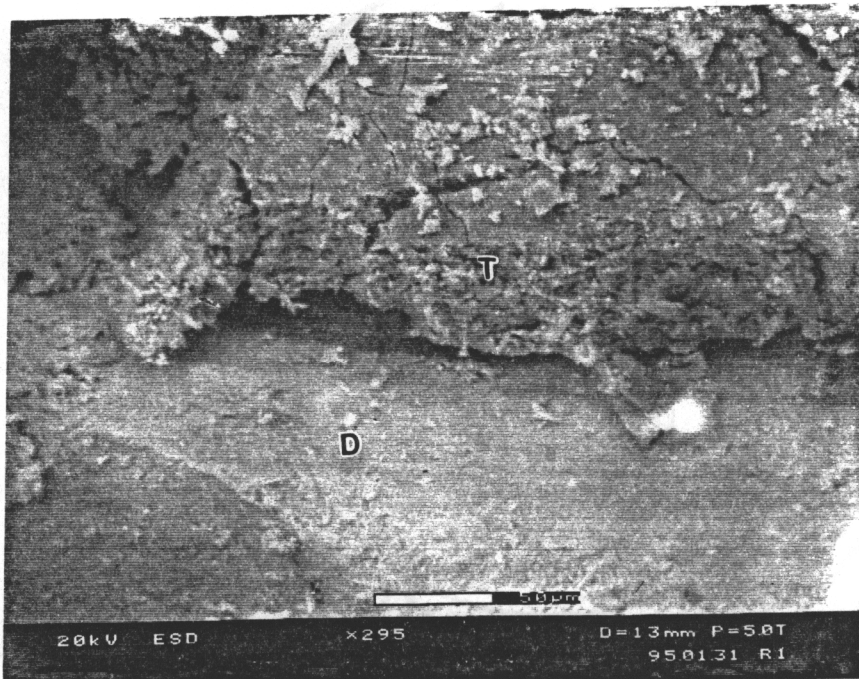


Figure 36: The bottom part showing dentin (D); the top part showing the cement (T) still bonded to dentin at X295.

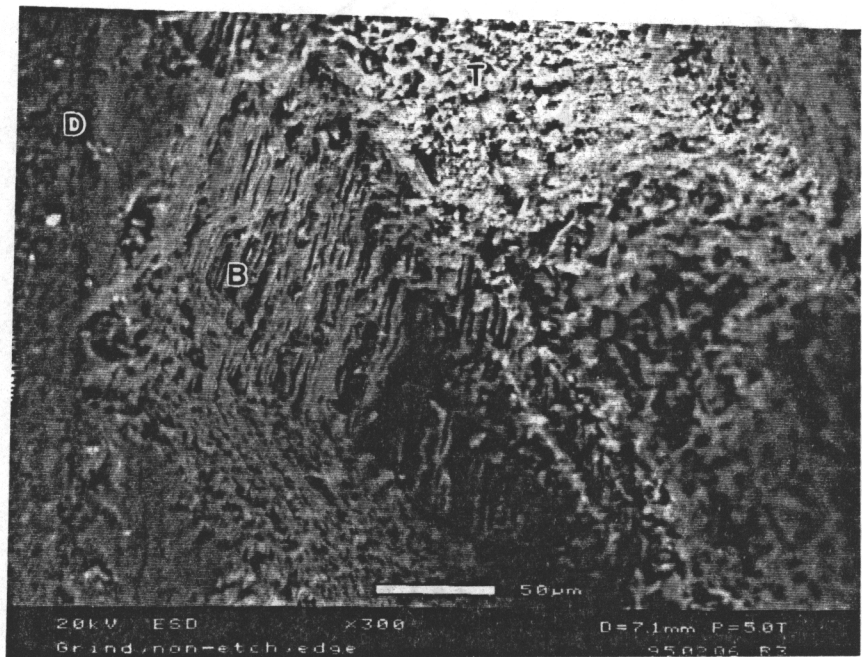


Figure 37: Dentin surface (D), dentin tubules (B) and cement debris (T) for Group G at X300.

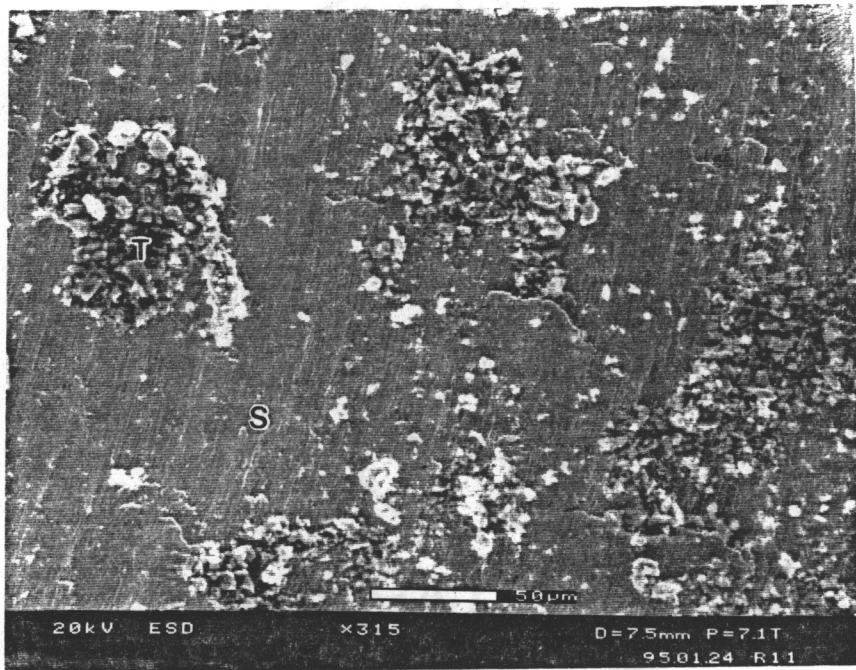


Figure 38: Cement Trace (T) bonded to steel rod (S) for Group U_{Tannic} at X315.

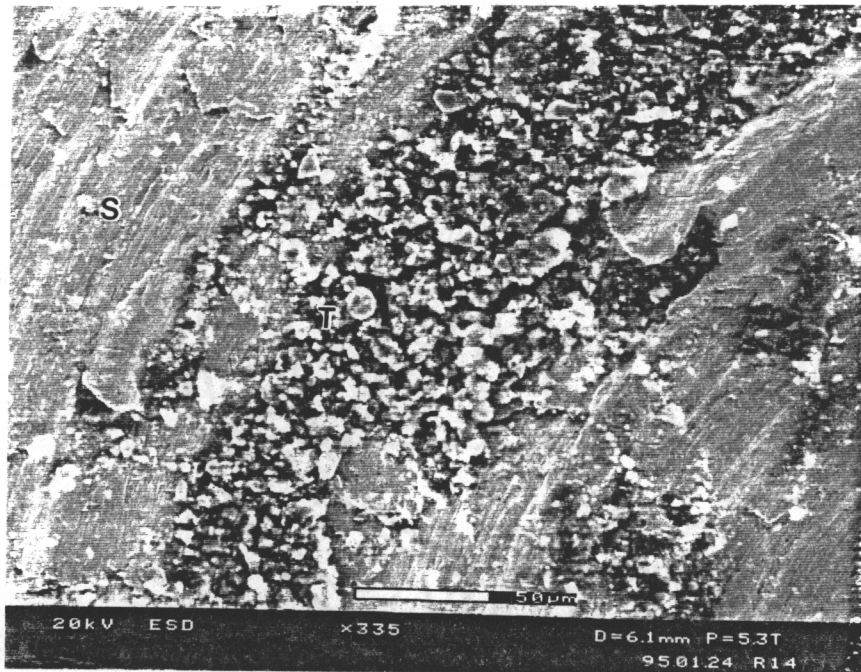


Figure 39: Cement trace (T) bonded to steel rod (S) for Group G_{tannic} at X335.

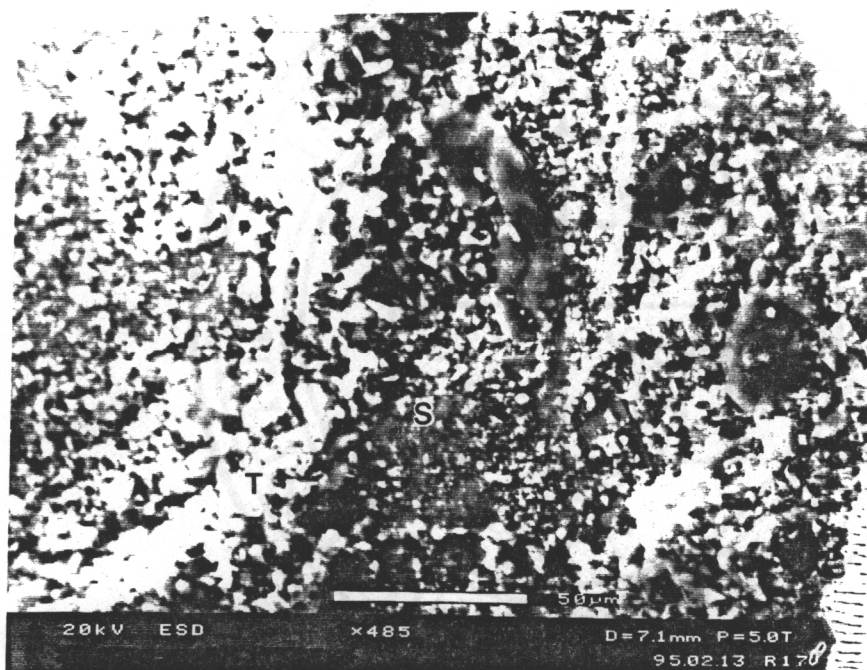


Figure 40: Cement (T) still bonded to etched enamel (S) for Group U_{Tannic} at X485.

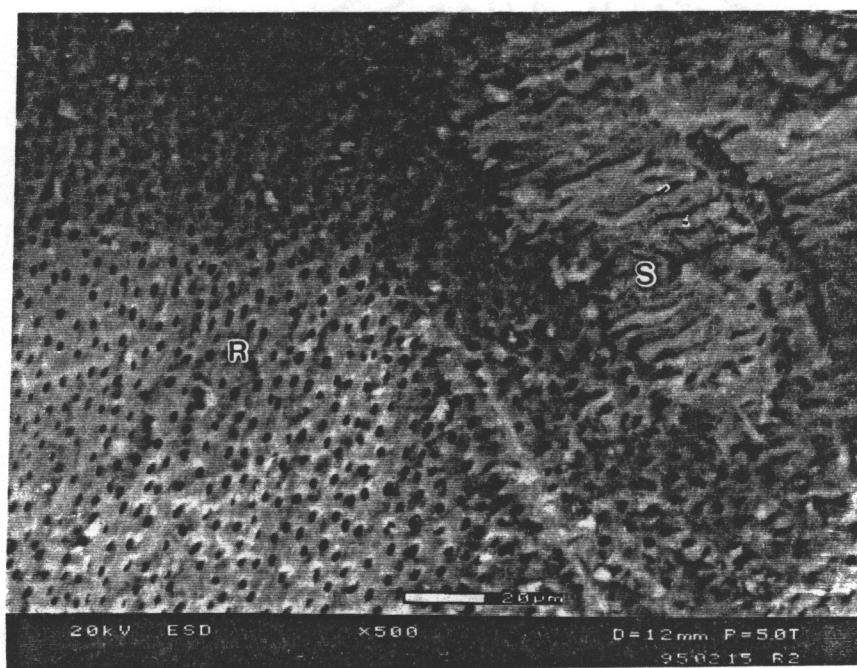


Figure 41: Cement trace (S) bonded to etched dentin (R) for Group U_{Tannic} at X500.

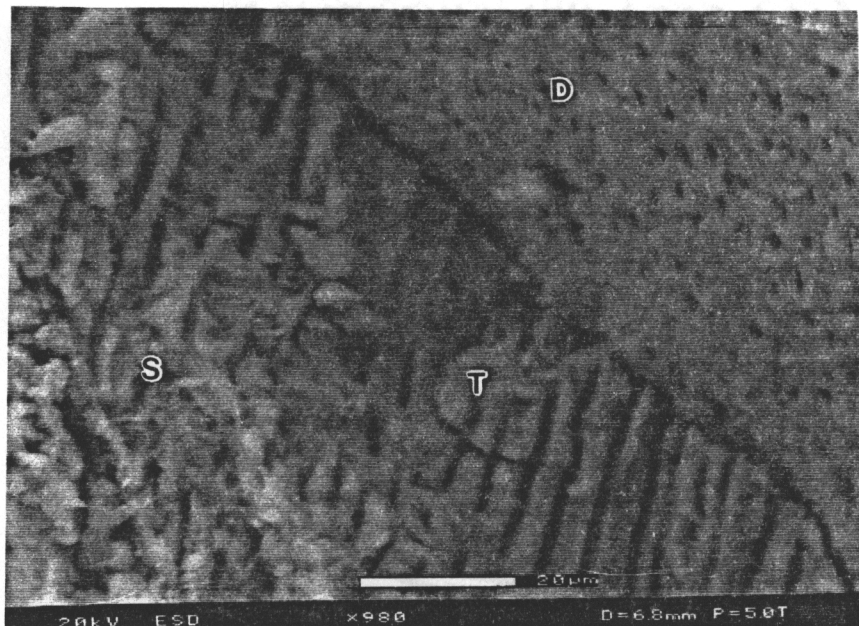


Figure 42: Dentin surface, including small pores (D), longitudinal tubules, and cement debris (S) shown for Group G_{tannic} at X980.

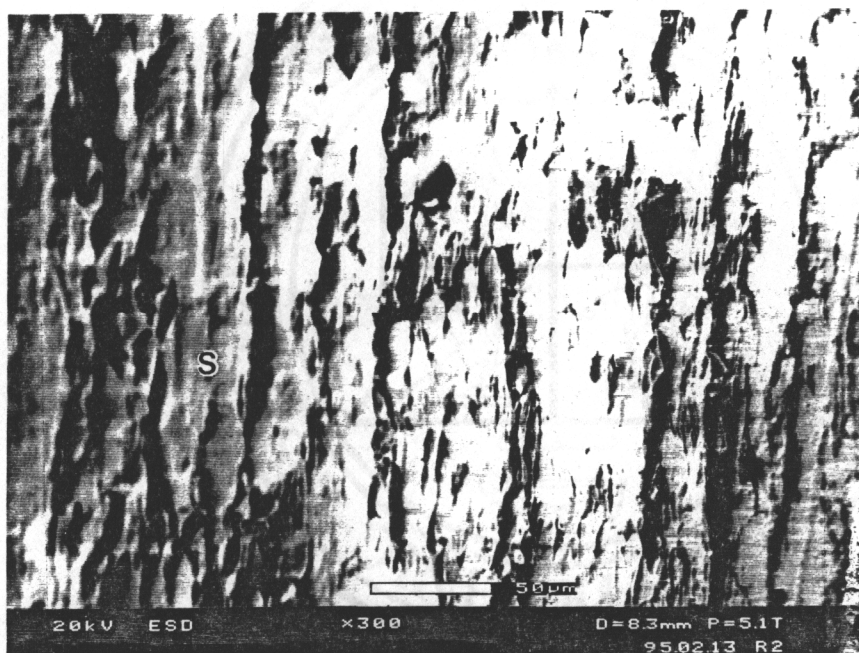


Figure 43: Micrograph of steel rod (S) for Group D₄₈ at X300.

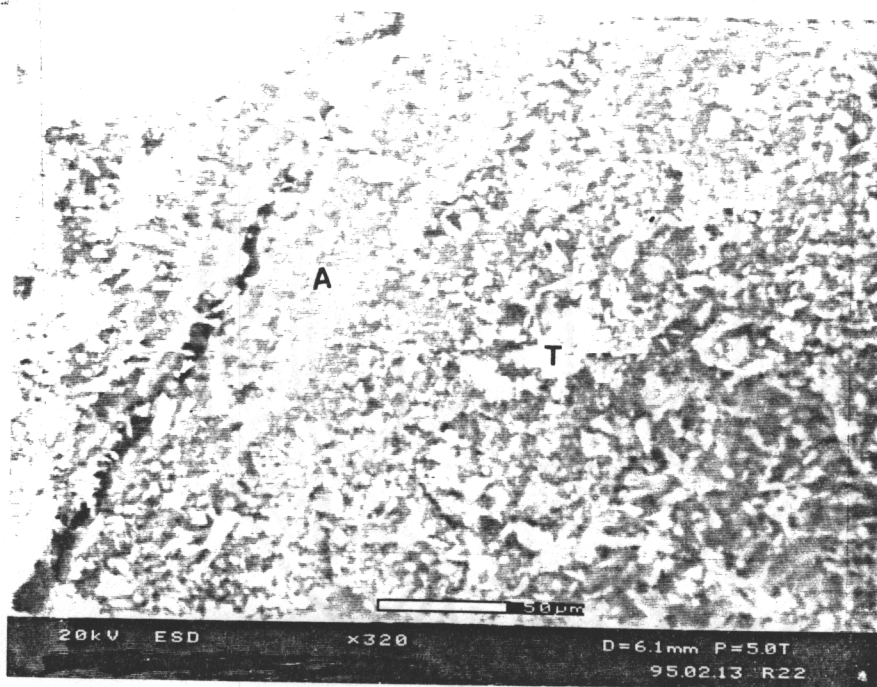


Figure 44: Cement debris (T) covering enamel surface (A) for Group D₄₈ at X320.

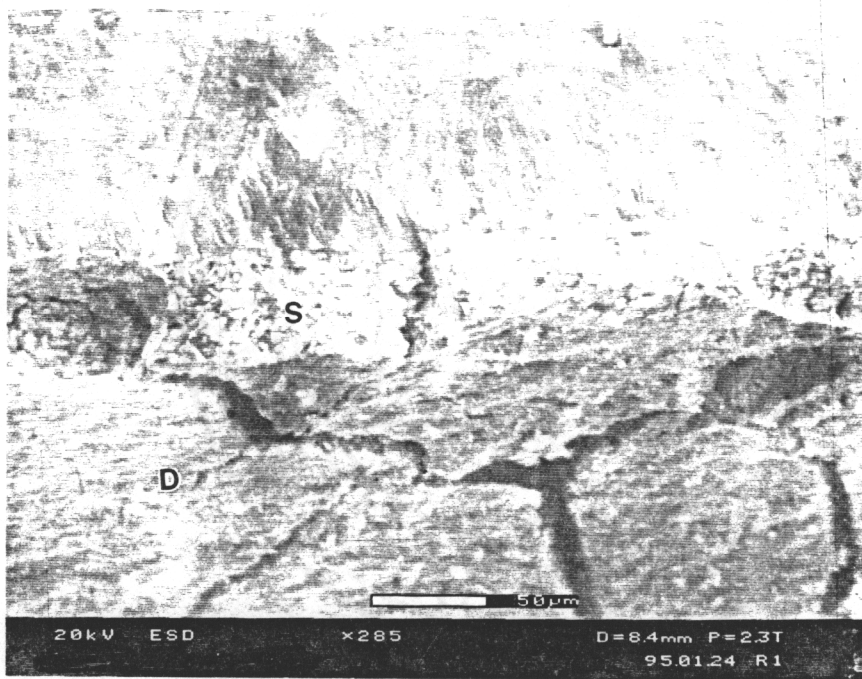


Figure 45: Cement debris (S) covering dentin surface (D) for Group D₄₈ at X285.

3.4.Glass-Ionomer Cement (VitrebondTM):

3.4.1. Chemical properties:

3.4.1.1. Contact angle measurements:

The average and standard deviation of the contact angles of water and methylene iodide for each cement sample mixture at different ratios were measured and are summarized in Table 20. Using these results, the polar, dispersive components of the surface tension and the total surface tension were calculated by applying the relationship 12. All these results are listed in Table 21. In addition, by increasing the liquid fraction in the cement, the contact angle of water on the cement decreases reflecting a rise in the polar surface tension. However there is no significant change in the contact angle of methylene iodide. The rise in the liquid fraction in the cement paste results in better wetting as evidenced by the decrease in the contact angle made with the polar component and the corresponding rise in the polar surface tension.

3.4.1.2. Fourier transform infrared spectroscopy (FTIR):

The absorbance spectra of the dental cement formed from the aluminosilicate glass and aqueous polyacrylic acid, after one hour of setting time, are reported in Appendix (B). The glass, liquid and the mixtures with solid/liquid ratios of 60/40, 50/50 and 40/60 are amenable to analysis by infrared spectroscopy. This technique is used to characterize the vibrational mode of the cement as the solid/liquid ratios changes. The stretching and bending vibrational modes of the liquid and the powder spectra as well as their corresponding frequencies in cm^{-1} are listed in Table 22.

Table 20: Average contact angle measurements of water and methylene iodide for each cement mixed ratio.

Powder/Liquid ratio	Average θ_1 (water)	Average θ_2 (Methylene Iodide)
60/40	31 ⁰ (± 6)	32 ⁰ (± 2)
55/45	19 ⁰ (± 5)	36 ⁰ (± 3)
50/50	17 ⁰ (± 3)	43 ⁰ (± 5)
45/55	20 ⁰ (± 1)	44 ⁰ (± 4)
40/60	21 ⁰ (± 2)	43 ⁰ (± 5)

Table 21: Average surface tension components for each cement mixed ratio.

Powder/Liquid Ratio	Polar γ_s^p dyne/cm	Dispersive γ_s^d dyne/cm	Total γ_s dyne/cm
60/40	35 (± 4)	29 (± 2)	63 (± 2)
55/45	43 (± 1)	26 (± 1)	68 (± 0.5)
50/50	46 (± 2)	25 (± 0.5)	71 (± 2)
45/55	46 (± 2)	25 (± 0.5)	71 (± 2)
40/60	45 (± 4)	25. (± 1)	70 (± 2)

Upon mixing the cement and letting it set for an hour, IR analysis revealed a peak at 1170 cm^{-1} representing C-C stretching, and a peak at 1635 cm^{-1} representing C=C stretching. As the powder and the liquid cure by the photoinitiated reaction, crosslinking occurs through the polymerization of pendant vinyl groups, which can be observed by following the decrease of IR peak absorbance in the spectral region of 1635 cm^{-1} and the increase of IR peak absorbance in the spectral region of 1170 cm^{-1} . By comparing the ratio of C-C to C=C IR peak absorbance values for each cement ratio, the highest ratio was obtained for the formulation containing the highest glass fraction in the cement. This data shows that the highest degree of cure results by using a higher weight percentage of glass, and the lowest was for the system possessing the highest liquid fraction.

3.4.2. Thermal properties:

3.4.2.1. Thermogravimetric analysis (TGA):

Thermal characterization of each sample fraction was done using Thermogravimetric Analysis (TGA). A plot of weight percent loss vs. temperature from 35°C to 455°C was obtained as shown in Figure 46 for each of the samples. The TGA thermogram shows a fairly rapid weight loss from 35°C to 150°C representing water and possibly unpolymerized HEMA as indicated by the infrared spectroscopy. Around 100°C the 40/60 ratio has 10.4 % weight loss total or a 17.3% weight loss relative to the liquid while the 60/40 ratio has 5.37% or a 13.4% weight loss relative to the liquid. From 150°C to 350°C the decreased slope indicates a decrease in the rate of the volatile loss. At these higher temperatures, depolymerization may result from the weight loss observations. For example, depolymerization would result in acrylic acid being produced which boils at 142°C . Above 350°C the slope is indicative of the rapid weight loss resulting from the decomposition of the organic component of cement mixture. The percent char yield for each cement sample ratio at 455°C is shown in Table 23. The highest 60/40 residual

Table 22: Vibrational modes and frequencies for the liquid and powder Vitrebond™ [50].

Liquid	Vibrational Mode	Frequency (cm ⁻¹)
C=C	Stretching	1630
C-C	Stretching	1182
C-O	Stretching	1300-1321
O-H	Bending	1405
CH ₃	Asymetrical Bending	1455
C=O	Stretching	1715
O-H	Stretching	2956
C-H	Stretching	2956
Glass (Si-O)	Stretching	968

Table 23: Percentage char yield for each cement ratio at 455° C.

Cement Ratio (Powder/Liquid)	% Weight Left at 450° C
60/40	71%
55/45	70%
50/50	67%
45/55	62%
40/60	57%

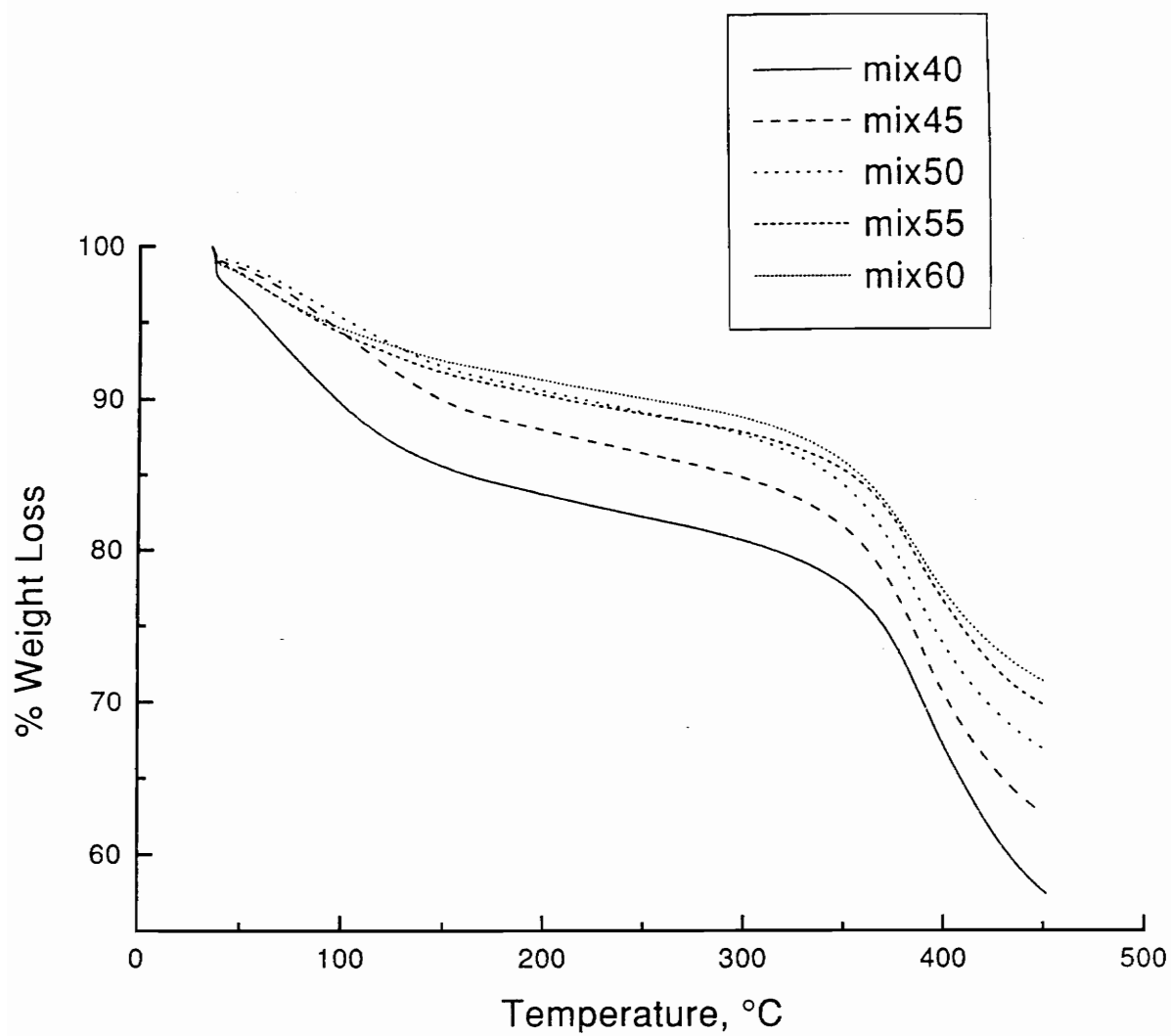


Figure 46: TGA plot for each cement sample ratio.

weight while the 40/60 has the lowest. The greater % weight loss corresponds with increasing weight percentage of liquid in the cement.

3.4.3.Mechanical properties:

3.4.3.1.Hardness measurements:

The average Vickers hardness at varied loads, and its standard deviation, are determined for each cement ratio using equation (8). These values are shown in Table 24. By increasing the load from 100g to 300g for each sample, the average hardness for each sample ratio decreases as noticed in Table 24. Visual cracks were observed at 300g.

The cement softened with decreasing glass fraction in the cement. The excess of the liquid fraction in the cement may plasticize the cement lowering its stiffness. The liquid additive may also prolong the setting time, thereby, lowering the apparent hardness. The highest average hardness is obtained for the 60/40 ratio. In this case, if tested at the same time after mixing, larger fraction of the cement grains may cause the paste to dry out in a shorter period of time increasing hardness. The variation of hardness within each ratio was significant especially for the 60/40 ratio.

Table 24: Average hardness of each cement sample at varying mix ratio, cured for one hour as a function of loading.

Powder/ Liquid Ratio	Average Hv 100g	Average Hv 200g	Average Hv 300g
60/40	127 (± 26)	90 (± 6)	74 (± 10)
55/45	81 (± 5)	72 (± 5)	62 (± 8)
50/50	70 (± 5)	65 (± 6)	61 (± 5)
45/55	70 (± 5)	66 (± 6)	61 (± 5)
40/60	28 (± 3)	21 (± 3)	12 (± 2)

4. Discussion:

4.1. Dentin quality discussion:

4.1.1. Contact angle measurements:

4.1.1.1. Comparison between the unetched and etched dentin specimens:

Acid etching resulted in lower measured contact angles using water on dentin. Sulfuric acid also reduced the measured contact angle of methylene iodide on dentin. These results could arise from either changes in the surface chemistry or the surface morphology of dentin. Dentinal surface wetting is affected by the acidity in the etchant. Wetting may be also affected by the hydrophobic-hydrophilic balance on the dentin surface due the pH of the acid solution used. Furthermore, etching increases dentin roughness, thereby leading to better wetting. From the optical microscopy results, pores on the surface of dentin associated with collagen tubules were observed when etched with sulfuric and tannic acids. It is more likely that the one minute acid treatment removes dentin smear layer and increases the roughness of the dentin surface. The rougher topography of the etched dentin for one minute with 20% tannic acid and 8.5 % sulfuric acid may enhance wetting.

The dispersive contact angles measured on untreated dentin are similar to Baier's values [7]. The polar contact angles measured on untreated dentin are higher than Baier's values. This may be associated with the difference between bovine dentin and human dentin composition, the time of extraction, the effect of storage, humidity, or dentin surface contamination [1,5,7,27,28,29]. Moreover, the contact angles we found in tannic and sulfuric acid treated surface are quite lower than measured by Baier's who used different etchants. In addition to the reasons cited above, acid exposure time, the level of acidity, concentration, or the acids dissociation characteristics in the solution may contribute to these changes[7]. This present study is in accordance with Baier's Chang,

and others who demonstrated that dentin etching render the dentin surface more wettable, and rougher both of which are more likely in favor better adhesion [1,7,35,66].

4.1.1.2. Thermally aged dentin specimens:

The observed contact angle of the methylene iodide droplet on denatured surface dentin specimens changes with the aging time. The average calculated contact angle of methylene iodide is lower than its standard deviation. The precision in the measurements was poor. It was assumed that the methylene iodide droplet was being absorbed in bulk. By dehydrating dentin specimens, water loss increases the hydrophobicity of dentin and improves the interaction of the methylene iodide with dentin. In addition, microvoids and microcracks were observed on dentin samples exposed at 65°C, allowing an easier pathway for absorption of methylene iodide. Figure 10 illustrates the microcracks occurring in dentin after 24 hours of denaturing time. Schwartz and Galligan also suggested that dentin became more hydrophobic when allowed to age in the dry state [1] which agrees with this study.

Finally the work of adhesion results of the aged dentin specimens compared to the initial and the etched ones showed that the forces of attraction between the water of the initial and etched specimens are greater than those of the aged ones. Again this likely related to the hydrophobic behavior of dentin when dehydrated.

4.1.2. Hardness measurements:

4.1.2.1. Comparison between the unetched and etched dentin specimens:

This study has demonstrated that the average dentin hardness decreased monotonically from 76(\pm 3) Hv to 68(\pm 1) Hv and 61(\pm 4) Hv upon etching with tannic and sulfuric acid for 60 sec respectively. Additional etching for 15 sec with tannic and sulfuric acid cause a decrease in dentin hardness to 42% and 33% from its original value, respectively. The dentin surface is softened with etching. The present study is in accordance with those of Moon et al, and Paghnini et al. who reported that a significant

loss of surface hardness can occur in 15 sec using phosphoric and citric acids as shown as Table 10 [8,9]. The present values are lower than Paghini's hardness values. The difference of etchants, the composition of the tooth and the storage effects are likely variants in the absolute hardness values [1,5,7,27,28,29]. Tannic and sulfuric acid show similar etching effects on the hardness like citric and phosphoric acid. Therefore etching causes dentin surface demineralization by lowering calcium concentration and reducing the dentin hardness.

4.1.2.2. Thermally aged dentin specimens:

Drying studies were conducted to reveal information about the change in the dentin hardness. Dehydrated dentin exhibited a decrease in the average dentin hardness. The loss of water content in the dentin was one reason that dentin hardness was affected. After rehydration, the dentin hardness partially recovered. Water must be a factor influencing the hardness recovery of dentin. Furthermore, the stability of the organic matrix may be affected at 65°C because dentin hardness recovery was not complete. Collagen fibers may be crosslinked at this temperature. Caldwell and et al. suggested that hardness decreases with aging which resulted in a surface "softening" of enamel [41]. Totah suggested that that dentin hardness scale increases with drying [43]. There is a contradiction between these studies because enamel is harder than dentin [1,2,19], it is likely that dentin will also "soften" with aging.

The controversy in hardness results may suggest that neither enamel nor dentin really "soften" with aging. These tissues may embrittle upon dehydration. Therefore hardness testing does not really tell if the material is softened simply because the hardness value decreases. This statement is supported by Figure 10 where major cracks were seen on the surface of aged samples prior to hardness testing, indicating embrittlement. These cracks on the surface of dentin may lower the apparent hardness values. Neither Totah nor Caldwell described the dentin surface morphology prior to hardness testing [41,43].

The hardness values increased again upon rehydration for two days but did not recover their original values before denaturing. This may also be associated with permanent damage that results upon dehydration.

4.2. Torsional testing:

4.2.1. Effects of etching on unground and ground teeth:

From the average tensile strength for unetched specimens drawn from Wilson's study as shown in Table 5, enamel and dentin had almost the same tensile bond strength which contradicts that obtained from this study [62]. When the enamel wall is not ground, the average torsional shear strength value was higher than when it was removed. The difference in these results may be associated with the geometry of the tests, and the assumption made in equation (VI). Torsional testing may give a better control of stress situation. The difference in results may also be associated with the preparation method, and cement thickness which depends on the rod location. The mechanical properties and chemical composition of Vitrebond are different than the ASPA cement used by Wilson [62]. The bond strengths of Vitrebond to enamel and dentin in this study are higher than ASPA cement. The finding that tannic acid increased the bond strength of Vitrebond to dentin agrees with Wilson [62] but not with Evje [11]. Nonetheless, the average values of the torsional shear strength for etched specimens were twice that measured by Wilson. This again may be associated with the difference in test geometry using different load direction, and the utilization of a different cement brand. The dentin bond strength values found in this study are lower than these found by Mitra. Besides the difference in the test geometry, Mitra exposed Vitrebond to a visible-light source. In this study, Vitrebond cement was self-cured before debonding [48].

Chiba et al. as well as Paghini have already suggested that the surface hardness decreases upon etching which leads to lower dentin bond strength [9,10]. From this study, tannic and sulfuric acid have been shown to decrease the dentin hardness, but they do not lower the dentin bond strength upon etching. This may be associated with the difference in the acid chosen and the exposure time, itself. According to another study [6], if the dentin is etched prior to cement bonding, the calcium ions are separated from the dentin apatite and the possibility of bonding between the carboxylic acid groups of poly (alkenoic acid) and the acid groups of both apatite and collagen is decreased. It

seems that mechanical interlocking and wetting to etched dentin surface were the main reasons for enhanced adhesion. There is also the possibility that the concentrations of tannic and sulfuric acid do not completely demineralize the dentin surface prior to adhesion testing. In this case, chemical interactions must also contribute.

4.2.2. Effects of thermal aging on enamel and dentin bond strength:

The finding that thermal exposure of dentin decreases the adhesion of glass-ionomer cement with dentin agrees with Maldonado[63]. Contrary to Maldonado, the adhesion of glass-ionomer cement to enamel decreases upon thermal exposure. This may be associated with the difference in the procedures. The present study is in accordance with those Jameson et.al who indicated that dentin prior to adhesion bonding induces a brittle behavior [14]. In accordance with their study, our study was an indirect study of the enamel. This may suggests that both enamel and dentin also show a brittle behavior upon thermal exposure which was observed under ESEM.

4.2.3. Effects of mixing ratios on enamel and dentin bond strengths:

A variation in the powder/liquid ratio affected significantly the bond strength of enamel and dentin. According to 3M, the recommended powder to liquid ratio is 1 to 1.4 by weight [17]. The highest bond strength values obtained for enamel and dentin are between 1 to 1.23 powder to liquid ratio. By increasing the powder to liquid ratio from 1.23 to 1.5 the bond strength decreases at least 20%. To obtain a maximum bond strength, the powder to liquid ratio has to be in the range of 1 to 1.3.

4.3. ESEM analysis:

The mechanism of adhesive failure was difficult to detect due to the procedure done after torsional testing. The cavity was cut longitudinally and ground on the edge of the cavity after failure and prior to ESEM evaluations. Grinding exposed dentin and enamel to humid environment and heat. The glass-ionomer cement may have debonded from enamel and dentin during grinding. The steel rod was not treated with any chemical

solvent prior to adhesion testing. The steel rod may be also contaminated and may effect the mechanism of failure. These two effects should be taken into consideration when analyzing the failure mechanism. The fact to be considered in the ESEM study is that the strength of the cement-bond stainless steel was greater than the strength of the cement tooth bond. From the ESEM results, the enamel exhibits cohesive failure within the cement except for the aged ones. Dentin exhibit an adhesive and cohesive failure for most of the cases. Contrary to Smith, part of the cement was removed from the tubules for most of the cases [16]. In accordance with Charlton [65], the majority of dentin failure is a combination of both cohesive and adhesive failure. However the failure for aged teeth samples is unexplainable because no trace of cement was seen on the rod. It is more likely that the steel rod was contaminated prior to adhesion testing. Debris of cement was left on the enamel and dentin. Major cracks were observed on those enamel and dentin samples showing a brittle behavior. Flaws may be created during thermal exposure and prior to adhesive testing.

4.4. Glass-ionomer cement properties (Vitrebond^{T.M}):

4.4.1. Chemical and thermal properties:

In order to obtain wetting, the surface free energy of the liquid adhesive has to be less than the surface free energy of the dentin [6]. The results obtained from the contact angle measurements on the cement paste show that the surface free energy of the cured adhesive is greater than the surface free energy of dentin. In addition, these results show that the cement paste became more hydrophilic when the liquid fraction is increased in the paste. This is probably due to an increase in the content of water and HEMA in the cement paste. However, the contact angle measurements were taken after the cement paste cured. It is likely that the thermodynamic properties of the adhesive changes from pre-cured state to the cured state. Thus, the contact angle results may not be completely valid and, therefore, the extent of adhesive wetting on dentin cannot be concluded from this study.

The infrared spectroscopic studies show that the cement paste becomes less crosslinked when the fraction of liquid increases in the paste. This means that vinyl groups, (pendant or from HEMA), have not all reacted. This suggests that the presence of the powder, somehow facilitates the photoinitiated curing reaction to some extent. The IR studies indicate that the reaction of the vinyl groups in the cement is more complete when the liquid fraction in the cement is decreased. The TGA analyses support this finding since the highest weight loss was obtained for the highest liquid fraction in the cement.

4.4.2. Mechanical properties:

An increase in the powder to liquid ratio led to increases in the superficial hardness of the paste. This means that the paste becomes stiffer, and higher strength is achieved. This finding agrees with Crisp's study who demonstrated that cement hardness increases at higher powder fraction in the cement paste. Visual cracks were observed on each sample surfaces at 300g. The cracks may initiate at 200g. At 300g, the cracks may already propagate. Brittle fracture, may occur for the 60/40, 55/45, and 50/50 ratio. In addition brittle fracture preceded by a little plastic deformation may occur for the 45/55 and 40/60 ratios. Thus, as the cement separates along the cracks, new surfaces may be created [67]. This may affect the changes in the hardness readings at 200g and 300g.

4.4.3. Effects of cement mixing properties on enamel and dentin bond strength:

By increasing the fraction of the powder in the paste from 55% to 60 % by weight, the bond strength decreases at least 20%. From the hardness test observations, the cement paste becomes brittle which is more sensitive to stress concentration when subjected to a bond strength test. However by increasing the fraction of the liquid in the paste from 45 % to 60% by weight, the bond strength decreases at least 17%. This may be associated with the unpolymerized HEMA detected from the IR results. The unreacted HEMA may act as plasticizer reflecting a decrease in the torsional bond strength.

5. Conclusions:

5.1. Summary:

The initial thrust of this study was to evaluate the effects of 20% w/w tannic acid and 8.5 % w/w sulfuric acid on dentin wettability and hardness, and to evaluate the effects of thermal aging and rehydration on dentin prior to adhesive bonding. From this study it was found that:

- Acid treatment of the dentin surface results in three effects:
 1. Changes in the hydrophobic-hydrophilic balance of dentin surface.
 2. Roughening of the dentin surface.
 3. Decreasing the dentin hardness.

- Thermal aging and rehydration on dentin results in:
 1. Decreasing dentin surface hydrophilicity .
 2. Identifiable cracks on dentin surface indicating a brittle behavior. While rehydration partially restores dentin toughness.

A second thrust was to use torsional testing to gauge bonding characteristics to dentin subjected a number of process conditions, and to analyze the mechanism of failure. Torsional testing was also utilized to identify the effects of Vitrebond^{T.M} mixing ratios on bonding. This research has found that:

- Higher bond strengths are obtained for unground teeth. This is attributed to greater mechanical interlocking and more chemical interactions when the enamel wall is not removed. Enamel is essential for better adhesion.

- Tannic acid acts as a hydrating conditioner increasing the bond strength of unground teeth after thermal exposure.
- Weaker strengths are measured for ground teeth. This is related to lower mechanical interlocking and lower chemical interaction within dentin. In addition, the cement may infiltrate poorly to the smear layer covering the dentin.
- Acid treatment enhances adhesion to both enamel and dentin.
- Cohesive failures within the cement are mostly observed during enamel debonding procedure. Adhesive and cohesive failures are detected during dentin debonding procedure.
- Inappropriate mixing decreases the bond strength of the cement to both enamel and dentin.

A third thrust was to evaluate the properties of the dental cement at different mixing ratios in order to provide a better understanding how improper cement mixing affects adhesion. From the experimental plan it was found that:

- The cement paste shows a brittle behavior as the powder fraction increases in the cement. This behavior is not enhancing adhesion. Excesses of liquid in the paste leads to incomplete polymerization of HEMA in the paste. This results in lower adhesion.

5.2. Future Work:

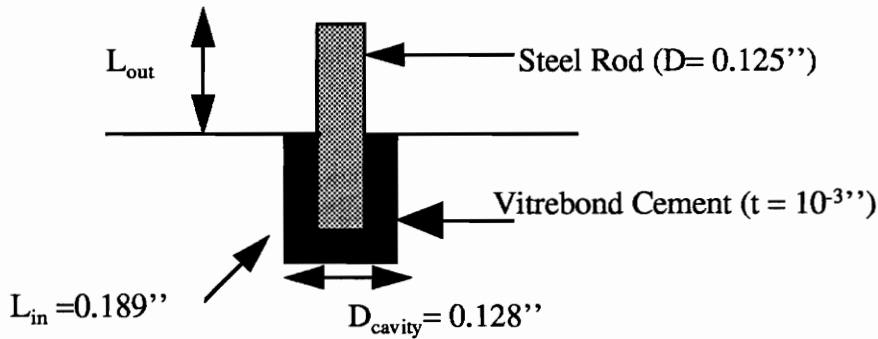
In proceeding with further research, additional experiments must be performed:

- Studying the effects of tannic acid and sulfuric acid on dentin surface wettability and hardness by prolonging the etching time and measuring its effect on dentin bond strength.
- Curing the glass-ionomer cement using a visible light prior to the adhesion test.

- Treating the steel rod with chemical agents such as phosphoric acid followed by acetone or abrasive agents such as alumina blasted prior to the adhesion test.
- Improving the fixturing of the torsional testing.
- Determining the contact angles of the cement paste at different mixing ratios before curing.
- Studying the kinetic properties of the glass- ionomer cement at different mixing ratios in order to give better understanding of working times of these cements.

Appendix A:
Torsional Shear Strength Derivation

The torsional shear strength is derived from the following equations, given the geometry in Figure 11. One assumption in this derivation is made is that the stress at the bottom area of the cylinder is neglected . The bottom area is determined to be around 15% of the overall cylinder area. The rod was adjusted in the center of the cavity.



$$T = F * r \quad (\text{I})$$

where T is the torque at failure in N.m, F is the force in N, and r is the radius of the rod in m [68].

$$T / r = F \quad (\text{II})$$

$$F = \tau * A \quad (\text{III})$$

where τ is the torsional shear strength in MPa, A is the area of the rod in m^2 [69].

Replace (III) in (II)

$$\tau * A = T / r \quad (\text{IV})$$

$$A = \pi * (D) * L_{\text{in}} \quad (\text{V})$$

where D is the diameter of the rod in m, and L_{in} is the length of the steel rod in the cavity in m.

Replace (V) in (IV)

$$\begin{aligned} \tau &= T * / (D) / 2 * [\pi * (D) * L_{\text{in}}] \\ \tau &= 2 * T / \pi * (D)^2 * L_{\text{in}} \end{aligned} \quad (\text{VI})$$

Appendix B:

Infrared Spectra

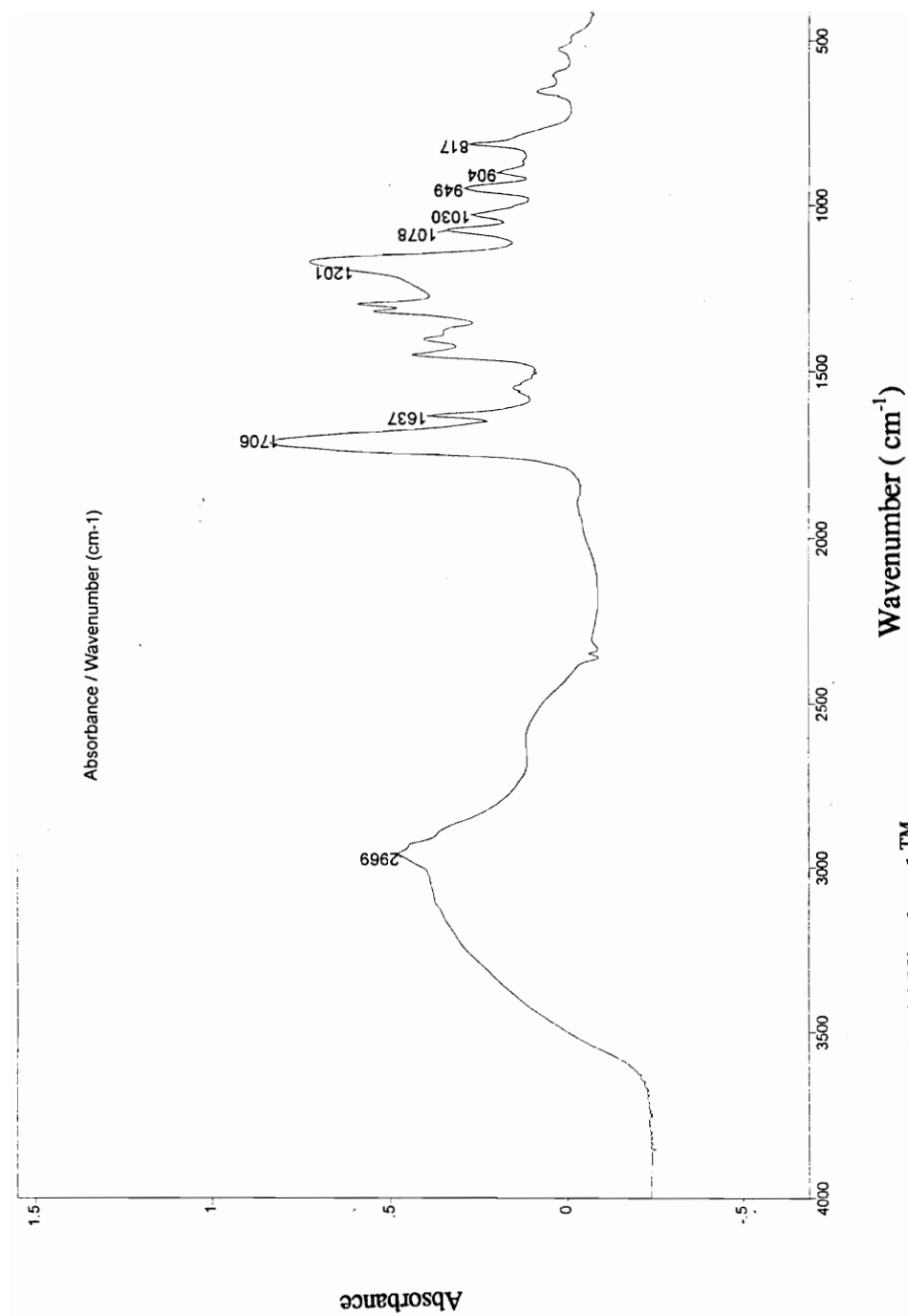


Figure 47: Liquid Vitrebond™ spectrum.

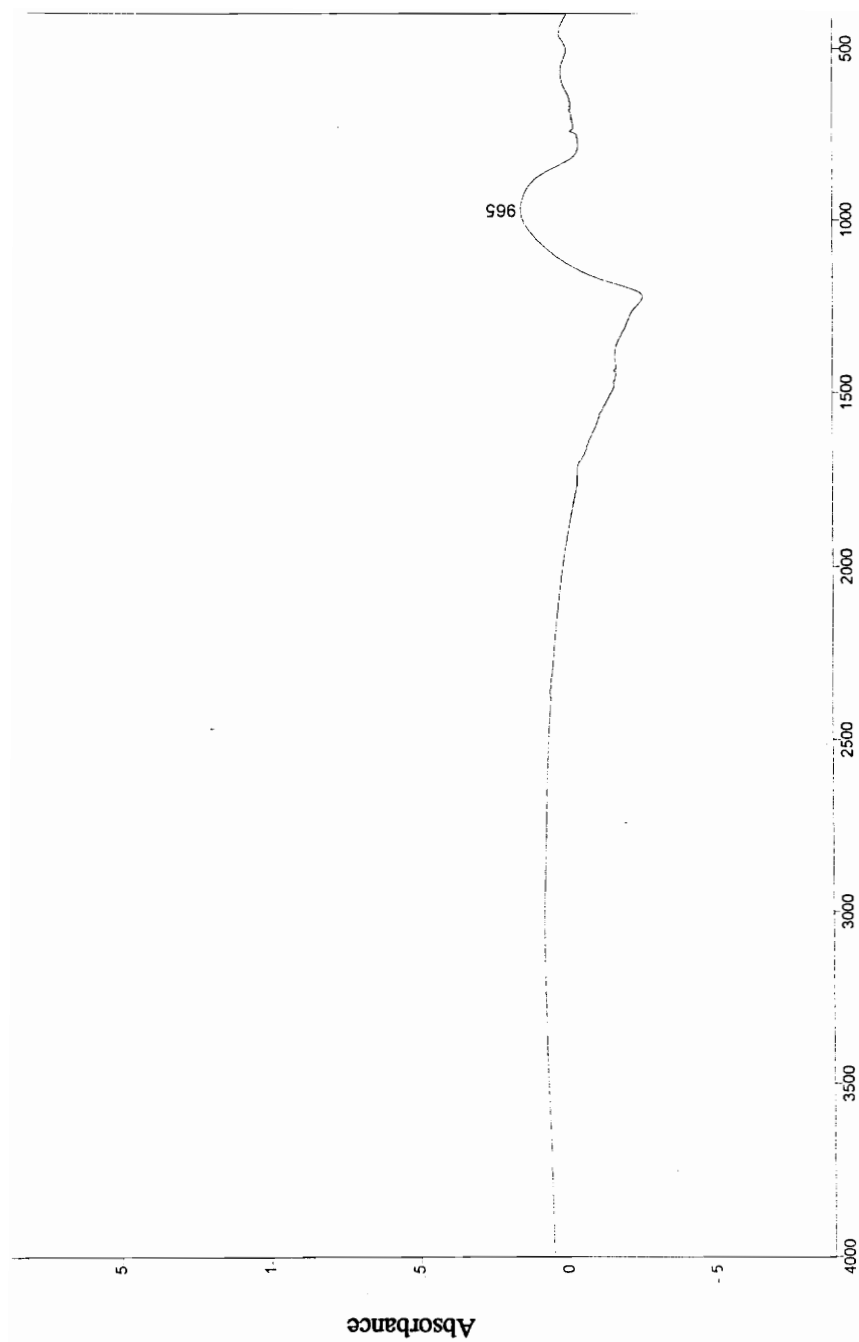


Figure 48: Powder Vitrebond™ spectrum.

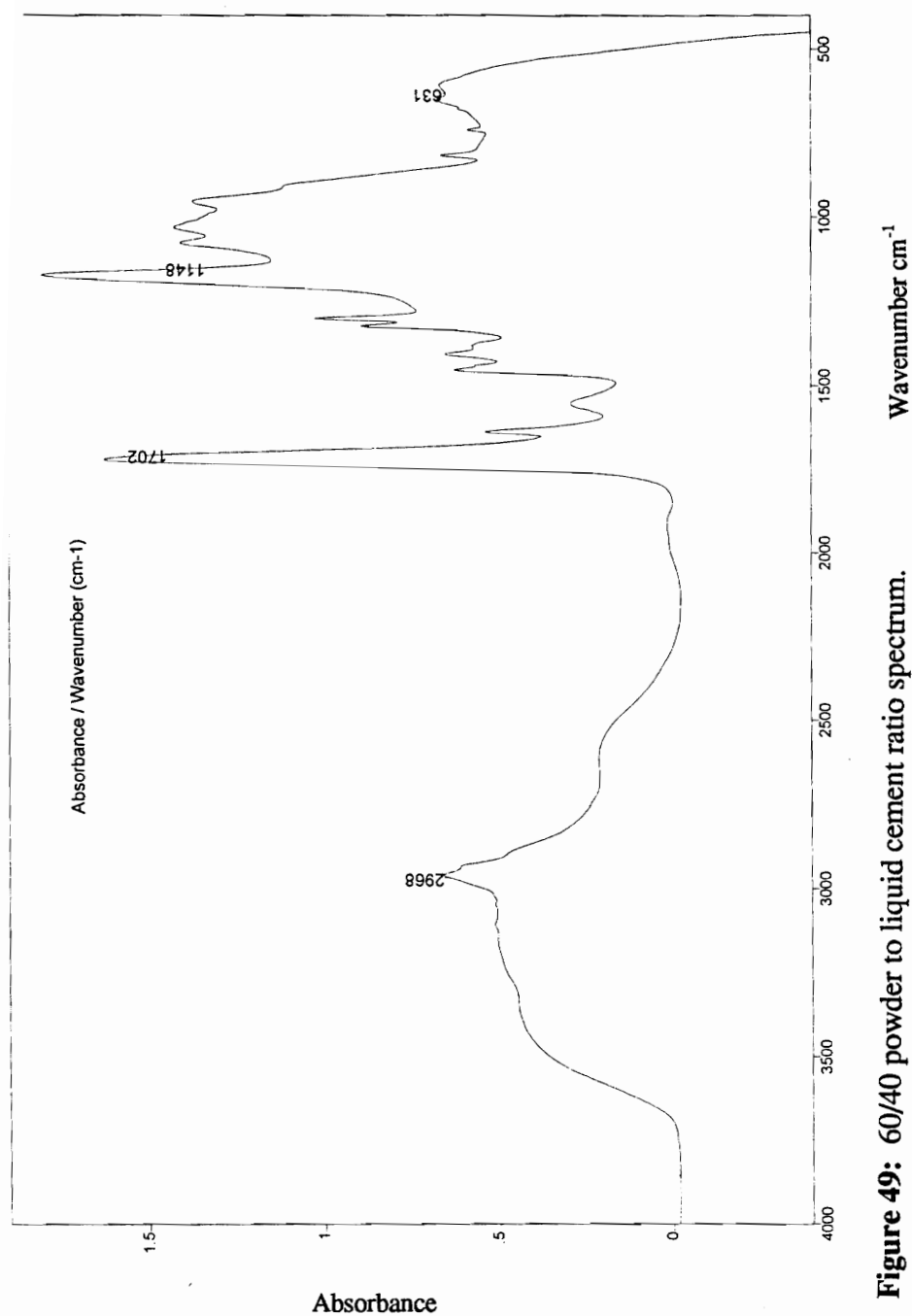


Figure 49: 60/40 powder to liquid cement ratio spectrum.

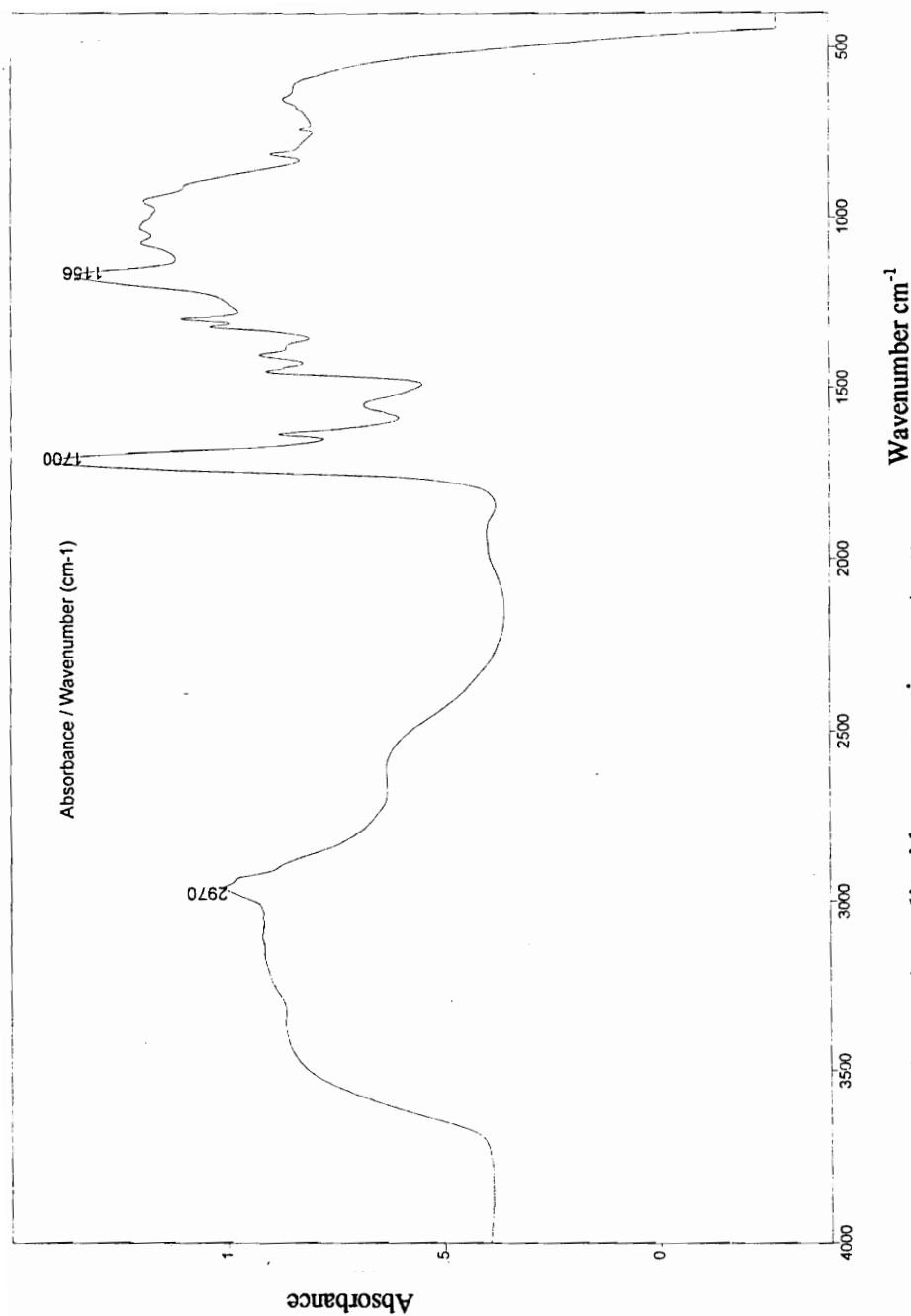


Figure 50: 50/50 powder to liquid cement ratio spectrum.

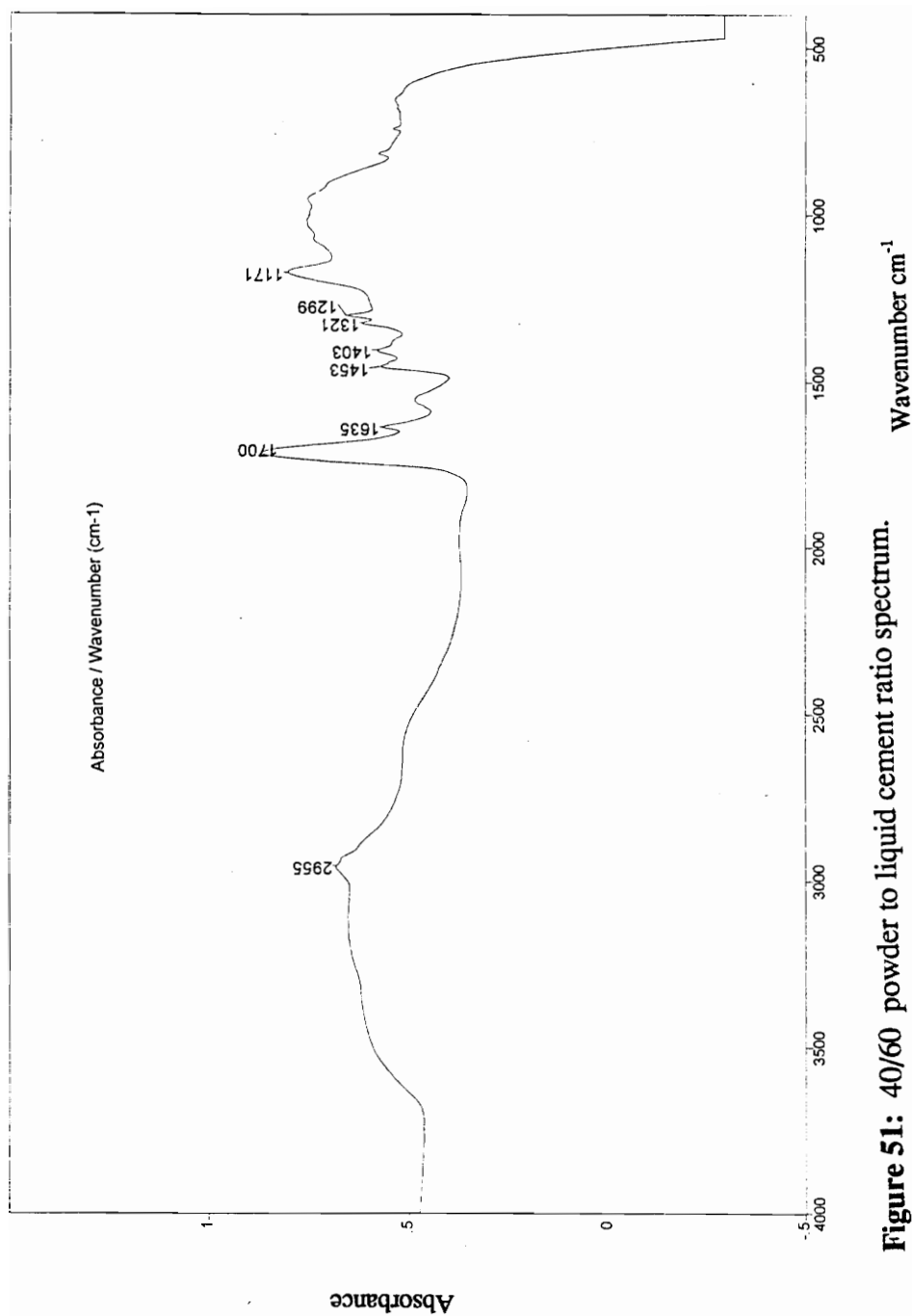


Figure 51: 40/60 powder to liquid cement ratio spectrum.

References

- 1: Hair, M. L., The Chemistry of Biosurfaces, Volume 2, Marcel Dekker, New York, pp. 732-770,(1972).
- 2: Retief, D. H., "Clinical Applications of Enamel Adhesives", *Operative Dentistry*, **5**, pp. 44-49, (1992).
- 3: Barkmeier, W. W., Cooley, L., "Laboratory Evaluation of Adhesive Systems", *Operative Dentistry*, **5**, pp. 50-61, (1992).
- 4: Soderholm, K. J. M., "Group Report", *Dental Materials*, **7** (22), pp. 74-83, (1991).
- 5: Watanabe, I., Nakabayashi, N., "Measurement Methods for Adhesion to Dentine: The Current Status in Japan", *Journal of Dentistry*, **22** (2), pp. 67-71, (1994).
- 6: Ruyter, I. E., "The Chemistry of Adhesive Agents", *Operative Dentistry*, **5**, pp.32-43, (1992).
- 7: Baier, R. E., "Principles of Adhesion", *Operative Dentistry*, **5**, pp. 1-9, (1992).
- 8: Moon, P. C., Davenport, W. L., "Microhardness of Acid-Etched Dentin", *Journal of Dental Research*, **55**, p. 910, (1976).
- 9: Paghini, M., G'Sell, C., "Tooth Microstructure and Composite Adhesion", *Journal of Biomedical Materials Research*, **27**, pp. 975-981, (1993).
- 10: Erickson, R. L., Surface Interactions of Dentin Adhesive Materials, *Operative Dentistry*, **5**, pp. 81-94, (1992).
- 11: Evje, Ø. G. A., "Bend Test for Measuring Cement-Dentin Bond", *Dental Materials*, **4**, pp. 98-102, (1988).
- 12: Renson, C. E., "Scanning Electron Microscopy of Human Dentine Specimens Fractured in Bend and Torsion Tests", *Archives Oral Biology*, **19**, pp. 447-449, (1974).

- 13: Morse, R. D., "Age-Related Changes of the Dentin Pulp Complex and Their Relationship to Systematic Aging", *Oral. Surg. Med. Pathol*, **72**, pp. 721-745, (1991).
- 14: Jameson, M. W., Hood, J. A. A., Tidmarsh, B. G., "The Effects of Dehydration and Rehydration on Some Mechanical Properties of Human Dentine", *Journal of Biomechanics*, **26 (9)**, pp. 1065-1067, (1993).
- 15: Van Der Graaf, E. R., Bosch, J. J., "Changes in Dimensions and Weight of Human Dentine After Different Drying Procedures and During Subsequent Rehydration", *Archives Oral Biology*, **38 (1)**, pp. 97-99, (1993).
- 16: Smith, D. C., "Polyacrylic Acid-Based Cements Adhesion to Enamel and Dentin", *Operative Dentistry*, **5**, pp. 177-183, (1992).
- 17: Vitrebond, Manufacturer's Information, 3M Center, St Paul, Minnesota 55144-1000.
- 18: Pearson, J. C., "Physical Properties of Glass-Ionomer Cements Influencing Clinical Performance", *Clinical Materials*, **7**, pp. 325-332, (1991).
- 19: Park, J., Lakes, R., Biomaterials, an Introduction, pp.186-187, 195-196, (1992).
- 20: Gwninett, A. J., "Structure and Composition of Enamel", *Operative Dentistry*, **5**, pp.10-17, (1992).
- 21: March, P., Martin, M., Oral Microbiology Second Edition, Van Nostrand Reinhold (UK), pp. 1-5, 1994.
- 22: Phillips, R. W., Elements Of Dental Materials For Dental Hygienists and Assistants, pp. 71-85, W.B. Saunders, Philadelphia, (1965).
- 23: Nakabayashi, N., Masuhara, E., Biomedical Polymers, pp. 85-111, (1980).
- 24: Mc Lean, J. W., "Clinical Applications of Glass-Ionomer Cements", *Operative Dentistry*, **5**, pp.184-190, (1992).
- 25: Smith, B., Wright, P. S., Brown, D., The Clinical Handling of Dental Materials, Second Edition, Butterworth-Heinemann LTD, pp. 2-10, 43-45, (1986).
- 26: Nelson, R. W., Intermediary Bases and Cementation, Advanced Restorative Dentistry, Second Edition, W.B., Saunders Company, pp. 63-76, (1984).

- 27: Causton, B. E., Johnson, N. W., "Changes in the Dentine of Human Teeth Following Extraction and Their Implication for In-Vitro Studies of Adhesion to Tooth Substance", *Archives Oral Biology*, **24**, pp. 229-232 (1979).
- 28: Goodis, H. E., Marshall, G. W., White, J. M., Gee, L., Hornberger, B., Marshall, S. J., "Storage Effects on Dentin Permeability and Shear Bond Strengths", *Dental Materials*, **9**, pp. 79-84, (1993).
- 29: Beech, D. R., Tyas, M. S., Solomon, A., "Bond Strength of Restorative Materials to Human Dentin: Post-Extraction Time", *Dental Materials*, **7**, pp. 15-17, (1991).
- 30: Busscher, H. J., Arends, J., "Determination of the Surface Forces γ_D^S and γ_P^S from the Contact Angle Measurements on Polymers and Dental Enamel", *Journal of Colloid and Interface Science*, **81** (1), pp. 71-79, (1981).
- 31: Jendresen, W. D., Baier, R. E., Glantz, P., "Contact Angles in a Biological Setting: Measurements in the Human Oral Cavity", *Journal of Colloid and Interface Science*, **100** (1), pp. 233-238, (1984).
- 32: Shaw, J. D., Introduction to Colloid and Surface Chemistry, Fourth Edition, Butterworth Heinemann, pp. 94-96, 151-156, (1992).
- 33: Meyers, D., Surfaces, Interfaces, and Colloids. Principles and Application, VCH, New York, pp. 349-358, 405-415, (1990).
- 34: Wu, S., Polymer Interface and Adhesion, Marcel Dekker, New York, pp. 133, 136, 149-151, 169-183, (1982).
- 35: Lee, H. L., Orlowski, J. A., Scheidt, C. G., Lee, J. R., "Effects of Acid Etchants on Dentin", *Journal of Dental Research*, **12** (6), pp. 1228-1232, (1973).
- 36: Okamoto, Y., Heeley, J. D., Dogon, I. L., Shintani, H., "Effects of Phosphoric Acid and Tannic Acid on Dentine Collagen", *Journal of Oral Rehabilitation*, **18**, pp. 507-512, (1991).
- 37: Pearce, J. A., "Laser Applications in Clinical Medicine", *Medical Instrumentation*, **4** (4), pp. 209-212, (1987).

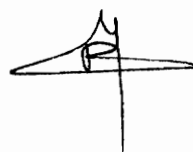
- 38: Holegar, J., "Thermogravimetric Examination of Enamel and Dentin", *Journal of Dental Research*, **55**, pp.547-548, (1976).
- 39: Hodge, H. C., Mc Kay, H., "The Microhardness of Teeth", *Journal of the American Dental Association*, **20**, pp. 227-233, (1933).
- 40: Hodge, H. C., "Hardness Tests on Teeth", *Journal of the American Dental Association*, **20**, pp. 271-279, (1933).
- 41: Caldwell, R. C., Gilmore, R. W., Timberlake, J., Pigman, J., Pigman, W., "Semiquantitative Studies of the Vitro Caries by Microhardness Tests", *Journal of Dental Research*, **37**, pp.301-305, (1957).
- 42: Hardness Measurements Handout, Leco DM 400 Digital Microscope.
- 43: Totah, V. P., "Increase in Hardness of Dentin upon Drying", *Journal of Dental Research*, **21**, pp. 99-101, (1942).
- 44: Crisp, S., Wilson, A. D., "Reactions of Glass-Ionomer Cements: The Precipitation Reaction", *Journal of Dental Research*, **53 (6)**, pp. 1420-1424, (1974).
- 45: Davies, E. H., Sefton, J., Wilson, A. D., "Primary Study of Factors Affecting the Fluoride Release From Glass-Ionomer Cements", *Biomaterials*, **14 (8)**, pp. 636-638, (1993).
- 46: Bagnall, R. D., "Adhesion in Dentistry: Part 2", *Materials Science and Technology*, **7**, pp. 786-794, (1991).
- 47: Vitrebond, Material Safety Data Sheet, 3M Center, St. Paul, Minnesota, 55144-1000.
- 48: Mitra, S. B., "Adhesion to Dentin and Physical Properties of a Light-Cured Glass-Ionomer Liner/Base", *Journal of Dental Research*, **70 (1)**, pp.72-74, (1991).
- 49: Crisp, S., Pringuer, M. A., Wardleworth, D., "Reactions in Glass-Ionomer Cements : II. An Infrared Spectroscopic Study", *Journal of Dental Research*, **53 (6)**, pp. 1414-1419, (1974).
- 50: Silverstein, R. M., Bassler, G. C., Morrill, T. C., Spectrometric Identification of Organic Compounds, Fifth Edition, Wiley, pp. 103-130, (1991).

- 51: Hegarty, A. M., Pearson, G. J., "Erosion and Compressive Strength of Hybrid Glass Ionomer Cements When Light Activated or Chemically Set", *Biomaterials*, **14** (5), pp.349-352, (1993).
- 52: Billington, R. W., Williams, J. A., Pearson, G. J., "Variation in Powder/ Liquid Ratio of a Restorative Glass-Ionomer Cement Used in Dental Practice", *British Dental Journal*, **169**, pp. 164-167, (1990).
- 53: Crisp, S., Lewis, B. J., Wilson, A. D., "Characterization of Glass-Ionomer Cements 2. Effect of the Powder: Liquid Ratio on The Physical Properties", *Journal of Dentistry*, **4** (6), pp. 287-290, (1976).
- 54: Crisp, S., Lewis, B. J., Wilson, A. D., "Characterization of Glass-Ionomer Cements 3. Effects of Polyacid Concentration on the Physical Properties", *Journal of Dentistry*, **5** (1), pp. 51-56, (1977).
- 55: Wilson, A. D., Crisp, S., Ferner, A. J., "Reactions in Glass Ionomer Cements: IV. Effect of Chelating Comonomers on Setting Behavior," *Journal of Dental Research*, **55** (3), pp. 489-495 (1976).
- 56: Wasson, E. A., "Reinforced Glass-Ionomer Cements-A Review of Properties and Clinical Use", *Clinical Materials*, **12**, pp. 181-190, (1993).
- 57: Eleanor, A., Nicholson, W. & J. W., "Effect of Operator Skill in Determining the Physical Properties of Glass-Ionomer Cements", *Clinical Materials*, **15**, pp. 169-172, (1994).
- 58: Van Noort, R., Brown, D., Causton, B. E., Combe, E. C., Fletcher, A. M., Lloyd, C. H., "Dental Materials: 1988 Literature Review", *Journal of Dentistry*, **18** (5), pp. 5-23, (1990).
- 59: Hull, D., An Introduction to Composite Materials, Cambridge University Press, pp.39-41, (1981).
- 60: Beech, D .R., "A Spectroscopic Study of the Interaction Between Human Tooth Enamel and Polyacrylic Acid Polycarboxylate Cement", *Archives Oral Biology*, **17**, pp. 907-911, (1972).

- 61: O'Brien, W. J., Rasmussen, S. T., "A Critical Appraisal of Dental Adhesion Testing", Adhesion Joint Formation, Characteristics and Testing, Ed. KL. Mittal, Plenum Press, New York, pp. 289-305, (1984).
- 62: Powis, D. R., Folleras, T., Merson, S. A., Wilson, A. D., "Improved Adhesion of a Glass Ionomer Cement to Dentin and Enamel", *Journal of Dental Research*, **61** (12), pp. 1416-1422, (1982).
- 63: Maldonado, A., Swartz, M. L., Phillips, R. W., "An in Vitro Study of Certain Properties of a Glass Ionomer Cement", *Journal of the American Dental Association*, **96**, pp. 785-791, (1978).
- 64: Barakat, M. M., Powers, J. M., Yamaguchi, R., "Parameters That Effect in Vitro Bonding of Glass-Ionomer Liners to Dentin", *Journal of Dental Research*, **67** (9), pp. 1161-1163, (1988).
- 65: Charlton, D., "Dentin Surface Treatment and Bond Strength of Glass- Ionomers", *American Journal of Dentistry*, **7** (1), pp. 47-49, (1994).
- 66: Blosser, R. L., "Time Dependence of 2.5% Nitric Acid Solution as an Etchant on Human Dentin and Enamel", *Dental Materials*, **6**, pp. 83-87, (1990).
- 67: Anderson, J. C., Leaver, K. D., Rawlings, R. D., Alexander, J. M., Materials Science, Third Edition, Van Nostrand Reinhold, pp. 211-212, 218-219, (1985).
- 68: Greener, E. H., Harcourt, J. K., Materials Science in Dentistry, Waverly Press, pp. 44-62, (1972).
- 69: Adams, R. D., Wake, W. C., Structural Adhesive Joints in Engineering, Elsevier Applied Science, pp. 125-126, (1984).

Vita

The author is the daughter of Riad H. and Wadad. H. Hamandi, born November 24, 1970, in Ashrafieh, Beirut, Lebanon. She graduated from Zahrat-el-Ehsan, Beirut, in August 1989. She decided to continue her higher education in America. The author started her undergraduate studies in Radford University in August 1990. After receiving her Bachelor's of Science in Chemistry in June 1993, she decided to pursue her Master's degree in Materials Science and Engineering at Virginia Tech.

A handwritten signature in black ink, consisting of a stylized, abstract shape with a vertical line extending downwards from its base.